# The Kinematic & Neuromuscular Basis of *Drosophila* Larval Escape

Patricia Cooney

Submitted in partial fulfillment of the
requirements for the degree of
Doctor of Philosophy
under the Executive Committee
of the Graduate School of Arts and Sciences

COLUMBIA UNIVERSITY

2022

# Abstract

The Kinematic & Neuromuscular Basis of *Drosophila* Larval Escape

Patricia Cooney

Escape behavior is the critical output of rapid sensorimotor processing in the brain that allows animals to sense danger and avoid it. The circuit structures and mechanisms that underlie escape are still under investigation. Drosophila larvae are an advantageous system for studying the neuromuscular circuitry of escape behavior. When threatened with harmful mechanical touch, heat, or light, larvae perform C-shaped bending and lateral rolling, followed by rapid forward crawling. The sensory input and neural circuitry that promotes escape in the larva have been extensively characterized, but we do not understand how bending and rolling motor programs are generated by the larval neuromuscular system. This work identifies the movement patterns, muscle activities, and motor circuit features that drive escape behavior. High-speed imaging approaches reveal that larvae select between four distinct, interchangeable patterns of escape rolling, and that each pattern consists of synchronous rotations of every segment as the larva rotates. Investigating electron microscopic reconstructions of premotor and motor neurons elucidates premotor to motor connectivity patterns that could underlie sequential muscle activity that circumnavigates the larva and propels synchronous rotation along the whole body. Volumetric Swept Confocally-Aligned Planar Excitation (SCAPE) microscopy uncovers that, unlike larval crawling, a well-studied form of larval locomotion that is driven by bilaterally symmetric peristaltic waves of muscle activity, the muscle activity during bending and rolling occurs in a circumferential sequence that is synchronous along the larva's segments. Muscles neighboring the dorsal and ventral midlines of the larva demonstrate left-right symmetric activity during rolling, and ventral muscles appear to drive the propulsion. Shifts in magnitude of left-right symmetric activity in midline muscles allow the larva to transition from initial escape bending into escape rolling. Preliminary computational predictions of PMN activities confirm the likely necessity of strong ventral muscle coactivity for driving escape. Probing specific PMNs during rolling demonstrates

robustness of circuits controlling escape and requires further investigation, alongside the role that sensory feedback could play in this behavior. Altogether, these data reveal a new circuit organization and motor activity pattern that underlie the coordination of muscles during an escape sequence. Future work could reveal circuit components necessary for escape, including the mechanistic basis for action selection, behavioral maintenance, and behavioral flexibility.

# Table of Contents

# List of Figures

# Acknowledgments

To start, I'd like to thank my mentors who guided me through my first experiences as a scientist. Chris Korey, my primary undergraduate advisor, provided an ideal learning environment and balance of guidance and independence to allow me to love doing science. Since 2012, your support in helping me find and participate in as many opportunities for growth as possible, and your openness to sharing your career experiences with me have made immeasurable positive impacts on my life. Thank you for being a steady source of wisdom and encouragement; for teaching me how the scientific process can be challenging, fun, and fulfilling; and for helping to open my eyes to the vast world around me. I'd also like to thank Melissa Hughes, my secondary undergraduate advisor, for providing my first glimpses into the breadth of fascinating animal behaviors, for encouraging me to embrace unknown possibilities, and for being the first to teach me how to ask questions, interpret data, and draw conclusions from experiments. Thanks to Trisha Folds-Bennett, Beth Meyer-Bernstein, Anton Vander Zee, and everyone at the College of Charleston Honors College for exposing me to opportunities I had never considered before and supporting me unwaveringly to achieve. Next, I'd like to thank Ruben Portugues for guiding me through my first experiences with advanced neuroscience techniques and for introducing me to the fun of collaborative research projects ("hackathons"). From the Portugues lab, I'd also like to especially thank Laura Knogler, Andreas Kist, and Daniil Markov for including me in your work and your thought processes, teaching me new concepts of experimental design and data analysis, and sharing your experiences as graduate students and postdocs.

Next, I'd like to thank my mentors in graduate school who have seen me through the most challenging stage of my development as a scientist so far. First and foremost, Wes, thank you for providing an environment and a mentoring relationship that gave me the opportunity to feel like a

valuable colleague, to gain confidence in my knowledge and abilities, and to challenge me to think more rigorously and critically about scientific discovery. Thank you for encouraging me to be a leader, for treating me with compassion and patience through difficult times, for giving me the freedom to cultivate my interests and develop collaborative skills, and for providing me with positive feedback and encouragement throughout this journey.

Aref Zarin, thank you for serving as a secondary mentor to me throughout the bulk of my graduate school career. You have provided me not only with a great deal of technical insight for my project, but also with guidance on project development and management, encouragement and support through rough patches, and tangible excitement and passion for the discovery of new knowledge. Thank you for continuously treating me as a colleague whose opinions and ideas you respect. It has been a joy to share and discuss ideas, however far-fetched or concrete, with you.

I'd like to thank my collaborators and committee members as well. Wenze Li, thank you for teaching me many important aspects of imaging, image processing, and data analysis, and for contributing guidance, advice, and encouragement to improve our work and help me improve as a scientist. I am immensely grateful to have learned from and worked with you—a brilliant scientist and a wonderful person. Elizabeth Hillman, thank you for challenging me to become more knowledgeable, more skilled, and more rigorous to ensure the best work possible, and thank you for providing your expertise to shape our scientific goals. Richard Mann, thank you for providing mentorship throughout my rotation with you and later throughout my thesis project, guiding me in the pursuit of questions that contribute to a meaningful, impactful body of work. Ashok Litwin-Kumar, thank you for taking time and effort to discuss my project from a computational perspective, and for teaching me how experimental and theoretical work can meaningfully coalesce. Rick Hormigo and Tanya Tabachnik, thank you for your support in improving and

maintaining our behavioral equipment, for troubleshooting new ideas with me, and for being wonderful colleagues to collaborate with.

I'd also like to thank Ai Yamamoto and Darcy Kelley for providing me broader mentorship throughout grad school. Darcy, thank you for helping me to identify and seek out the experiences I wanted to have while in grad school, and helping me become more confident in myself early on. Ai, thank you for providing me guidance through project management and career exploration; for encouraging me to be proud of and take ownership of my work; and for teaching me how to advocate for my work and myself.

To my mentors and colleagues from the Grueber and Mann labs, thank you. Lalanti, thank you for teaching me the wonders of working with flies, for showing me how exciting doing science can be, and for encouraging the formation of good, disciplined habits early on. Sam G., thank you for teaching me more about experimental planning, rigor, and how to present science well. Grace, thank you for teaching me patience, endurance, and encouraging me to stay positive and curious, and showing me how to be kind to myself and others. Rebecca, thank you for being my lab "big sister" for the first few years of my PhD, teaching me about balance as a graduate student, and resetting my perspective throughout. Davys, thank you for being a great source of intellectual excitement, encouragement, and grounding. Shan, thank you for being a constant friend in the lab—I am so grateful to have shared so closely the milestones of this experience with you, I will always be grateful for your insights, and I am glad to have grown with you. To Raffi, Abby, and Nova, for bringing new excitement and fresh ideas to the lab. To the rest of the Grueber lab, past and present, thank you so much for contributing to a great environment for doing research and discussing science!

Finally, thank you to my friends who have cared for me throughout this process. To my NBB cohort, you have all been wonderful colleagues and friends to discuss science and life with, and to learn from. I'd especially like to thank Mike, Amin, Dan, Taiga, Michelle, Liz and Claire for being great sources of support and fun these past few years. Especially, Taiga, thank you for always being thoughtful and sharing your experiences, thoughts, and ideas selflessly. Liz, thank you for being a tremendous emotional support to me, encouraging me to push through tough times, and reminding me to take stock along the way. Claire, thank you for being a reliable source of connection, compassion, kindness, joy, laughter, tears, understanding; for reminding me to be confident in myself; for helping me to grow; for being my New York family; for being the best fellow dog mom; for being my tether. Lloyd, thank you for being a supportive friend full of kindness and warmth through the last couple years. Sarah, Clare, and Thalia, thank you for your support and for sharing your worlds with me to remind me of what all is out there in life beyond science. Tatiana, thank you for always treating me with kindness and patience and believing in me in all that I do. Kelsey, thank you for being a dear friend to me throughout our time at different grad schools—I've learned so much from discussing our experiences, and I'm grateful to have your authenticity and humor in my life.

Finally, thank you to my family for supporting me to pursue my dreams. To my sister Kathleen for reminding me to keep perspective and not forget to enjoy many aspects of life. To my mom and dad, for encouraging me to push for more, and to be proud of my work and my growth; for reminding me to have a sense of humor and seek out joy; for sacrificing time and energy on me so that I could live a life of freedom and opportunity; for supporting me in all of life's pursuits. Thank you.

# Dedication

I dedicate this thesis to the brilliant women of generations past who pushed me to choose a life of adventure, discovery, and satisfaction, and without whom, I doubt I would be here. To Anna Beth Cooney, Kathleen Gover, Margaret Nevens, and Mary Gover, scientific and artistic minds, who taught me to be curious and pursue any opportunities that life presented me. To my mother, Tamara Cooney, the smartest and most resilient person I know. You taught me the power of endurance and persistence through difficulty, the joys of learning and asking questions, the worthiness of not settling for less, and the importance of cultivating one's interests and pursuing new passions throughout life.

# Chapter 1: Introduction

Animals are distinct from other organisms because of a handful of coevolved traits, including the presence of a nervous system and the ability to move. Movement is arguably the most important function of the nervous system. It is essential for animals to perform tasks critical to their survival: locate resources, find mates, and escape danger. Fascinatingly, animals can perform a seemingly infinite repertoire of motor behaviors with a finite number of neurons and muscles in order to effectively engage with the environment around them at any instant. Foundational thinker and Nobel Laureate in the study of ethology, Nikolaas Tinbergen proposed that behaviors could be understood through a hierarchy of modules[1]. Namely, any behavior (*e.g.* fighting) can be decomposed into stereotyped components of movement (*e.g.* punch, kick, duck), into stereotyped motion of body parts (*e.g.* pull back arm, make fist), into stereotyped contractions of muscle groups (*e.g.* contract bicep, contract finger flexors), and finally into stereotyped motor unit drive (*e.g.* activate motor neurons innervating bicep and finger flexors). Tinbergen hypothesized that the infinite complexity of animal behaviors could be reduced into a combinatorics problem within this hierarchy of modules. Simply recombining particular body part movements, and thus the motor unit and muscle activities that drive them, could yield the infinite behavioral repertoires that animals perform.

Evidence has emerged to support this hierarchy of modules, spanning from neurons to muscles to body motion to behavior. For example, mice perform sub-second behavioral modules, including darting, pausing, and walking bouts, that change in duration and order to generate unique behavioral responses to environmental changes, like the introduction of a predator's scent[2]. Behavioral modules can either occur as independent events, such as in sequences, or as simultaneous events. For instance, male rats perform multiple types of ultrasonic vocalizations during social interactions with female rats, employing single-module calls—comprised of uniform, stereotyped muscle contractions and air pressure profiles—and complex calls that involve the combination of multiple single-module calls[3]. Muscle modules, coactive groups of muscles, produce specific body part motion, and can be employed combinatorically to generate specific behaviors or multiple behaviors. For example, some muscle modules in frog legs demonstrate

shared activity patterns across jumping, swimming and walking, while others demonstrate activity dedicated for only one of these behaviors[4]. Finally, motor circuit modules, the motor and premotor neurons active during a particular behavior coordinate muscle modules. Motor circuit modules can be selectively active during specific behaviors or demonstrate variable activity patterns across behaviors. For example, the majority of interneurons active during leech swimming are also active during crawling. Some of these interneurons demonstrate distinct activity patterns for each behavior, while others show unique activity patterns for a single behavior alone[5]. Though Tinbergen's framework for understanding behavior at multiple scales has revealed many insights into the generation of movement, much of this work has not successfully integrated measures from across the hierarchy that yields behavior. Further, until recent advances in neuroscience and behavioral techniques, mechanistically linking the modules that comprise complex behaviors to the sensory contexts that promote them has proven difficult.

In this thesis, I uncover multiple hierarchical levels of a sensory-evoked behavior: I elucidate the body movements, muscle activities, and motor circuits that underlie *Drosophila* larval escape. The genetic tractability and tools, functional imaging resources, and circuit connectome data available in the *Drosophila* larva model, alongside its well-characterized sensory circuitry and behavioral responses to sensory input, make this investigation of motor circuit functions in escape behavior particularly fruitful for understanding sensorimotor transformations in the brain. To preface my experimental work, in this chapter, I will introduce current knowledge on how motor circuits generate movement, and how sensory information is transformed by the brain into motor responses in the form of rapid, flexible escape behaviors. I will close by detailing how sensation, particularly sensing potential harm, and locomotion occur in *Drosophila* larvae.

## 1.1 Fundamentals of Movement

At its most complex, movement allows animals to perform high-level functions, like social communication and artistic expression. At its simplest, movement allows animals to survive. In vertebrates, the neural circuits that control and generate movement are broadly distributed and hierarchically organized.

Motor learning, planning, and initiation are controlled by population activity in cortical regions, while repetitive, stereotyped movements are controlled by circuits in the brainstem. Subpopulations of neurons in the brainstem project to distinct spinal circuits that are organized in a manner that promotes flexible recruitment of specific movement components[6]. In this section, I will summarize how motor circuits are organized, how they generate multiple movement patterns, and how motor circuit architecture can contribute to behavioral sequences.

Though brain circuits are required for higher-level aspects of movement, the spinal cord is remarkably autonomous in generating reflexive movements and self-sustained movement patterns[7]. First observed in the decerebrate cat, spinal cord circuits can sustain rhythmic locomotion without input from the brain[8,9], as well as withdrawal reflexes[7]. These spinal circuits consist of motor neurons (MNs), organized into motor neuron pools, that project to a specific functional group of skeletal muscles. The MNs receive input from premotor neurons (PMNs) that excite or inhibit specific motor neuron pools, and from proprioceptors within the muscles that the MNs innervate[6,7]. When vertebrate spinal MNs become excited, they release acetylcholine into neuromuscular junctions, exciting the specific group of muscle fibers that they project onto, and causing muscle fiber depolarization[9]. As the muscle fibers with common MN input depolarize, calcium influxes into the muscle. This calcium influx then triggers actin-myosin interactions that power muscle contraction[9]. Though the motor units—single MN to muscle fiber groups—are the driving force of movement, the activation and coordination of these units is controlled by the PMNs. Just as the MNs are organized into functionally related MN pools, PMNs are spatially segregated based on the functional roles of the MNs they project to: PMNs for trunk muscle coordination are bilaterally symmetric, while PMNs for limb muscle coordination are ipsilateral to the MNs and muscles they innervate; PMNs that control flexor movement are located laterally in the spinal cord, while PMNs that control extensor movement are located medially[6]. This functionally based spatial segregation of PMNs simplifies how descending input might initiate a given movement pattern[6]. For example, stimulation of specific spinal cord regions in the frog evokes distinct reflexive or repetitive movements[10]. Though descending input could be thought of as a singular selector of behavior, descending neurons can also act combinatorically to evoke

precise movement components. For example, in flies, a morphologically similar group of descending neurons combinatorically contributes to wing beat amplitude during flight[11], showing that descending activation of lower motor circuits is not merely an "on/off" signal for behavior.

Both motor circuits that control rhythmic movements and those that control non-rhythmic movements act through muscle synergies—groups of muscles with congruent functions[10]. While these muscle synergies, and the motor units that control them, are coordinated in a fixed way for one behavior, the same motor units and muscles must be multifunctional—reused in a different coordinated manner to generate other behaviors[12]. For example, in frogs, some muscle synergies are specific to swimming and jumping, but others are shared across these behaviors[4]. The same principles hold true at the level of the spinal circuits driving movement, where premotor neurons show shared and distinct patterns for driving different behaviors. For example, in turtles, the PMNs that drive coordination of a particular scratching behavior demonstrate a distinct activity pattern during other behaviors[13]. Similarly, population analysis of PMN activities during swimming and walking in the leech show that many PMNs are active for both behaviors but with different activity timing[5]. While some of these active PMNs are necessary for both behaviors, others demonstrate dedicated function[5]. This principle of circuit reorganization and multifunctionality is essential to the diverse repertoire of behaviors that any single animal can perform.

Though descending control serves as an appealingly simple mechanism for how animals select the motor patterns they will perform, emerging evidence suggests that maintenance of movement—and therefore also transitions between distinct movement patterns—could be regulated in part by local interactions within premotor circuits. In flies, for example, muscle activity patterns that drive singing versus flight are distinct, and these behaviors are mutually exclusive; yet activation of a song-inducing descending neuron during flight does not cause the fly to transition from flying into singing, suggesting that flying premotor circuits could be competitively inhibiting song premotor circuits, and therefore prohibiting descending neuron-based behavioral switches[14]. Further, in *Drosophila* larvae, transitions into sequential movements and preventions of behavioral sequence reversals are mediated by lateral disinhibition and feedback disinhibition, respectively[15]. Specifically, larvae probabilistically perform "hunching" or

"bending" behaviors in response to a wind stimulus, with the most common behavioral sequence consisting of hunching followed by bending. To drive this order of motor circuit activation, interneurons that promote hunching indirectly disinhibit bend-promoting interneurons over time to allow transition, and bend-promoting interneurons indirectly disinhibit themselves further to sustain bending behavior[15]. The role of descending input versus autonomous motor circuits in behavior generation requires further investigation under naturalistic settings across taxa. Overall, from these findings, we can conclude that lower-level motor circuits can perform complex, multifaceted behavioral functions, and are organized in a way that permits precise recruitment and behavioral flexibility. Studying lower-level motor circuit function can enrich our understanding of how animals behave adaptively in their environments.

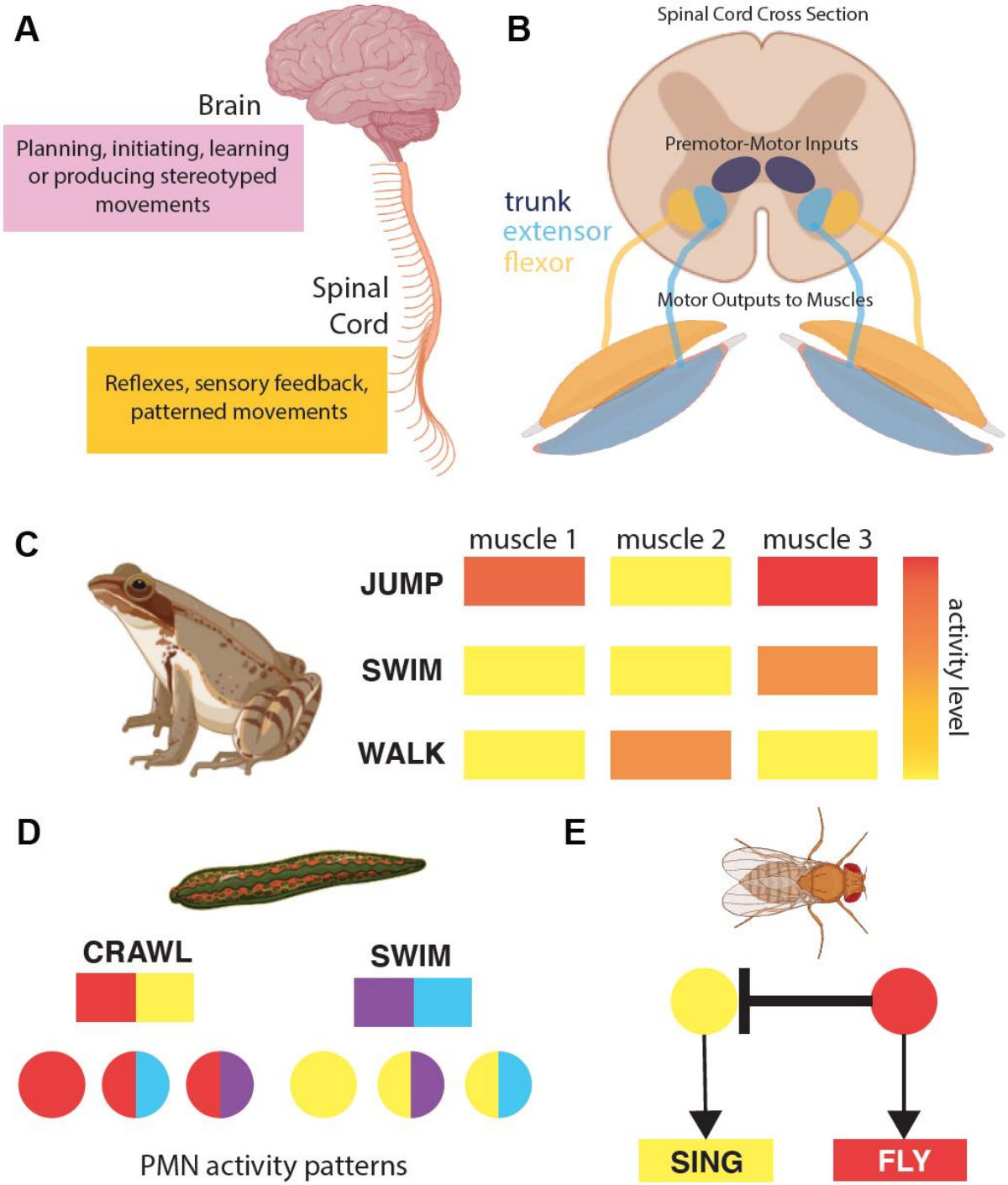


**Figure 1.1: Motor Circuits & Control Principles.** (**A**) General distribution of motor control between brain and spinal cord. (**B**) Spinal cord cross section showing spatial-functional relationship of premotor inputs to motor neurons. (**C**) Example muscle synergy overlaps and distinctions in three different frog behaviors. (**D**) Example premotor neuron multifunctionality, where some PMNs are uniquely active during one phase of a single behavior, and others are active in both behaviors. (**E**) Action selection mediated by descending neurons in flies demonstrates behavioral hierarchy via neural circuits.

## 1.2 Sensorimotor Processing & Escape

The life of an animal is a constant cost-benefit analysis: one must use energy efficiently and conservatively to optimize chance of survival. Distinct movement patterns allow animals to actively select between lower energy, slower movement and higher energy, faster movement based on the urgency of the animal's needs. Detecting potential harm elicits more powerful and flexible locomotor behaviors than forms of locomotion used for exploration and resource-seeking. Motor circuits and muscles must therefore be activated by sensory cues in a manner separate from how they are activated in other, non-threatening contexts. Here, I will highlight common features of escape behaviors across taxa, alongside the sensory circuits that promote such behaviors and the so-far identified motor circuit components that drive these unique forms of movement.

**Features of escape behaviors**

Across taxa, the movements that comprise escape locomotion involve sequences that differ fundamentally from those that comprise exploratory locomotion. The key tenets of escape usually include: 1) depending on the stimulus type and intensity, an initial withdrawal from the source of harm; or an initial pause to assess the source of potential harm and perform preparatory movements; and 2) rapid, high-powered movement to evade the source of harm[16–18]. Initial reflexive withdrawal movements in escape are generally prompted by direct mechanosensory stimulation, and span crayfish tail-flip responses[19], fish fast-starts or C-bends[20], and rodent paw withdrawals[21]. Alternatively, many animals pause as an initial response to a potential threat, determined by visual input or other distance-based cues. For example, in response to select visual cues, flies, crabs, locusts, and rodents freeze prior to performing escape locomotion[16–18,22]. During this freezing stage, animals gather more sensory information about the potential threat[17,18,22], and can integrate threat-related sensory information with sensory feedback to perform preparatory movements that shape their escape locomotor trajectories[16,21,22].

The subsequent locomotion away from danger can either entail more vigorous activation of exploratory locomotor circuits or, more commonly, completely different bodily coordination than exploratory locomotion. In response to looming stimuli, larval zebrafish perform an initial escape bend followed by burst swimming that is a combination of higher velocity and higher bend angle tailbeats than non-escape maneuvers, but relies on fundamentally similar locomotor coordination[23]. On the other hand, quadrupedal animals like mice and horses exhibit fundamentally distinct gaits to locomote at different speeds. At slow speeds, mice and horses "walk", wherein three or four of their feet contact the ground simultaneously, touching the ground in an alternating sequence: left forelimb footfall, right hindlimb footfall, right forelimb footfall, left hindlimb footfall[24,25]. At maximal speeds, these quadrupeds show no left-right alternation, with synchronous footfalls of two out of four legs at a time that propel them to cover substantially more ground over time[24,25]. The emergence of distinct gaits to fit contextual locomotor speed requirements is also observed in limbed insects. For example, at slow speeds, flies primarily exhibit tetrapodal or wave gaits, where at least four or five feet are on the ground at the same time, respectively[26]. At maximal speeds, flies primarily exhibit tripod gaits, where front- and hindlegs on one side have synchronous footfalls with a midleg on the contralateral side in a repetitive alternating pattern[26]. Distinct descending neurons can induce particular speeds of locomotion in flies, suggesting that descending control selectively activates context-specific central circuits to meet locomotor needs[27]. However, both quadrupeds and hexapods alike demonstrate seamless transitions through locomotor patterns as they change speeds, where intermediate speeds involve hybridity of limb coordination seen at lower speed and higher speed gaits, highlighting the complexity of gait selection and the likely interconnected nature of spinal circuits that coordinate fluid, adaptive locomotion[24,26].

Escape sequences are flexible, allowing each animal successful evasion given its current state and the competitive co-evolution of predator-prey interactions. Animals demonstrate adaptive initiation of escape, and adaptive switching in necessary motor output mid-behavior[16,18,28,29]. Flies and rats alike alter escape responses based on sensory feedback about current body position. For example, a rat's initial stance when presented a noxious mechanical or heat stimulus impacts its behavioral response: if in a bipedal stance

and presented a noxious hindlimb stimulus, the rat is less likely to withdraw its paw, or it shifts into a quadrupedal stance prior to paw withdrawal[21]. Similarly, when presented a looming stimulus, the magnitude and direction of a fly's escape jump vector depend directly on its center of mass location during stimulus presentation[30], highlighting the importance of integrating current state with impending threat when executing escape behavior. Some animals have been shown to pick suboptimal escape strategies to prevent predictability, essentially adding noise to predator-prey interactions and undermining co-evolution of more effective predatorial behaviors. For example, cockroaches tend to select suboptimal escape trajectories from a fixed angular set away from a wind current, allowing them to avoid predation through combining distance from predator's attack and a metric of unpredictability[28]. This flexibility in selecting initial escape response to a threat is crucial to survival. Animals also demonstrate flexible switches in behavioral strategy mid-escape. For example, crabs can update their escape direction as direction of visual input changes[17]. Other animals employ different components of the escape sequence probabilistically. Nematodes, even with the same optogenetic noxious stimulation, flexibly alternate between reverse locomotion, pausing, and escape omega turns[31]. Flies and mice alternate flexibly between freezing and fleeing escape strategies[32,33]. These key aspects of escape make it an excellent behavior for understanding the neural transfer of constantly updated sensory information, both external and self-generated, into rapid action selection.

**Neural circuits of escape as a basis for action selection**

The richness of these behaviors has made them a central focus for investigating how neural circuits achieve action selection. The main neural circuit bases of initial, reflexive withdrawal from harm have been primarily attributed to command neuron systems, balanced with parallel circuitry to invoke less immediate escape responses. First identified as a neural mechanism for inducing the crayfish tail-flip response, command neurons are usually pairs or small groups of neurons that are downstream of sensory inputs and, when activated, induce a rapid motor response[19]. Specifically, in the crayfish tail-flip response, strong mechanosensory input is channeled to one of two sets of giant fiber neurons—named for their large-diameter axons that permit fast action potential conductance—based on localization along the body. These

GFs project to phasic motor circuits, and upon firing, activate stereotyped segment contractions that either induce backward propulsion in response to rostral stimuli or forward flipping in response to caudal stimuli[19]. Meanwhile, parallel non-GF circuitry responds to lower intensity sensory input in a combinatorial manner, and promotes more flexible escape responses, including directed jumping and swimming behaviors[19]. Similar mechanisms have been identified in insects[16,22,34]. For example, in flies, escape jumps are induced by looming stimuli, where faster looming stimuli cause flies to execute short-mode takeoffs with less control over trajectory, while slower looming stimuli cause flies to execute long-mode takeoffs that include a preparatory wing motion and result in more precise trajectory selection[34]. Giant fiber descending neurons, similar to the giant fibers in crayfish, are necessary and sufficient for driving short-mode takeoffs[34]. GFs integrate information from visual interneurons that encode distinct features of looming stimuli[35], and project to jump muscle motor neurons and other interneurons[36]. When GF input surpasses a threshold, GFs fire a single action potential that triggers short-mode takeoff, whereas when visual input is subthreshold, parallel circuits trigger alternative escape strategies, including long-mode escape and freezing[37]. Sometimes, GFs will fire a spike but parallel circuits that initiate wing movements in response to looming stimuli take over and initiate long-mode escape instead[34,37]. Similar circuits are observed in fish to induce fast-start responses and subsequent swims[20,23]. Interestingly, many of these command neurons are not required for some degree of escape response to be initiated, highlighting the importance of alternative, parallel mechanisms in inducing escape. Other systems appear to promote escape strictly via combinatorial coding of sensory interneuron populations, rather than any command-like circuitry. For example, in crickets, the detection of wind direction, which impacts escape trajectory choice, is encoded by sensory interneurons that have very broad receptive fields individually, but upon firing in synchronous pairs provide finer directional tuning of wind detection[16]. Some mixture of command neuron-based and population-based neural circuits could be responsible for initial escape responses across taxa.

Neural mechanisms that trigger context-dependent switches in escape locomotion patterns have also been identified. Most commonly, these switches are governed by descending control where selecting the distinct descending signal depends on competitive inhibition. For example, in flies, a specific pair of

descending neurons is necessary for freezing behavior to occur in response to an inescapable looming stimulus, and sufficiently induces freezing behavior in a walking speed-dependent manner[32]. Though the circuit mechanism for balancing this freeze activation versus escape is unknown, silencing this descending neuron increases the probability of the fly performing other escape modules[32], suggesting a role for competitive inhibition of circuits. In mice, freezing versus fleeing is also flexibly interchangeable based on threat imminence[38]. This flexibility is governed by competitive inhibition and feedforward disinhibition interactions across brain regions. Namely, the central nucleus of the amygdala contains molecularly distinct subpopulations of neurons that laterally inhibit each other[33]. Greater activity in one subpopulation results in either freezing or flight. Shifting the activity balance between these regions alters escape output[33]. Projections from the central nucleus of the amygdala disinhibit the ventral periaqueductal gray to induce freezing behavior through premotor outputs to the medulla[38]. Selecting appropriate locomotor speed and coordination patterns during escape is dependent on subpopulations of excitatory neurons in the midbrain[39]. Namely, both the cuneiform nucleus and the pedunculopontine nucleus contribute to slower, alternating gaits, while the cuneiform nucleus alone is necessary and sufficient for inducing synchronous leg movements that comprise escape bounding[39]. The cuneiform nucleus is downstream of other brain regions linked to processing pain and escape, including the dorsal periaqueductal gray, suggesting that collectively, the periaqueductal gray mediates freezing versus locomotion, and subsequently influences locomotor pattern selection[39,40]. The exact sensory integration mechanisms that drive activity differences in the above-mentioned circuits, and the descending mechanisms through which they activate spinal circuits that coordinate bounding are unknown. Altogether, these findings have provided insight into sensory bases and descending control mechanisms that promote and select escape motor programs, respectively, and demonstrate how stereotypy and flexibility can be balanced via neural control.

**Motor circuits driving escape**

Little is known, however, about the motor circuit mechanisms that underlie and coordinate escape-specific movement. In larval zebrafish, high velocity, high frequency swim bouts have been linked to

recruitment of dorsal excitatory spinal interneurons, while slower swim bouts rely on ventral excitatory spinal interneurons[41]. Spatial recruitment of inhibitory interneurons for these two locomotor speeds is inversely related to excitatory interneuron recruitment[42]. The fast, powerful 'bound' gait that emerges in quadrupedal animals is thought to be coordinated by contralaterally-projecting excitatory and inhibitory interneurons in the spinal cord, though their identity and exact mapping within the spinal cord remains unknown[25]. This hypothesis emerged because: 1) the ablation of inhibitory interneuron populations that maintain hindlimb alternation at low speeds and 2) the excitatory interneuron populations that maintain hindlimb alternation at high speeds, both result in bounds at all speeds[24]. This suggests that another interneuron population could be bypassing or inhibiting these alternation circuits to generate synchronous limb movements when quadrupeds are under threat. Interestingly, opposite of the spatial-functional relationship of spinal interneurons in larval zebrafish, ablation of dorsal inhibitory interneurons disrupts slower locomotion only[24]. These findings highlight the relationship between functional significance and spatial location in spinal cord circuits for regulating locomotor mode switching in escape. However, they also demonstrate the complexity of untangling the exact spinal circuit components and mechanistic bases by which animals rapidly and flexibly switch locomotor modes. By gaining traction on the motor circuits that underlie escape, we can uncover the precise interactions between parallel circuits promoting probabilistic sequences, and we can better understand the mechanisms through which motor circuits coordinate diverse motor outputs.

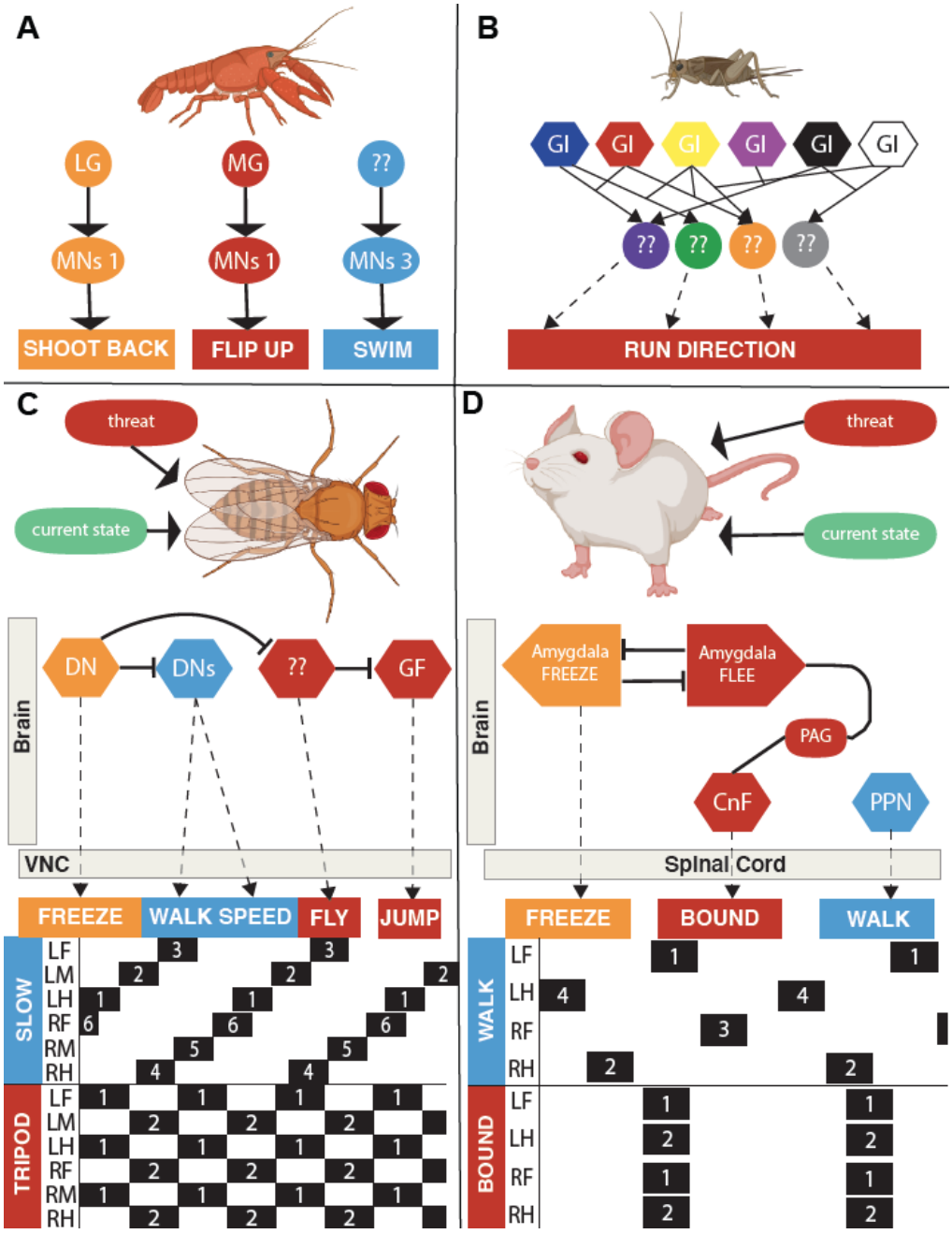


**Figure 1.2: Escape Behaviors & Circuits.** (**A**) Command neurons (lateral giant, LG; and medial giant, MG) drive two distinct rapid escapes in crayfish, while unknown neural components drive slower escape movements. (**B**) Population of giant interneurons (GIs) combinatorically code wind direction and subsequent escape trajectory in crickets. (**C**) Flies integrate different types of threat and current behavior to determine subsequent escape, mediated by descending neurons (DNs) with hierarchical relationships that permit behavioral flexibility. Gaits of fly walking differ based on context, where slower gaits consist of wave-like progression, and faster gaits consist of tripod alternations. (**D**) Mice integrate threatening stimuli with current behavioral state, and flexibly alternate between freezing, fleeing (bounds, fast locomotion), and walking (slow locomotion). Action selection in escape is mediated by the

amygdala, and gait selection is mediated by brainstem nuclei (periaqueductal gray, PAG; cuneiform nucleus, CnF; pontine peduncular nucleus, PPN). Walking gait is comprised of left-right, front-hind alternation pattern, while bounds are comprised of left-right synchronous, front-hind alternation.

## 1.3 Sensation & Movement in *Drosophila* Larvae

### The *Drosophila* larva as a model for sensorimotor circuit investigation

The brain is a remarkably complex organ: it perceives the present (sensation), integrates perceptual information with instincts and previously learned responses (internal state, memory), and drives behaviors advantageous to survival (movement). Though the human brain and its rich capacity for cognition, emotion, identity, and creativity fascinate, the complexity of human behavior and the vast capabilities of the human brain make it difficult to study. To understand the exact neural mechanisms by which the brain orchestrates coordinated behavior as a product of self and sensing environment, neuroscientists investigate the brain using models. Models allow us to gain insight into more complex phenomena and form conclusions about how these phenomena work at a simpler level[43,44]. In the pursuit of understanding how the brain transforms sensory information into coordinated responses, an ideal model would demonstrate robust behavior in response to some cue, contain a relatively simple brain, be easy to observe and highly manipulatable for testing hypotheses, and would show conserved or representative features that make its neural mechanisms generalizable to other systems[43,45]. The *Drosophila* larva is an ideal model for investigating how the brain transforms sensory information into behavioral responses.

*Drosophila* have a relatively short life cycle and reproduce in large numbers rapidly, making them ideal for high-throughput experiments and population-level understanding of variable biological phenomena like behavior. After egg-laying, the *Drosophila* embryo develops for roughly one day before hatching and becoming a first instar larva[46]. Over the next four days, the larva transitions into second and then third instar stages[46]. The larva grows in size and increases the number of synaptic connections between neurons during this period but does not change circuit connection patterns substantially during the larval stages of development[47]. As the larva matures, it demonstrates more robust, but not fundamentally distinct,

behaviors[48]. The larva then pupates and eccloses as a sexually mature adult fly by day 10, that can mate and generate more offspring.

The larval nervous system is comprised of a ventral nerve cord, analogous to the vertebrate spinal cord, and brain lobes, that altogether contain about 10,000 neurons[49,50]. In the past decade, efforts to reconstruct every larval neuron and its connections have been made with electron microscopic (EM) connectomics[50–58], a work in progress that will allow comprehensive circuit diagrams to guide mechanistic insights into how neural computations are made, like in *C. elegans*. The extensive use of *Drosophila* as a model for genetic inheritance[59], development, and the first investigation of the genetic basis of behavior[60] has made *Drosophila* a highly tractable model organism[61]. Namely, a wide repertoire of tools has been developed for visualizing, ablating, observing activity and connectivity of, and manipulating activity of neurons in *Drosophila*[62]. Many of these tools in neuroscience rely on binary expression systems, such as Gal4-UAS[63], an exogenous paired transcriptional activator and upstream activation sequence from yeast that allows combinatorial expression of transgenic tools in specific tissues. A number of binary expression-based libraries—where specific enhancers have been used to drive transcriptional activator expression (*e.g.* Gal4, LexA, QF)—have been generated, and have publicly documented tissue expression patterns[64,65]. When paired with upstream activator sequence-linked tools (*e.g.* UAS-GFP, LexAop-GFP, QUAS-GFP), these binary expression-based libraries make consistent, reproducible expression of tools in specific cells a simple matter of setting up crosses between two fly strains, rather than having to generate a novel transgenic animal strain for every experiment.

On top of ease of use for experiments, *Drosophila* show conserved features with other organisms: they share many neurotransmitters and general circuit structures with mammals, and roughly 75% of genes linked to human disease have analogs in the *Drosophila* genome[66–68]. Further, larvae show a broad repertoire of behaviors that are conserved across taxa, ranging from sensorimotor decision-making to associative learning. Though *Drosophila* adult flies share the wide breadth of tools for circuit mapping and manipulation, and demonstrate richer behavioral complexity than larvae, adults have 10-fold more neurons than larvae, and the larva's smaller size and cuticle transparency make approaches for measuring whole-

body movements and muscle activities, as well as manipulating neural activity with optogenetics, more feasible. In this section, I will summarize our current extensive knowledge about how the larva senses the world around it and behaves accordingly, and our capacity to glean more about the mechanisms of brain function from this model.

**Somatosensation & somatosensory circuits in *Drosophila* larvae**

The *Drosophila* larval body wall is composed of three thoracic segments and nine abdominal segments. Somatosensory neurons, including chordotonals, mechanosensors, nociceptors, and proprioceptors cover the larval body in a segmentally repeated, stereotyped manner[69–73], providing the larva the ability to sense air current and vibration[71–73], gentle touch and noxious cold[74–76], noxious mechanical touch and noxious heat[72,74,77–90], and self-generated body deformation[91,92] , respectively. These neurons have been well-characterized morphologically, exhibiting type-specific dendritic morphologies and territories in the body wall[69], as well as corresponding type-specific axon morphologies and projection areas within the ventral nerve cord[93]. The type-specific axonal projection territories determine what downstream neurons these somatosensory neurons synapse with: mechanosensors and nociceptors target ventromedially in the ventral nerve cord, and proprioceptors target dorsolaterally, closer to the motor neuropil[70]. Activation of any single somatosensory neuron type induces a stereotyped behavioral response; yet many second order sensory interneurons act as initial sites of sensory integration, receiving inputs from multiple classes of somatosensory neurons[54,56,86,87,89]. Multisensory activation impacts second order sensory interneuron processing, and modulates behavioral responses[87,89].

Larval nociceptors, called class IV dendritic arborization neurons (cIVs), demonstrate the greatest dendritic complexity of the somatosensory neurons[69]. Their dendrites are highly branched and collectively tile the entire body wall, allowing the larva to detect noxious stimuli anywhere on their bodies[69]. cIVs are polymodal nociceptors that, via distinct molecular mechanisms, respond to noxious heat, noxious mechanical touch, and noxious short-wavelength light[77,79,80,83,88,90,94–96]. cIVs are necessary and sufficient for escape behavior[78,85]. When strongly activated either naturalistically—via heat probe, forceful touch, or

parasitic wasp attack—or through optogenetics, cIVs induce larval escape behavior[48,56,71,77–80,82,83,85,87,88,97]. Larval escape behavior generally consists of a sequence of C-shaped bending, lateral rolling while remaining bent, and fast forward crawling[56,77,78,85,87], though this sequence can differ based on stimulus modality and strength[78,82,85,96]. This nocifensive sequence allows the larva to effectively defend itself against and escape from parasitoid wasps upon nociception caused by the wasp ovipositor penetrating the larval body wall[78,85]. Notably, escape rolling is faster than fast crawling alone, wherein larvae move at ~3-5mm/s across the substrate compared to ~1.5mm/s during fast crawling[71,78], and rolling allows the larva to effectively fling an attacking wasp off its body[78,85], making this behavior useful for both predatorial escape and for escape from other environmental sources of harm.

Performance of each module of the escape sequence is probabilistic[56,71,85,87], consistent with the flexibility and variability of escape behavioral sequences across taxa described in the previous section. Escape sequence variability in the larva thus far has been linked to different mechanisms of sensory transduction[82], and different components of somatosensory circuits being activated[54,86,87,89]. For example, distinct avoidance behaviors can be induced through modality-specific cIV activation patterns[82,85]. Specifically, in response to noxious heat, cIVs exhibit high-frequency spike trains, followed by pauses in activity and resultant calcium influxes to dendrites, whereas in response to noxious short wavelength light, cIVs exhibit lower firing rate and no large dendritic calcium influxes[82]. These cIV activity patterns parallel modality-specific behavioral responses in larvae, where noxious heat induces the full escape sequence[56,71,72,77,78,80,82,83,85,87,88,97]; whereas noxious short-wavelength light induces only fast crawling away from the light[82,96]. The exact link between how cIV activity patterns differentially activate downstream circuits remains mysterious.

The probabilistic occurrence of escape behavioral modules has also been linked to differences in multisensory integration. For example, parasitic wasp attacks—that involve a combination of gentle touch information as the wasp lands on the larva, followed by noxious touch of the wasp stabbing the larva with its ovipositor—result in variable behavioral responses based on type of sensory input and location of sensory input to the larva's body[78,85]. Specifically, larvae primarily select between forward crawling,

turning, C-shaped bending only, and bending and rolling as their initial response to wasp contact before transitioning into secondary behaviors[85]. Escape rolling is most commonly triggered when the wasp has contacted the larva in mid-segments, usually correlates with having sustained injury from the wasp's ovipositor, and almost always results in the larva transitioning back into forward crawling[85]. Meanwhile, crawling and turning behaviors are most likely if the wasp contacts the larva's head or tail and does not injure the larva, consistent with previous studies observing gentle touch-based behavior alone[74,85].

The characterizations of second-order sensory interneurons that receive nociceptive input have provided further insight into the mechanisms for integrating sensory modalities and promoting context-specific behaviors. The downstream interneurons that nociceptors synapse onto has been EM-reconstructed[47,54,56,86,87,89]. Many of the reconstructed interneurons receive input from multiple sensory modalities[54,56,86,87,89], and exhibit indirect circuit convergence onto 'Goro', a command neuron, that is sufficient to induce rolling, but does not promote subsequent fast escape crawling[54,56,86,87]. For example, a group of 'Basin' interneurons receive mechanosensory and nociceptive inputs and respond most intensely to a combination of vibration (mimicking wasp flight) and nociception (mimicking ovipositor stabbing)[87]. These interneurons facilitate rolling and serve as one of the first of many points of neural circuit convergence of mechanosensory and nociceptive inputs in the ventral nerve cord and brain[87]. Another type of second-order nociceptive interneuron, the 'Down-and-Backs' (DnBs), receive noxious input as well as gentle touch input, and promote escape rolling indirectly through Goro neurons as well[56]. Interestingly, the DnBs are specifically necessary for full-magnitude escape bending and are sufficient for inducing the entire escape sequence. Their likelihood of inducing escape rolling is dose-dependent, but they are not required for rolling to occur[56]. DnBs are presynaptic both to motor regions and other nociceptive circuit components like the Goro pathway, providing an additional circuit-based mechanism for sensory integration and flexible engagement of escape modules[56]. By contrast, one type of nociceptive interneuron, 'medial Clusters of cIV Second-order Interneurons' (mCSIs), is both necessary and sufficient to induce escape rolling completely, even when Goro command neurons are silenced[86]. mCSI activity does not impact Basin-Goro circuit activity, but mCSIs are functionally upstream of motor neurons[86], some of which are also direct downstream

partners of DnBs[56]. These studies of second-order sensory integration and escape promotion reveal parallel mechanisms for escape, as observed in other animals.

In summary, the study of nociception and its escape-promoting circuits in the larva highlight the rich perceptual basis through which larvae flexibly select behaviors. Though the somatosensory circuitry—and consequently, a few downstream candidate premotor neurons—that are necessary for escape have been identified, this sensory-focused investigation of escape has demonstrated the complexity of multisensory parallel processing that promotes escape, as in other neural circuits that promote robust, flexible escape behaviors. Gaining greater clarity on the circuit mechanisms that use this multi-stream information to selectively promote probabilistic, modular behavioral sequences requires dissection of the motor output mechanism. By characterizing motor circuits and neuromuscular activities during escape, we can yield insight into the mysterious "black box" between sensory processing and resultant behavior in the future.

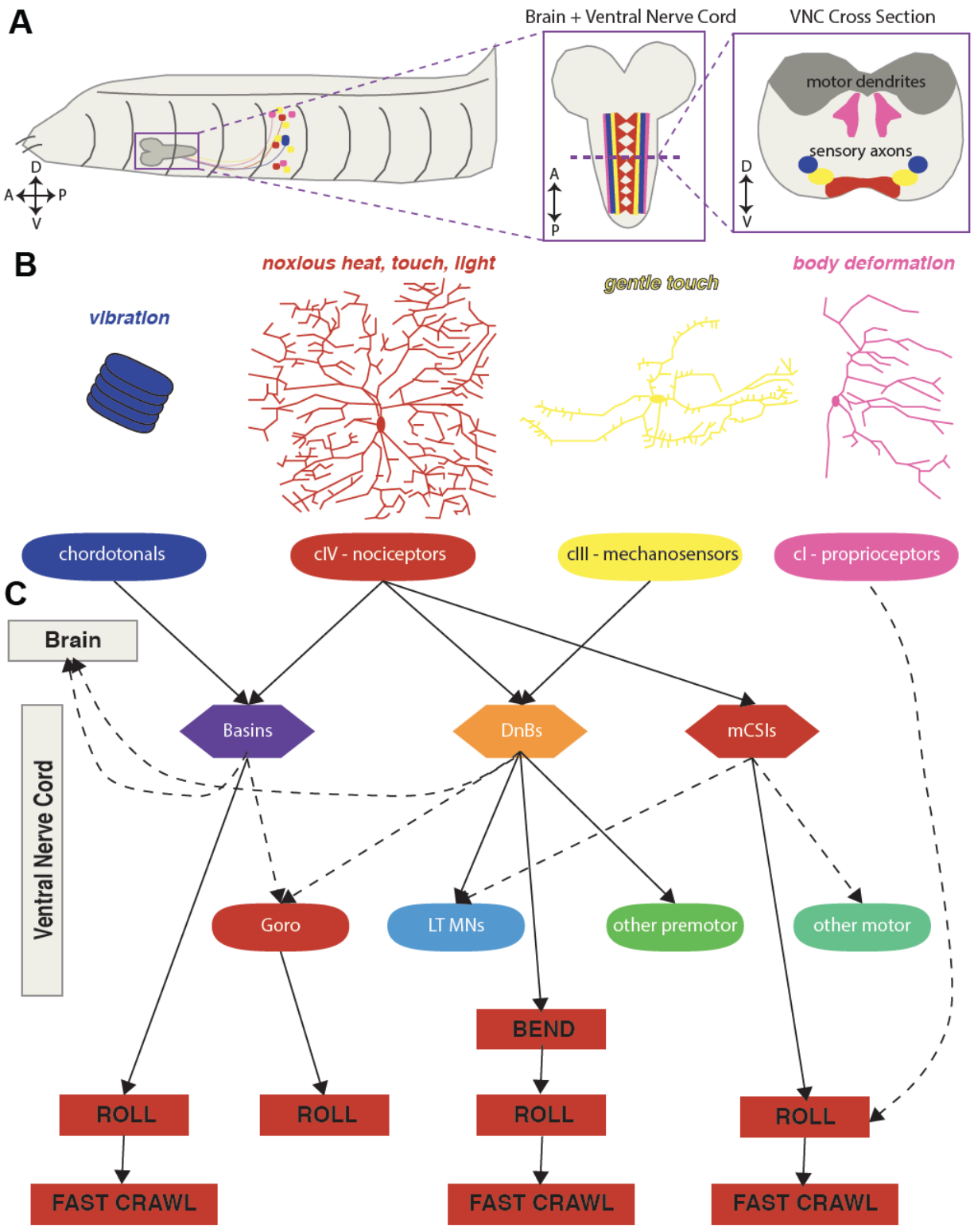


**Figure 1.3: Nociceptive Circuits in *Drosophila* Larvae.** (**A**) *Drosophila* larva body, showing mouth hooks, segments, brain & ventral nerve cord, and sensory neurons in body wall projecting axons to the ventral nerve cord. Sensory neurons have stereotyped soma and dendrite positions in the body wall. They also have distinct axon projection regions in the ventral nerve cord, with

nociceptor axons most ventral and medial, and chordotonal axons most dorsal and lateral. Proprioceptor axons project axons closer to motor neuropil. (**B**) Sensory neuron classes have unique morphologies and functions. (**C**) Nociceptive interneurons, Basins & DnBs, integrate input from multiple sensory classes and promote escape behavior. Goro command neurons are downstream of both Basin and DnB circuits and strongly promote rolling but do not promote fast escape crawling after rolling. mCSIs may act independently of the Goro command circuit to promote the escape sequence.

### Movement & motor circuits in *Drosophila* larvae

Though the motor basis of larval escape has not been studied, larval muscles and motor circuits, alongside their roles in body coordination during crawling, have been extensively characterized. Each hemisegment of the body wall contains thirty muscles, varying in shape, size, and orientation[98]. Six distinct spatially oriented groups of muscles have been identified—dorsal and ventral longitudinal muscles, dorsal and ventral oblique muscles, ventral acute muscles, and lateral transverse muscles[98,99]. Longitudinal muscles run along the anteroposterior axis of the larva, while transverse muscles span dorsoventrally, and oblique and acute muscles demonstrate intermediate angles of orientation[98–100]. Like vertebrate muscles, larval body wall muscles are composed of actin and myosin filaments[101]. In the presence of calcium and ATP, myosin heads form cross-bridges along the actin filaments, resulting in contraction and force generation[101]. Larval body wall muscles are simpler than vertebrate muscles in many ways. For example, body wall muscles are single muscle fibers which attach indirectly to the larval cuticle[101]. This general architecture is unlike vertebrate muscles, which contain multiple, independently activatable fibers. Further, body wall muscles are isopotential, meaning that their lengths are less than two times the time constant. This means that any electric potential in the muscle is the same at all points in the muscle, simpler than vertebrate muscles[101]. Body wall muscles are also supercontractile. Their z-discs in each sarcomere are perforated, allowing them to contract to less than 50% of their resting length[101]. Because of this supercontractile capability, body wall muscles exhibit a different force-length relationship than that seen in vertebrate muscles. Body wall muscles continue generating greater force at minimum length[101]; whereas vertebrate muscles reduce force generation at maximum contraction. Finally, larval body wall muscles do

not fire action potentials—rather, depending on the amount of glutamate released by presynaptic motor neurons, these muscles exhibit graded potentials of extracellular and intracellular calcium[101]. Muscle activity onset precedes muscle shortening during behavior, and each of the above-mentioned features make the activities within muscles and the forces they generate easily quantifiable by observing calcium indicators expressed directly in the muscles[58,102,103].

Four types of motor neurons (MNs) innervate the body wall muscles[99,100]. Type I motor neurons are excitatory, glutamatergic, and have two different projection patterns: type Ib MNs innervate unique muscles or pairs of muscles with large boutons, while type Is MNs innervate large groups of muscles with small boutons[100–102]. One type Is MN innervates most dorsal muscles, one innervates most ventral muscles, and one innervates lateral muscles[100,102]. Though type Ib and type Is MNs demonstrate highly correlated peak activities, type Ib MNs show greater firing rates and longer firing duration during muscle contraction than type Is MNs during crawling[102]. Type Is MNs are higher threshold than type Ib MNs and have therefore been proposed to be recruited for increased force generation during high-power movements[100,104]. This is analogous to tonic versus phasic motor relationships across taxa. Mammalian motor units are recruited according to Henneman's Size Principle, where smaller motor units are recruited early and demonstrate tonic activity to generate more constant, lower-level muscle force; meanwhile, larger motor units demonstrate phasic activity and are recruited later in movement to further increase force output. This principle of easily recruited, tonic, low-force motor units and muscles versus higher threshold, phasic, high-force motor units and muscles has been observed across systems and behaviors, including in adult *Drosophila* walking and flight, respectively[105,106], and even in crayfish escape circuitry[107]. Evidence for the functional role of type Is MNs in larval behavior is lacking[100,102]. The other two types of MNs are thought to play modulatory roles in locomotion: type II MNs show broad innervation of nearly the entire hemisegment and release the neuromodulator octopamine, while type III MNs innervate muscles near the midline in segments 2-5 only and release insulin-like peptide[100]. The exact roles of these modulatory MNs in locomotion remain unknown.

Just as spatial organization of circuits in the vertebrate spinal cord can aide in dictating ordered recruitment of muscles[41,108], and just as larval somatosensory neurons demonstrate functional segregation in the ventral nerve cord[93], MNs develop precise dendritic patterns in the adult and larval *Drosophila* ventral nerve cords to form myotopic maps[99,109–112]. Specifically, in the larva, MNs that innervate lateral muscles tend to have the most lateral dendritic fields in the dorsal neuropil, MNs that innervate ventral muscles tend to have the most medial dendritic fields, and MNs that innervate dorsal muscles tend to have intermediate mediolateral dendritic field placement[58,111,112]. Because a given MN's location impacts which premotor neurons it receives input from, myotopic maps have strong functional implications for organizing motor drive and thus generating behavior. For example, when the development of precise dendritic field localization of MNs in *Drosophila* adults is genetically perturbed, coordinated walking behavior is disrupted[110], likely based on the alteration of which premotor neurons (PMNs) are driving these leg MNs. In the larva, each MN receives input from an average of 32.5 PMNs out of roughly 236 segmentally repeated PMNs (~118 segmentally repeated pairs), and each PMN projects to an average of eight MNs[58]. Some PMNs show selective innervation of MNs that belong to a single coactive muscle group, or muscle module, identified in forward or backward crawling, but others show mixed selectivity relative to MN recruitment order during this behavior[58]. MNs innervating specific coactive muscle groups responsible for forward and backward crawling have postsynapses that are not fully spatially segregated[58], leaving open the possibility that MN dendrite organization is conducive to muscle modules of other behaviors.

Larval crawling, and the premotor and motor circuits that coordinate it, have been heavily characterized[100]. Forward and backward crawling are composed of sequential shortening, lifting, and elongation of segments from tail to head or head to tail, respectively. This form of locomotion relies on three fundamental components of muscle coordination: 1) muscles within a segment must fire sequentially to allow independent segmental compression, lifting, and elongation phases; 2) muscles across segments must coordinate to allow propagation along the larva's length for body translation; 3) muscles on the left and right sides must co-contract with similar timing and amplitude to permit a straight trajectory. Specific neural circuits have already been linked to each of these fundamental tenets. Intrasegmental coordination

involves a phase delay between morphologically and functionally opposed muscles. The mechanism for this phase delay has more than one mechanistic basis[100]: 1) MNs that drive these muscles demonstrate some non-overlapping excitatory PMN drive[53]; and 2) an inhibitory PMN within the segment inhibits MNs that share excitatory drive but drive muscles that must fire later than their intrasegmental counterparts during crawling[53]. Intersegmental coordination involves propagation of muscle contractions along the segments of the larva, and is coordinated by 1) feedforward inhibition, where an excitatory PMN, A27h, in one segment excites specific MNs, while also exciting an inhibitory PMN that inhibits the next anterior segment's A27h neuron, preventing premature contraction of the same MNs in neighboring segments[52]; and 2a) feedback inhibition, where MNs in more posterior segments are actively inhibited while muscles in more anterior segments are contracting[113], and 2b) feedback inhibition where MNs of early-active muscle groups in the next anterior segment are inhibited while late-active MNs groups in the adjacent posterior segment are excited by a feedback neuron in the anterior segment[57]. Left-right symmetric amplitude of contractions during crawling are regulated by segmentally repeated interneurons that receive direct proprioceptive input from one side of the larva and output to contralateral MNs[51]. Other neurons have been identified as controlling specific higher-level aspects of locomotion. For example, crawling speed is partially regulated by a few anterior inhibitory neurons in the ventral nerve cord[114,115]. Action selection between forward and backward crawling has been partially attributed to a pair of descending neurons[55]. These features show some similarity to descending control of action selection in vertebrates.

The muscle activity patterns that drive forward versus backward crawling differ, where specific lateral muscles contract earlier in forward crawling, and specific dorsal and ventral muscles, especially the ventral obliques, contract earlier in backward crawling[100]. A connectome-based artificial neural network (ANN) that recapitulates forward and backward crawling has made predictions about the crawl-type specific firing patterns of PMNs, many of which show distinct activity patterns during these two modes of locomotion[58]. One PMN, A27h—shown to contribute to intersegmental coordination and selectively innervate some of the muscles differentially active in forward and backward crawling—has been shown experimentally to be active during forward crawling, but not backward crawling[52,58]. Another PMN, A18b

is active only during backward crawling[55]. Akin to multifunctional premotor neurons in the leech[5], many of these PMNs are likely relevant not only to forward and backward crawling, but also to escape behaviors. For example, when the inhibitory PMNs involved in limiting firing duration of select ventrally-projecting MNs during crawling [114] are silenced, roll number is reduced[56], but further investigation is needed. The rich knowledge of local premotor circuit mechanisms for regulating exploratory locomotion serves as an excellent foundation for characterizing motor circuit mechanisms in a broad behavioral repertoire.

**Sensory feedback in *Drosophila* larval behavior**

Animals receive sensory feedback about their own movements to help coordinate ongoing and shape future movements. Characterization of proprioceptor function during a variety of behaviors in *Drosophila* larvae is ongoing. Segmentally repeated subclasses of proprioceptors respond differently to muscle contraction, relaxation, and stretch in each segment of the body wall[92]. Because of this subtype response specificity, during forward crawling, the activities of each segment's proprioceptors collectively tile the segment's entire duration of movement[92]. Loss of sensory feedback through temperature-dependent short-term silencing of proprioceptors causes larvae to perform slower, uncoordinated crawling with more intense segmental contraction, where larvae are unable to keep upright[91]. Similarly, in fictive crawling preparations where larvae are partially dissected and lack sensory feedback, motor neurons still fire in a segmentally repeated sequence, but do so roughly ten times slower than in intact larvae[116]. These findings propose that proprioceptive feedback during larval crawling serves as a "mission accomplished" signal for segmental contraction, allowing faster propagation of the motor sequence[91,92,116]. During body bending, the escape module that occurs prior to and throughout rolling, dorsal proprioceptors along the bent segments of the larva are activated by segment contraction[92]. Silencing proprioceptors while inducing nociception reduces roll probability and roll speed[71,78]. Together, these data suggest that sensory feedback during rolling could contribute to initiation and propagation of the escape motor sequence, but further study of how sensory feedback impacts escape sequence transitions and kinematics is required.

**Towards linking sensation & movement via larval escape**

Altogether, the preceding work on *Drosophila* larval nociceptive circuits and larval exploratory locomotion make this model an ideal testbed for studying escape behavior. In this thesis, we target three of Tinbergen's hierarchical levels of behavior by asking: 1) how is the whole body coordinated during escape movement?; 2) how do muscles drive this coordinated movement?; and, 3) what neural circuit structures could coordinate these muscle activities? We uncover the kinematics, muscle activities, and neural circuit features that comprise escape, providing direct insight into how a compact and relatively simple nervous system can produce a rich behavioral repertoire in response to its environment. This work moves the understanding of larval escape from sensory circuits and general motion descriptions to precise observations of how larvae execute escape, laying the foundation for understanding the elusive neural mechanisms that link sensation and movement.

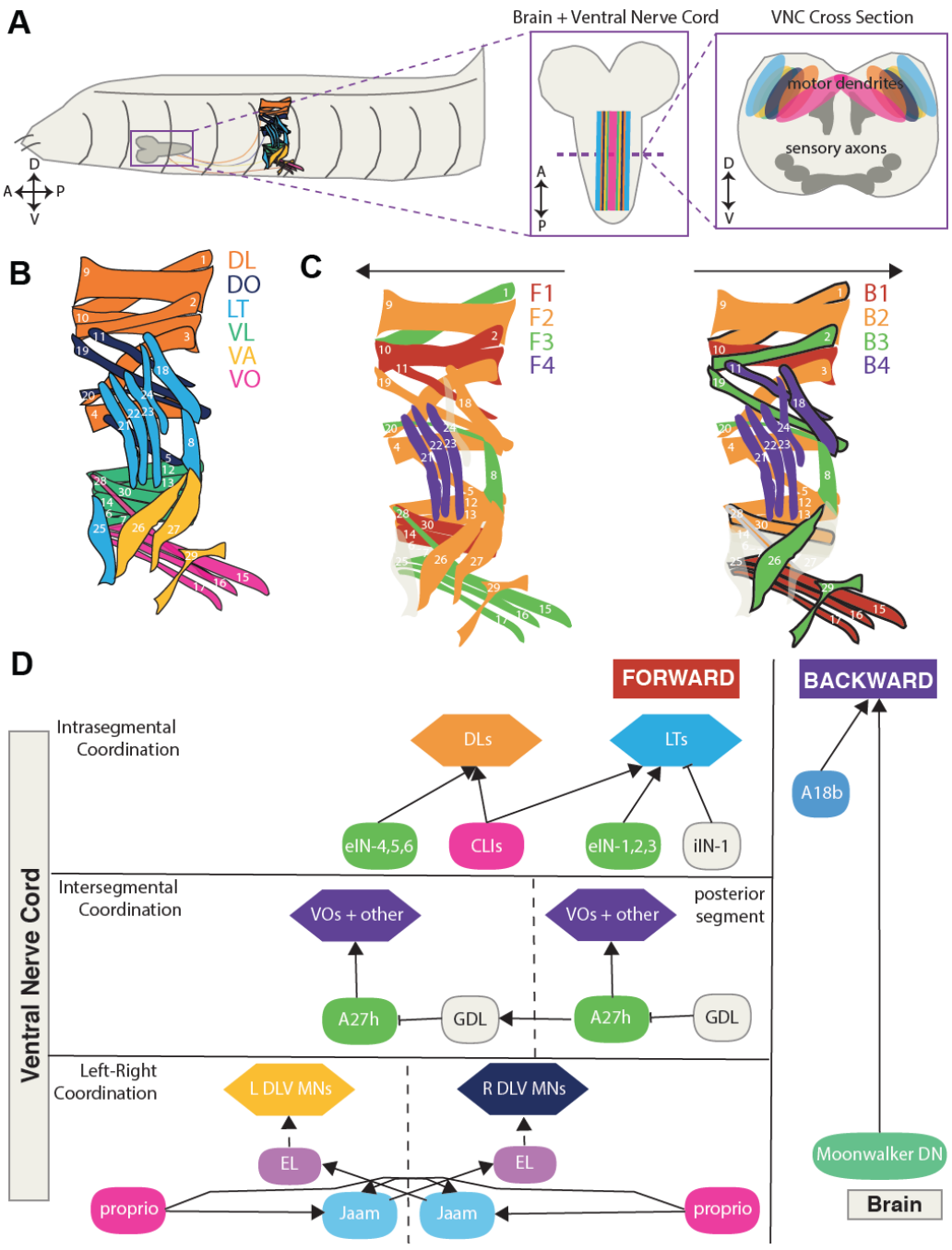


**Figure 1.4: Motor Circuits & Locomotion in *Drosophila* Larvae**. (**A**) *Drosophila* larva body, showing mouth hooks, segments, brain & ventral nerve cord, and muscles in body wall receiving input from motor neuron axons from the ventral nerve cord. Muscles have stereotyped locations, orientations, and shapes in each hemisegment. Most muscles receive 1:1 type Ib motor neuron innervation. The motor neuron somata and dendrites occupy largely overlapping regions in the dorsal neuropil of the ventral nerve cord, though the motor neurons that project to ventral oblique muscles occupy more medial territories and motor neurons that project to lateral transverse muscles occupy more lateral territories. (**B**) Single hemisegment of muscles, numbered and color-coded

by muscle groups: dorsal longitudinal (DL), dorsal oblique (DO), lateral transverse (LT), ventral longitudinal (VL), ventral acute (VA), and ventral oblique (VO). (**C**) Muscles color-coded by coactive muscle group or synergy activity timing during forward crawling (F1-F4) and backward crawling (B1-B4). Muscles that fall into a different coactive muscle group for backward compared to forward crawling have thick black boundaries. (**D**) Example motor circuit components driving four fundamental components of larval locomotion: intrasegmental coordination, intersegmental coordination, left-right coordination, and direction of movement.

# Chapter 2: The Kinematics of Escape[ϕ]

## 2.1 Introduction

Kinematics—the measurement of movement features independent of the forces that generate them—is the product of neuromuscular control and body-environment interactions. Characterizing kinematics has helped scientists to make predictions about and contextualize neural control of movement, revealing finer principles of control than those defined when collapsing complex behaviors into general heuristics. For example, by comprehensively tracking joint angles during walking in mice, unbiased classification techniques can identify mice that are healthy versus mice that are suffering from a spinal cord injury, highlighting that simple kinematic measurements can reveal circuit differences that impact behavior[117]. Further, other kinematics findings have revealed insights into specific circuit mechanisms of motor control. For instance, seeking to disambiguate the roles of distinct motor regions of the brain, Kawai *et al.* lesioned motor cortex before or after rats learned a lever-pressing task[118]. Interestingly, each rat developed its own kinematic strategy for waiting the exact amount of time necessary between receiving a cue and pressing the lever, as measured through joint tracking. After these trained rats underwent motor cortex lesion, each rat returned to performing its exact kinematic sequence for lever-pressing without issue. However, if untrained rats underwent motor cortex lesion prior to learning the lever-pressing task, they could not learn to perform it[118]. Therefore, evaluating detailed kinematics during behavior can reveal principles of how the brain performs motor control tasks. Kinematic features have also been closely linked to muscle firing and descending control in *Drosophila* flight.

[ϕ] I am thankful to my collaborators for their valuable contributions to this work. Grace Shin provided technical and conceptual guidance on behavior experiments. Rick Hormigo and Tanya Tabachnik provided training, guidance, and conceptual input for altering behavioral assays. Wes Grueber and Aref Zarin guided project conceptualization. Aref and Wes provided input on data analysis and the main text. This work comprises part of a manuscript in preparation.

Alterations in pitch during flight are controlled by the spiking of specific muscles that impact wing stroke amplitude[119]. Further, flies regulate their wingbeat amplitude asymmetrically to accommodate for wing damage and still fly straight. Neural manipulations performed in parallel with kinematic measurements revealed that wingbeat amplitude variation is controlled by 15 different pairs of descending neurons[11], a key finding in understanding the neural mechanisms of motor control. These studies, alongside numerous efforts to improve body part tracking for deeper interpretation of neural data relative to behavior[2,117,120], highlight the importance of being able to compare exact body movements to features of neural activity. Without recognizing subtle differences in body motion, it is impossible to successfully subdivide motor behaviors into respective motion modules, and thus to deeply understand the neuromuscular mechanisms of motor control.

Not only does the investigation of kinematics reveal aspects of low-level sensorimotor control of movement—kinematic observations can yield insight into fundamentally distinct behavioral decisions that operate via specific neural circuits. Specifically, in escape behaviors, the quantification of fine kinematics has proven to distinguish which neural circuits employ different escape strategies. For example, measuring center of mass position after postural adjustments but prior to escape reveals that flies integrate body position with approaching threat stimulus to determine escape jump direction[30]. This kinematic result highlights rapid decision-making driven by specific neuromuscular control processes. In another example, slight kinematic differences can reveal the use of completely different motor circuits in distinct behavioral contexts altogether. For example, in fish, feeding strikes, air breathing, and social interactions demonstrate similar general body movements to escape C-bends[121]. However, measurements of finer-level kinematics, including latency to bend and body angle, allow distinction between escape circuit-driven bending

versus bending driven by other sensorimotor circuits[121]. Altogether, these works demonstrate the utility of observing kinematic features in revealing aspects of the neural circuits that drive behavior.

Here, I measure the kinematic components of escape, finding fundamental similarities and differences across distinct escape induction methods. Escape bending and rolling consists of four patterns, dependent on the combination of bend direction and rotation direction. Larvae change their escape locomotor patterns mid-roll, though the frequency of switches varies based on method of escape induction and stimulus intensity. Sensory induction of escape results in greater variability in the motor program compared to command neuron activation at any intensity level, highlighting the likely role of parallel circuitry in driving flexible, context-dependent escape sequences. Unlike alternative models of bending and rolling, and unlike larval crawling, segmental rotation occurs synchronously along the entire larva, suggesting a non-peristaltic neuromuscular control mechanism. Bending occurs throughout escape rolling with the larva's numerous and diverse ventral musculature bending most strongly during rolling, potentially providing the driving force of this behavior. Body-substrate interactions might aide in propelling the larva during escape rolling. These findings reveal the fundamental motor components that likely drive escape and yield insight into how parallel circuits provide motor flexibility in this behavior.

## 2.2 Methods

*Fly Stocks:*

| **Reagent type (species) or resource** | **Designation** | **Source or reference** | **Identifiers** | **Additional information** |
|---|---|---|---|---|
| Genetic reagent (*Drosophila melanogaster*) | w1118 | | | Global heat + vibration assay line; global heat, body-substrate interactions |
| Genetic reagent (*Drosophila melanogaster*) | 38A10-LexA | BDSC | 54106 | cIV driver for thermogenetics and body-substrate experiments |
| Genetic reagent (*Drosophila melanogaster*) | LexAop-TrpA | Grueber lab | | Thermogenetic activator and body-substrate experiments |
| Genetic reagent (*Drosophila melanogaster*) | ppk1.9-Gal4 | Ainsley *et al.*, 2003 | | cIV driver for optogenetic experiments |
| Genetic reagent (*Drosophila melanogaster*) | 20xUAS-Chrimson | | | Optogenetic activator for cIV activations |
| Genetic reagent (*Drosophila melanogaster*) | R69F06-Gal4 | BDSC | # 39497 | Goro line |
| Genetic reagent (*Drosophila melanogaster*) | 44H10-LexA, Aop-GCaMP6f; Aop-mcherry | Aref Zarin | | Epiflourescent muscle imaging and optogenetics line |

| Reagent type (species) or resource | Designation | Source or reference | Identifiers | Additional information |
|---|---|---|---|---|
| Genetic reagent (*Drosophila melanogaster*) | 44H10-LexA, Aop-GCaMP6f; Aop-mcherry, UAS-Chrimson-mcherry | Aref Zarin | | Optogenetics line |

*Behavior Experiments:*

For behavior experiments, flies were reared at 25˚C and tested as third instar larvae. For each experiment, at least two sessions, performed on separate days, were performed for each genotype. Larvae were only tested once.

Behavior experiments, except for body-substrate interaction experiments, were conducted using FIM (Frustrated total internal reflection Imaging Method)[122]. Videos were acquired at 50 frames per second with a Basler ACE acA2040-90uc four megapixel near infrared sensitivity enhanced camera equipped with CMOSIS CMV4000 CMOS sensor. Camera was equipped with LM16HC-SW lens (Kowa), and BN880-35.5 filter (Visionlighttech). IR diodes (875 nm, Conrad) were used for FTIR imaging and images were acquired using Pylon camera software (Basler). Animals were placed on 0.8% agar surface ~2 mm thick (Molecular grade, Fisher Scientific).

For the global heat only, thermogenetic cIV activation, and global heat & vibration assays, we developed a novel implementation of FIM, where the agar surface was uniformly heated and temperature was read out using a Elitech STC-1000 and two 10 kOhm temperature probes. These probes measured temperature in the FIM table chamber, which was heated by four LUBAN Mini Hot Air Guns, and the agar substrate itself. For global heat and global heat & vibration experiments, the gel was heated to 42 degrees Celsius. For thermogenetic cIV activation experiments, the gel was heated to 34 degrees Celsius. Third instar $w^{1118}$ larvae were rinsed and transferred to a petri dish with 0.8% agar at least 10 minutes prior to

experimentation. Then, larvae were gently transferred with a paintbrush to the agar imaging surface. For global heat & vibration experiments, vibration was generated using Logitech Multimedia Speakers Z200 with Stereo Sound for Multiple Devices. The composite 1000Hz and wasp sound, played at 100dB, was previously published[72].

For optogenetic experiments, larvae were raised on molasses food with 1 mM all-*trans*-retinal (ATR). Larval care prior to experimentation was the same as in the assays described above. Two rings of Blue (470 nm) LED lights (WFLS-G30 × 3 WHT, SuperBright LEDs) of 5 inches and 8 inches diameter were placed approximately 5 inches underneath the FIM table. LED brightness was programmed for experiments using custom code in ARDUINO, as the LEDs' pulse width modulation was controlled by an ARDUINO Mega 2560 board. For 100% Goro activation experiments, blue LEDs were active at 2230 uW/mm$^2$. For 50%, 1090 uW/mm$^2$; for 15%, 160 uW/mm$^2$; for 2%, 40 uW/mm$^2$. An additional tracker IR LED (TSHA4401, Vishay Semiconductor Opto Division 875 nm) was mounted within the camera field of view to allow exact knowledge of when colored LEDs were on.

Larvae that failed to move at all during trials were excluded from any analysis. Bend and roll probabilities, number of rolls, roll latency, and bend and roll direction changes were quantified manually by evaluating TIFF stacks in FIJI (https://imagej.net/Fiji).

*Widefield Imaging:*

For widefield videos of mCherry in muscles during rolling, late first and early second instars were raised on grape juice agar with yeast. A thin 5% agar arena was generated on glass slides by compressing agar between slides spaced by two pieces of lab tape. The arenas were cut to be approximately 2x larval width and 1.5x larval length using a micro-knife (Fine Science Tools). Arenas were filled with a 50% glycerol-50% distilled water solution to slow down the rolling speed, covered with a coverslip (Fisherfinest Premium Cover Glass #1), and larvae were imaged immediately after mounting.

Larvae were imaged with a Zeiss Axio Imager A1 with a 10x EC PLAN-NEOFLUAR objective and XCite Fluorescence Lamp for muscle fluorescence acquisition. Videos were acquired at 50 frames per

second using a Basler ACE four megapixel near infrared sensitivity enhanced camera equipped with CMOSIS CMV4000 CMOS sensor. Rolling was induced in larvae of *44H10-LexA, Aop-GCaMP6f; Aop-mCherry* by placing a soldering iron (WESD51, Weller) set to 250 degrees Celsius on the glass slide near the larval arena until larvae rolled (**Figure 2.1**).

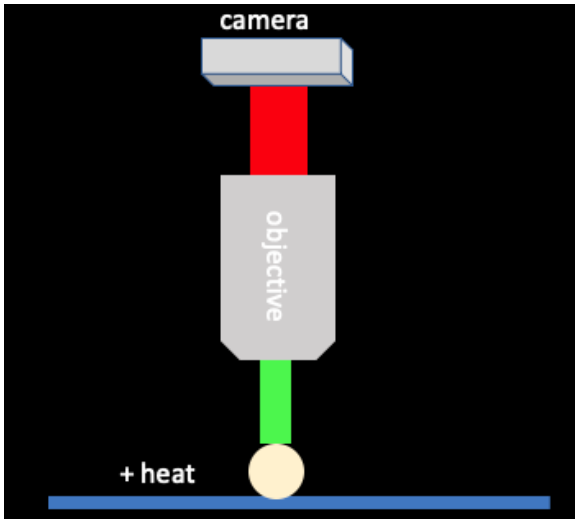


**Figure 2.1: Widefield imaging approach for observing muscle movement during escape.** Imaging setup for imaging muscles labeled with mCherry during heat-evoked rolling behavior.

*Curvature Analysis:*

The curvature analysis was performed as previously published[56]. In short, the boundary of the larva is divided into 300 evenly spaced points. Each point and its neighboring ten points are used to construct the arc of a circle. The curvature index at each point is 1/radius of the circle. To quantify which side of the larva was most bent during roll bouts, a curvature index of 0.05 was selected as a threshold. The number of boundary points greater than or equal to this threshold were counted on manually selected frames of each side passing through the bend, based on trachea, posterior spiracle, and internal organ position. These counts were used to determine relative curvature intensity of all sides of the larva.

Roll bouts for Curvature Analysis were defined as any single instance of 360 degree rolling without the larva's body straightening out or stopping rotation. Up to five rolls were counted per larva, based on the mean roll number per experimental group. The counts of which side was most or least bent and which bend-

roll pattern occurred were normalized by number of rolls per larva. For example, if one larva rolled five times, all five rolls were counted as 0.2 towards respective bend-roll pattern frequencies and max or minimum curvature sides. If one larva rolled two times, each roll was counted as 0.5 towards respective bend-roll pattern frequencies and max or minimum curvature sides.

For curvature-rotational velocity relationships, roll bouts were assessed for maximum number of points over CI threshold and for duration of roll. For curvature-translational velocity relationships, average number of points over CI threshold versus distance larval midpoint traveled was calculated for every 10 frames of behavior.

*Statistical Analyses:*

Initial sample sizes for global heat + vibration and 100% optogenetic Goro activation escape assays were designed to replicate recently published larval escape assay data[87]. Using these initial results, a power analysis was conducted in MATLAB to determine necessary sample sizes for each measured parameter for dose response optogenetic Goro activations ($p = 0.05$, effect size = 0.80). The most conservative estimated sample size, excluding the 'number of roll changes' parameter, was used ($n = 41$), such that all subsequent experimental groups exceeded this value. Sample sizes for comparative sensory activation were based on similar pilot experiments.

Statistical analyses were performed using custom programs written in MATLAB. For behavioral parameter differences across paradigms, Wilcoxon Rank Sum tests were used. Two-sided binomial classification tests were used for binary classifications of most or least bent side frequencies, as well as curvature analysis based on progression of roll sequence. For curvature-speed analysis, linear regression was performed.

Matlab codes for figure generation and statistical analyses are available in the following Github repositories:https://github.com/cooneypc4/larval_escape_manuscript and https://github.com/cooneypc4/thesis_behavcodes_2022.

*Body-Substrate Interactions:*

To observe body-substrate interactions during escape, larvae were placed on a 1% agar pad, tainted with 0.6% black ink for contrast. To induce escape via noxious heat, this agar pad was warmed on a Peltier device set to 42 degrees Celsius, controlled in close loop by FMC tc3265 software. Larval movement was observed and recorded at 5 frames per second using a Leica FireCam and its controller software, connected to a dissection microscope. Light sources were positioned from the side to allow visualization of larvae and tracks they made while crawling and rolling. Before and after images of the black ink substrate were captured for each trial, sometimes involving adjustment of light source angle to better visualize tracks made. Agar pads were changed between larvae to help isolate tracks to specific larval behaviors. After acquisition, behavior videos and images of tracks made were observed and body-to-track measurements were done manually in FIJI. In subsequent body-substrate interaction experiments, larvae were submerged in 3-plate glass wells in 95% ethanol or in a 50% Immersol W-distilled water solution and filmed as described above, or were observed in soft, well-churned molasses food, and illuminated with white light to induce Goro activation.

## 2.3 Results

**Sensory-evoked escape varies based on paradigm & demonstrates motor program flexibility**

Larval escape behavior is comprised of C-shaped bending, lateral rolling, and a transition into rapid forward crawling[56,71,87]. There are multiple methods through which one can induce larval escape behavior. These collectively involve naturalistic sensory stimulation[77,78,80,82,85,88], artificial sensory stimulation[56,78,87], and artificial command neuron stimulation[87]. Activation of only command neurons has demonstrated circuit-based variability in the escape sequence. Namely, command neuron activation generally results in rolling followed by crawling, but the crawling speed following command neuron-induced rolling is lower than crawling in the sensory-induced escape sequence[71]. While the probability of rolling has been measured across these distinct assays, little is known about how variable escape behavior is via different induction

methods. To quantitatively assess how differential circuit activation impacts motor programs, I measured behavior across four different escape-inducing assays.

First, we modified our behavioral assay to improve stimulation precision and readout for post-hoc analyses. This behavior-recording system is based on FIM (Frustrated total internal reflection Imaging Method), an imaging system that permits high-contrast visualization of body movement during larval behavior[122]. A new ARDUINO-based system was designed that allows for finer control over optogenetic LEDs. Using this new code base, users can pre-program brightness, duration, and repetitions of blue, green, red, IR or UV lights to stimulate light-sensitive proteins expressed in the larvae. A tracker IR light that can be independently coded to emit light at certain points in the behavioral trial was also added, allowing precise time-linking of stimulation to behavior (**Figure 2.2A,C**). Seeking body part resolution similar to that observed in subsequent models of FIM[123], the distance from acrylic surface and number of bronze spacers between lens and CMOS chip that provided ideal resolution for visualizing finer body features during rolling behavior was established. This permitted future body-side dependent observations via visualization of internal organs, trachea, posterior spiracles, and mouth hooks of the larva during behavior (**Figure 2.2B**). In total, these modifications made it possible to attain higher quality, more easily quantified images of body movement during behavior.

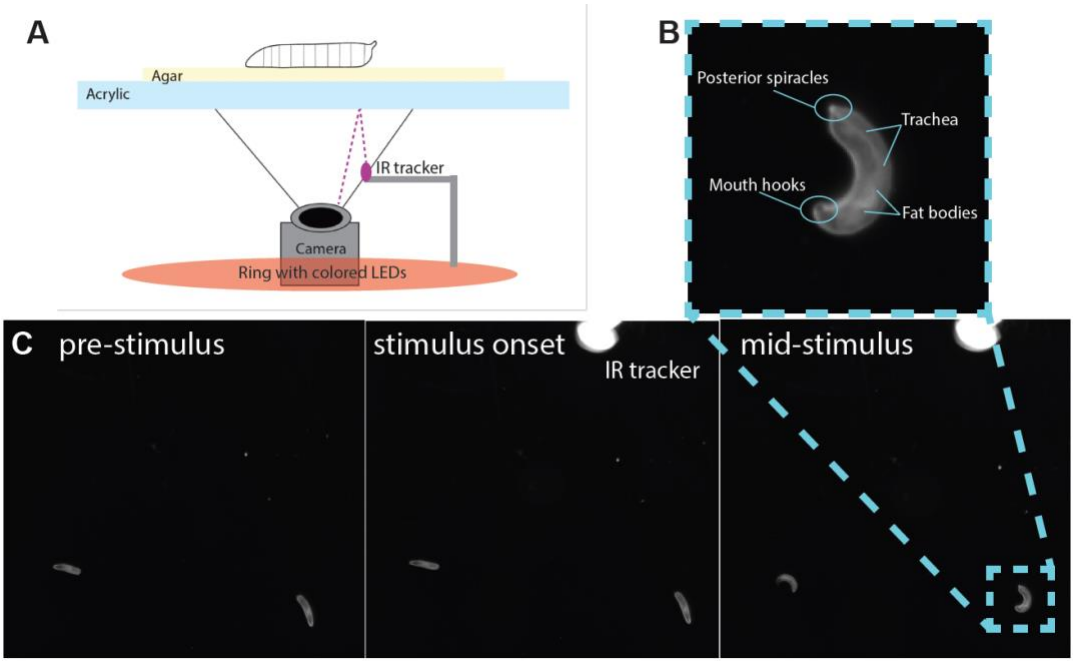


**Figure 2.2: Technical updates to behavioral imaging methods. (A**) Schematic showing FIM setup with camera, colored LEDs for optogenetic stimulation, and new IR tracker light below the acrylic surface where experiments take place. (**B**) Close-up of larva, showing that camera adjustments resulted in high-quality images where specific body parts are easily visualized, while also allowing imaging of multiple larvae at once. (**C**) Raw collected video frame where two larvae expressing optogenetic activator Chrimson in Goro neurons begin bending and rolling shortly after stimulus onset, as indicated by IR tracker.

To observe the kinematics of various sensory-evoked and downstream circuit-evoked escape, and to determine what method most effectively induces escape in the larva, I first evaluated escape using four assays with FIM: 1) global heat—placing the animals onto an agar gel uniformly heated to a noxious temperature, 2) thermogenetic cIV activation—placing the animals onto an agar gel uniformly heated to a sub-noxious temperature that activates dTRPA1 channels, 3) optogenetic cIV activation using Chrimson, and 4) optogenetic Goro activation using Chrimson. Probability of rolling and latency to roll across assays were similar to previous localized noxious heat experiments and optogenetic cIV activations[56,78] (**Figure 2.3A,D**). Heat-based stimulation, whether naturalistically noxious or inducing thermogenetic activation of cIVs, was most effective at inducing rolling, but resulted in the most behavioral variability (*i.e.* latency to roll, bend & roll direction changes; **Figure 2.3**). Optogenetic activation of Goro resulted in high probability

of rolling and number of rolls (**Figure 2.3A,C**), but demonstrated less variability in terms of escape motor program engagement. During sensory-evoked escape, larvae frequently changed bend direction and occasionally changed rotation direction (**Figure 2.3E,F; Figure 2.4**). This suggests that bypassing sensory circuits simplifies selection and maintenance of escape movements.

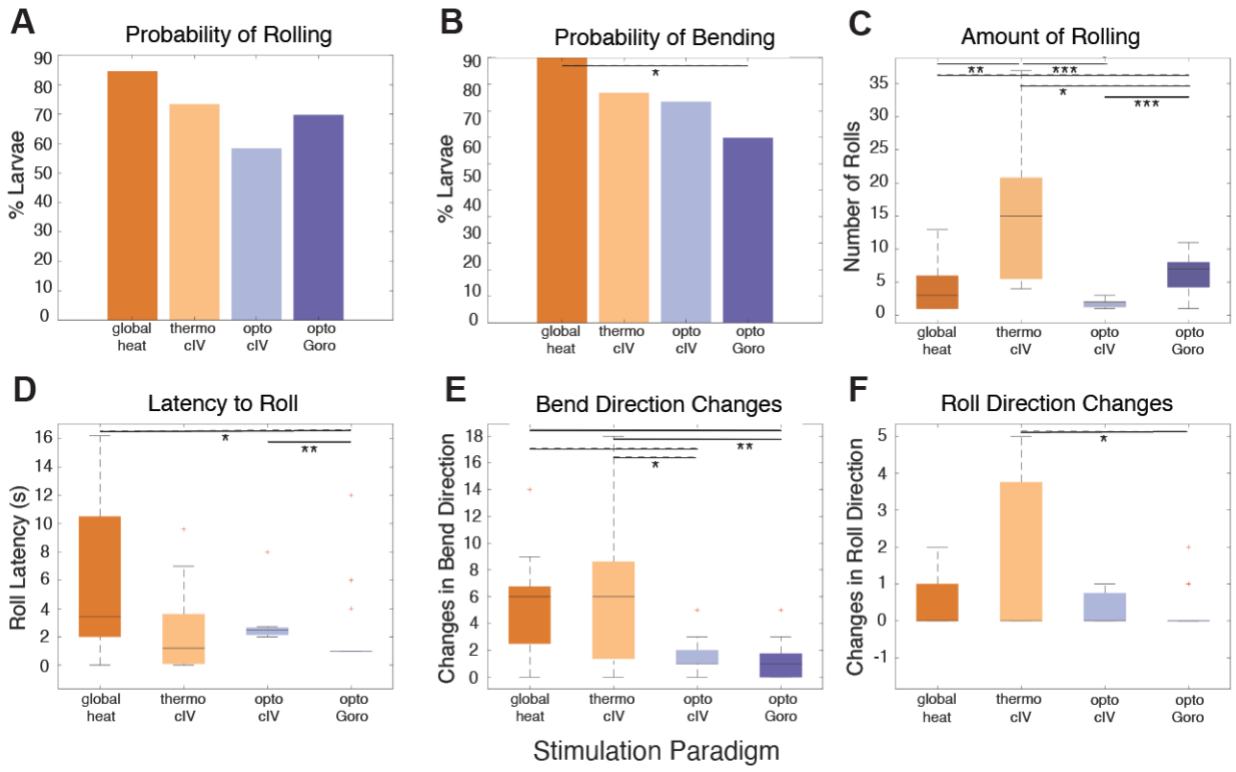


**Figure 2.3: Sensory-evoked escape varies based on method of activation.** (**A**) Percent of larvae that rolled during global heat (n = 13), thermogenetic cIV activation (n = 15), optogenetic cIV activation (n = 12), and optogenetic Goro activation (n = 32). (**B**) Percent of larvae that performed C-shaped bend during above assays. (**C**) Number of rolls performed of all larvae that rolled at least once across 30-second assays. (**D**) Number of seconds prior to roll onset across assays. (**E**) Number of changes in bend side during assays. (**F**) Number of rotation direction changes during assays. P values are indicated as *p<0.05, **p<0.01, ***p<0.001 as determined by Wilcoxon Rank Sum Test.

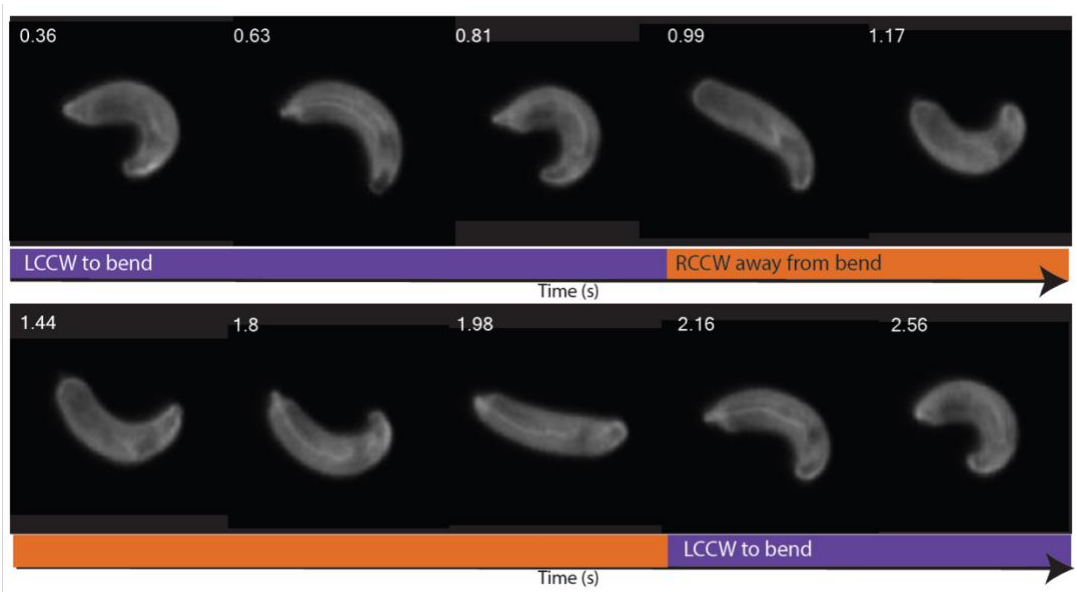


**Figure 2.4: Sensory-evoked escape involves motor program flexibility.** Single escape event during which larva changes escape motor program mid-behavior. Note that the body straightens between changes in bend direction, and that these changes in bend direction can occur irrespective of which side of the body is bent. Time indicated in seconds, top left of each frame.

### Larvae perform four distinct patterns of escape

Larvae bend to the left or right and roll away from the inside of the bend when escaping a focal noxious heat stimulus[78]. Vibration and nociception converge at Goro command neurons in the larval nervous system[87]. A vibration stimulus with frequencies similar to those occurring during wasp attack has been shown to enhance nocifensive rolling[72,87], so this was added to our global heat activation. I sought to observe whether the sensory circuits promoting vibration- and nociception-based escape produce similar escape motor programs as does Goro activation alone, or whether parallel circuits alter escape in response to sensory stimulation. To address this question, I compared behavioral responses between optogenetic activation of Goro neurons and global heat and vibration assay. I first sought to determine whether the entire repertoire of escape patterns is similar to, or different from, those induced by localized heat alone.

Initiation of rolling using heat & vibration or optogenetic Goro activation both induced four qualitatively different patterns of bending and rolling (**Figure 2.5A**). These four patterns of escape can be classified by two metrics: which side of the larva is bent and the direction that the larva rotates. A larva

bent to its left side can either roll (1) clockwise (CW) or (2) counterclockwise (CCW) relative to its posterior end. CW and CCW rolling leads to movement in opposite directions—translation toward the inside of the bend or translation away from the inside of the bend (**Figure 2.5B**). Similarly, animals bent to their right can roll in (3) CW or (4) CCW directions. Thus, rotation direction can be uncoupled from bend direction, and the former determines the direction of movement (**Figure 2.5A**). Larvae can change bend and roll directions during an escape bout. The four motor patterns and the ability to change patterns during escape underscore the flexibility of larval escape behavior.

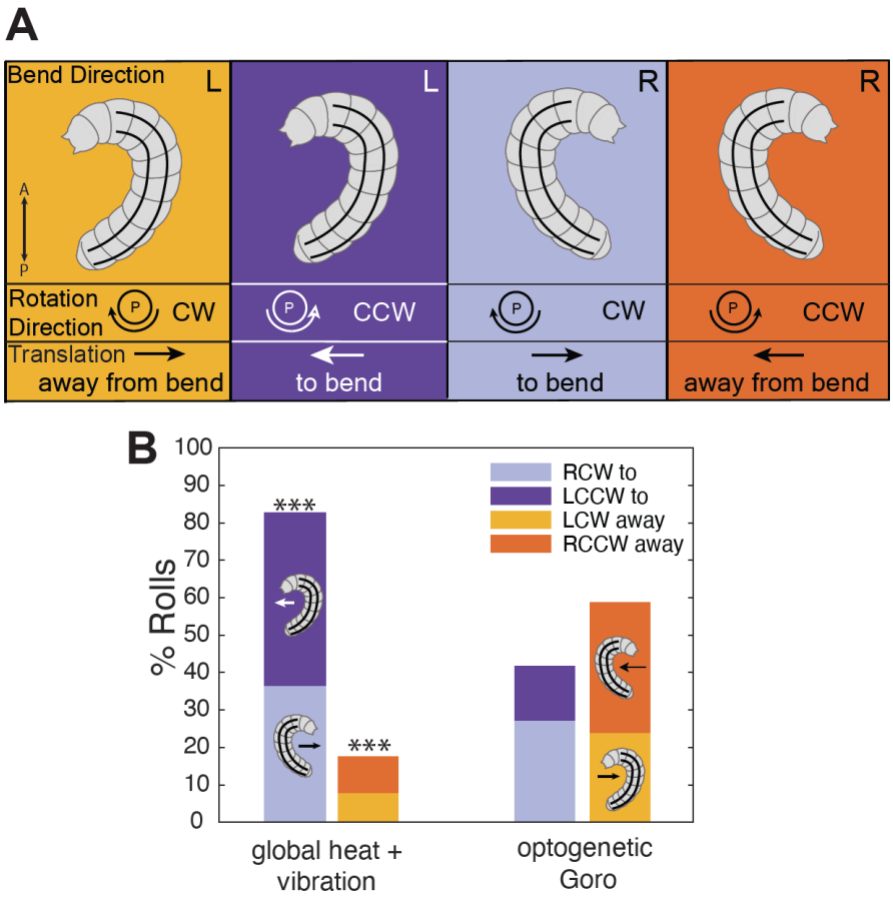


**Figure 2.5: Larvae perform four distinct patterns of escape.** (**A**) Schematic demonstrating bird's-eye view of four patterns of escape. This schematic shows that bend direction (L or R) and rotation direction (CW or CCW, from the perspective of the posterior end of the larva) determine translation direction (to bend or away from bend). Trachea indicate dorsal side of larva. (**B**) Frequency of four patterns when escape is induced via global heat and vibration assay (n = 52 larvae, 157 rolls normalized) or 100% optogenetic Goro activation (n = 93 larvae, 244 rolls normalized). P values are indicated as *p<0.05, **p<0.01, ***p<0.001, as determined by Binomial Test.

To understand if inducing escape through sensory circuits results in distinct motor program selection compared to inducing escape via command neuron activation, I examined how frequently the four patterns of escape locomotion are employed with each assay. The frequency of the escape patterns differed based on stimulus type. Surprisingly, given prior results with a localized heat probe[78], sensory-evoked activation (heat & vibration), was more likely to cause movement toward the inside of the bend, whereas optogenetic Goro activation results in roughly equal movement types (**Figure 2.5B**). The difference in escape pattern frequencies based on stimulus suggests a distinction between multisensory and command neuron-based escape, and between broad activation of nociceptors and dual activation of Goro command neurons. I compared additional metrics of this form of sensory-evoked escape and varying levels of optogenetic Goro activation. Our results indicate that Goro activation induced escape more consistently, more rapidly, and with fewer motor pattern changes mid-escape than the multisensory integration that converges onto Goro neurons (**Figure 2.6**). Further, assessing multiple levels of Goro activation intensity reveals that activation of Goro artificially is consistently distinct from sensory-based activation of the same pathway, again highlighting the potential role of parallel circuits in orchestrating specific features of this behavior.

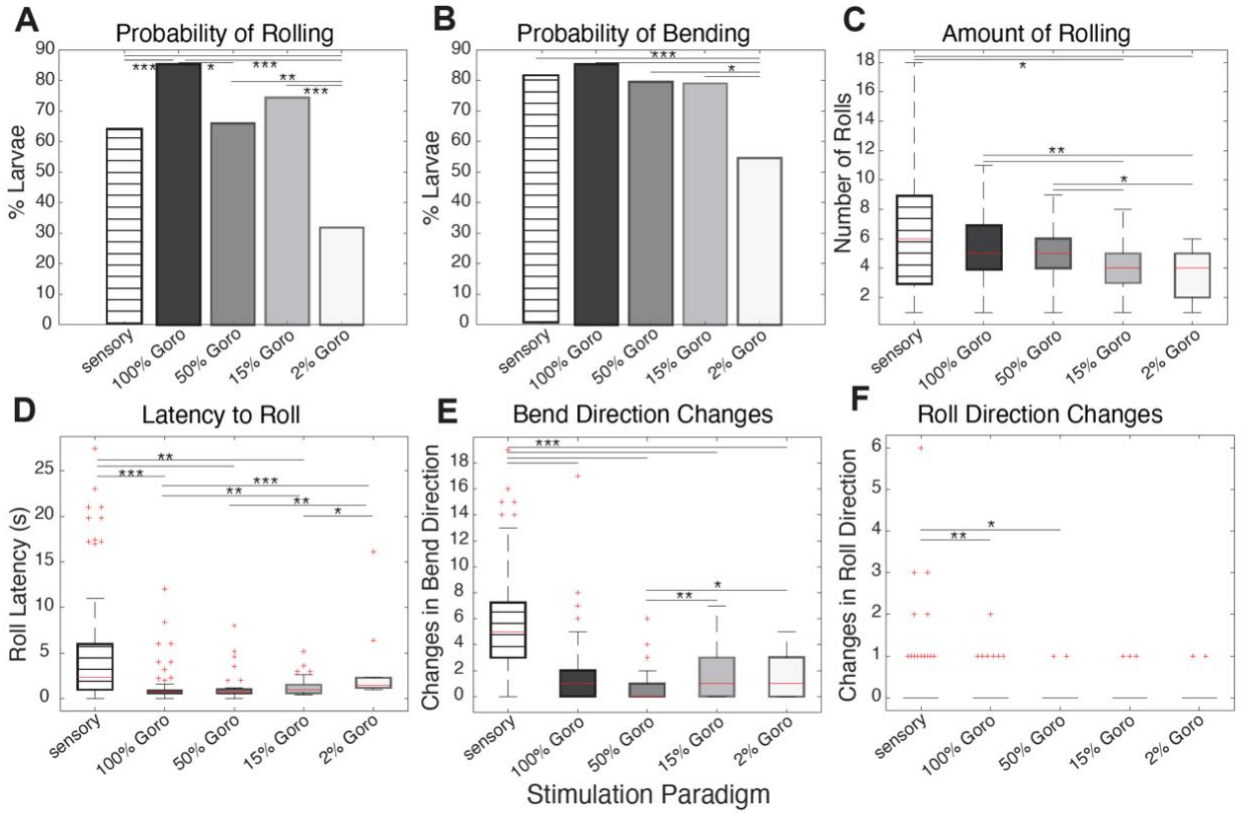


**Figure 2.6: Differences in sensory-evoked vs. different degrees of command neuron-evoked escape behavior.** (**A**) Percent of larvae that rolled during global heat and vibration assay (sensory) (n = 110), 100% brightness optogenetic Goro activation (100% Goro) (n=108), 50% brightness optogenetic Goro activation (50% Goro) (n=44), 15% brightness optogenetic Goro activation (15% Goro) (n=43), and 2% brightness optogenetic Goro activation (2% Goro) (n=44). (**B**) Percent of larvae that performed C-shaped bend during above assays. (**C**) Number of rolls performed of all larvae that rolled at least once across 30-second assays. (**D**) Number of seconds prior to roll onset across assays. (**E**) Number of changes in bend side during assays. (**F**) Number of rotation direction changes during assays. P values are indicated as *p<0.05, **p<0.01, ***p<0.001, as determined by Wilcoxon Rank Sum Test.

## Escape rolling is segmentally synchronous

The muscle motion that underlies larval rolling has not been characterized. To help guide our understanding of this form of locomotion, I compared it with well-characterized larval crawling. Larval crawling consists of segmentally peristaltic, left-right symmetric activation of muscle subgroups[100]. The premotor circuits that control this sequence of muscle activities prevent co-contraction of the same muscles in neighboring segments[52,57,113] and promote symmetric contraction of the same muscles within left and

right sides of the same segment[51]. This drives a propagation of segmental shortenings along the larva as it crawls.

Some robotic and computational simulations of C-shaped bending and lateral rolling in segmented systems invoke an intersegmental delay reminiscent of larval peristaltic crawling[124,125]. Specifically, in both the snake robot and the lamprey, bending and rolling involve a peristaltic progression of lateral followed by dorsoventral movements in neighboring segments—where the anterior neighboring segment moves laterally while the posterior neighboring segment moves dorsoventrally[124,125] (**Figure 2.7**). Because the larva lacks many easily observable external features, initial studies of crawling observed GFP in body wall muscles to track body motion[126]. To test if bending and rolling contains a peristaltic component like that observed in larval crawling or other bend-and-roll systems, and therefore might operate via similar neuromuscular mechanisms, I examined muscle positions during rolling using widefield epifluorescent imaging. I found that the same muscles across different segments appeared in the focal plane at the same time (**Figure 2.8**), suggesting that rolling does not consist of segmental peristalsis. Muscles were clearly shortened in length once they rotated into the bend (**Figure 2.8**), suggesting that muscles on the bent side of the larva are actively contracting.

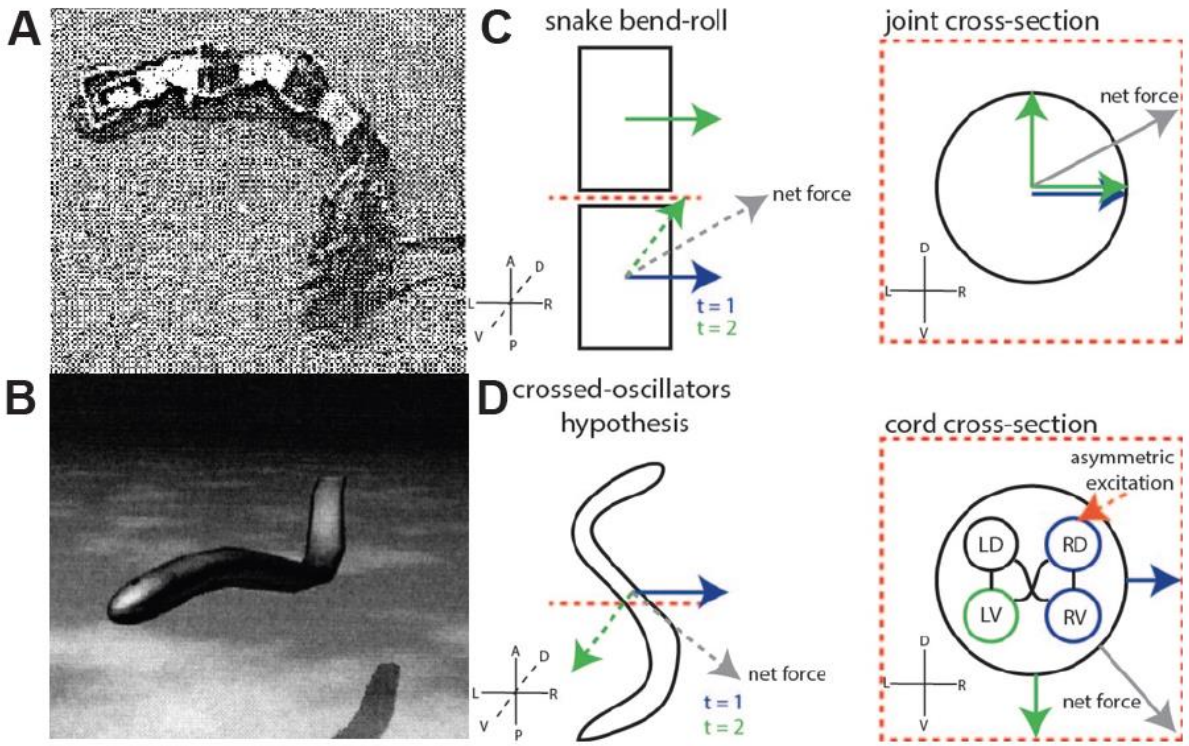


**Figure 2.7: Models of C-bending and rolling in other systems**. (**A**) Segmented snake robot structure from Chen *et al.*, 2004. (**B)** Lamprey simulation from Ekeberg *et al.*, 1999. (**C**) Programmed mechanism for bending and rolling in segmented snake robot. Progression of lateral and sequential dorsoventral segment motions occur in a peristaltic manner to drive bend and rotation. (**D**) Hypothesized neural circuit control scheme for generating bending and rolling in the segmented lamprey. Combined asymmetric lateral excitation to dorsal and ventral populations, followed by contralateral ventral excitation, occurs in a peristaltic manner. In both systems, lateral and dorsoventral forces in neighboring segments generate torque.

This data does not exclude the possibility that some muscle types might drive rotation by being active on the stretched side of the larva. However, these muscle movements led us to hypothesize that the specific muscle contraction sequence that drives escape would consist of a circumferential sequence rather than a segmental sequence, with muscle activity occurring primarily in the bend (**Figure 2.8B**). Under this hypothesis, we predicted that the muscle activity that drives rolling would consist of: 1) asymmetric activity in left and right lateral muscles, farther from the body midline, and 2) symmetric activity in left and right dorsal and ventral muscles, closer to the body midline (**Figure 2.8B**). This pattern of left-right asymmetric, segmentally synchronous muscle activity during rolling would stand in stark contrast to the left-right

symmetric, segmental propagation of muscle activity observed in larval crawling. This, in turn, would indicate that to drive escape behavior, motor circuits must function in a substantially different fashion than they do during forward crawling. In the next chapter, I test this hypothesis using synapse-level examination of motor circuits and high-speed analysis of individual muscle activities.

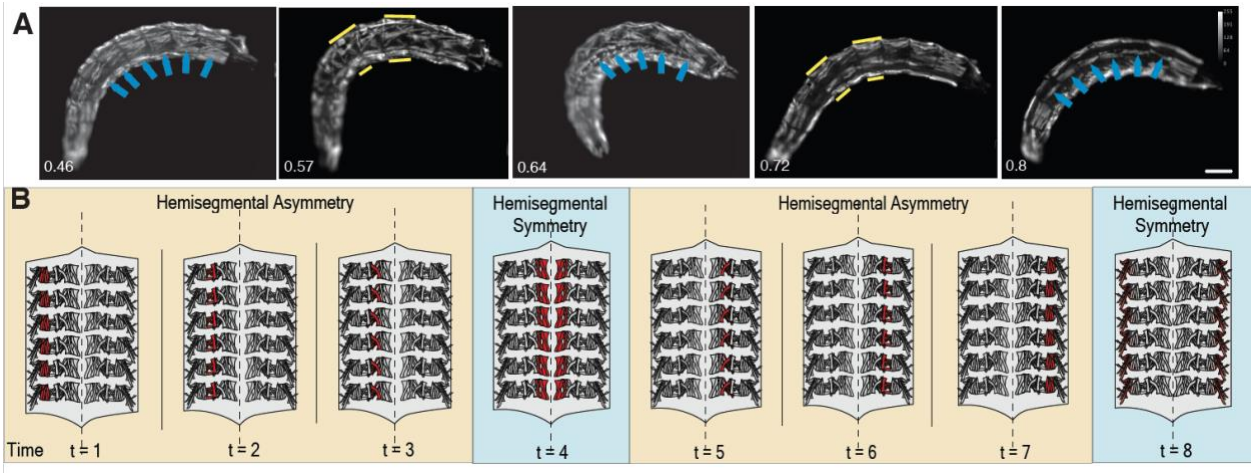


**Figure 2.8: Escape rolling consists of segmentally synchronous rotation.** (**A**) Widefield epifluorescent images of larvae expressing mCherry in muscles (n = 2 larvae). Appearance and position of muscles is synchronous along the entire larva (blue arrows) and muscles shorten within the bend (yellow lines). Scale bar = 100um. Time in seconds, bottom left. (**B**) Hypothesized muscle activity pattern that could generate segmentally synchronous muscle contractions. Coactivity of left and right sides would be exclusive to midline muscles (blue panels), while independent activity of left and right sides would be common in lateral muscles (gold panels).

### Muscle architecture correlates with bending strength

The C-shaped bend is a consistent feature of all patterns of escape rolling. As larvae progress through a roll, each side of the larva (lateral sides, dorsal and ventral) acquire a C-shape in sequence, yet different sides of the larva differ substantially in the number and orientation of muscles. For these reasons, I predicted that amount of bending during a roll bout might show variability and provide clues to the muscle activities that drive escape. Further, ablation of ventral, but not dorsal, muscles disrupts the larva's ability to perform forward crawling[103], suggesting that ventral muscles could be the primary source of force generation during larval locomotor behaviors.

Our data revealed that bending intensity indeed varied during single roll bouts. Specifically, during escape, the ventral side of the larva, with its 14 muscles, was consistently the most bent surface, whereas dorsal and lateral sides were less bent across assays (**Figure 2.9**). Thus, asymmetries in muscle architecture may allow each side of the larva to contribute differential levels of propulsion to escape rolling, as seen in exploratory locomotion[103]. I found the pattern of curvature changes to hold true for sensory-evoked and command neuron-evoked escape (**Figure 2.9C,D**). This suggests that distinct modes of escape activation, that are promoted via parallel circuits[56,86,87], converge to coordinate muscle groups in a similar manner.

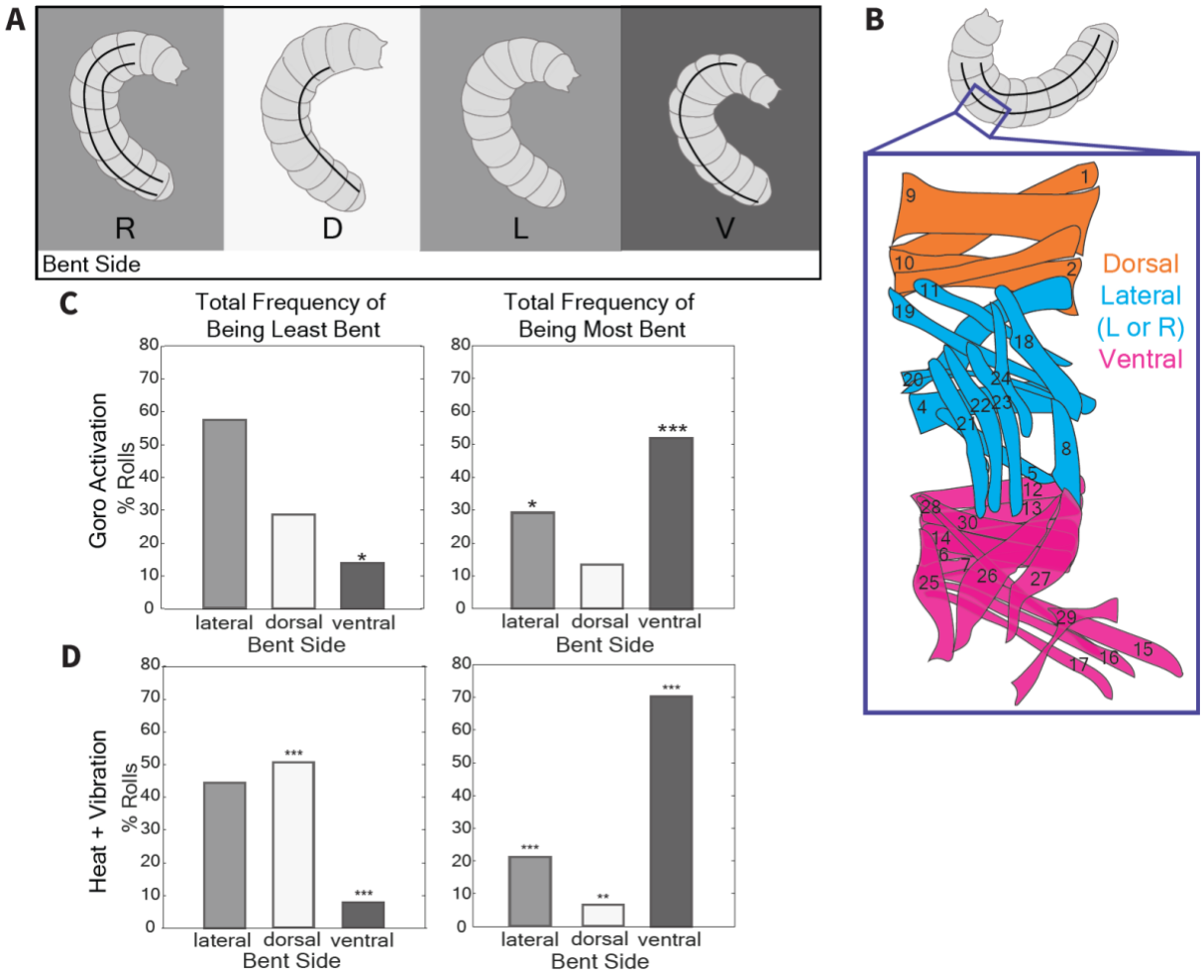


**Figure 2.9: Curvature changes during escape rolling demonstrate relationship between muscle structure and function.** (**A**) Schematic illustrating curvature changes based on which side of the larva's body is bent during a single right clockwise roll (R right → D dorsal → L left → V ventral). Trachea indicate dorsal side of larva. (**B**) Schematic of stereotyped muscles in each larval hemisegment, demonstrating numerical and morphological differences between dorsal and ventral muscle groups. (**C,D**) Bar plots

showing that the ventral side is least frequently the least bent and most frequently the most bent during escape induced via optogenetic activation of Goro neurons (**C**) (n = 93 larvae, 244 rolls normalized) or induced via heat and vibration stimulus (**D**) (n = 52 larva, 157 rolls normalized). P values are indicated as *p<0.05, **p<0.01, ***p<0.001, as determined by Binomial Test.

Because the progression of which side is bent varies based on bend-roll pattern selection and the ventral side emerged as the most prominently bent across behaviors, I hypothesized that the lateral side that is bent immediately prior to ventral bending might aide in increasing larval bend. I sought to test this hypothesis to uncover whether such a mechanism could contribute to force generation during escape. I found that the degree of curvature demonstrated on a lateral side of the larva during rolling is not dependent on escape pattern (data not shown; Binomial Test; p = 0.1537). This suggests that left and right sides contribute roughly equally to bend-roll movements.

**Curvature impacts body propulsion and could be recruited in a recurrent manner during escape**

Silencing Down and Backs (DnBs), nociceptive interneurons responsible for bending during escape, severely reduces degree of bending and decreases total roll number[56]. Though this manipulation leaves rolling behavior intact and does not impact roll latency, it has been previously shown to increase the amount of time that a single roll takes[56]. I first sought to confirm whether degree of bending while rolling contributes to larval rotational velocity during escape rolling (**Figure 2.10A**). I found a weakly positive, not significant correlation between body curvature and rotational velocity (**Figure 2.10B**). However, because of the observed increase in curvature on the ventral side of the larva during rolling (**Figure 2.9**), I predicted that bending on the ventral side could act as a propulsive force in generating escape movement. Therefore, I hypothesized that degree of bending would correlate with translational velocity—how fast the larva moves across the substrate. Preliminary time course data of curvature intensity and translational velocity during continuous rolling supported this hypothesis. Example rolls demonstrated that larvae slow down as they increase body curvature, then immediately following maximal curvature, accelerate (**Figure 2.10D,E**), as though the larva's body acts like a spring: compressing to store up energy, then expanding and

moving rapidly when the compression is released. However, just as maximal body curvature did not correlate with rotational speed, when population data were tested for a relationship between curvature and translational velocity, the relationship was insignificant (**Figure 2.10C**). A potential confound is that the slickness of the agar surface during experiments could vary slightly over time, which could alter rotational and translational speeds independent of body curvature measurements. Alternatively, it is possible that Goro activation fails to induce the full complexity of sensory-evoked escape bending and rolling—just as it fails to induce the fast crawling at the end of the escape sequence[87]—since previous curvature assessments were performed on global heat data.

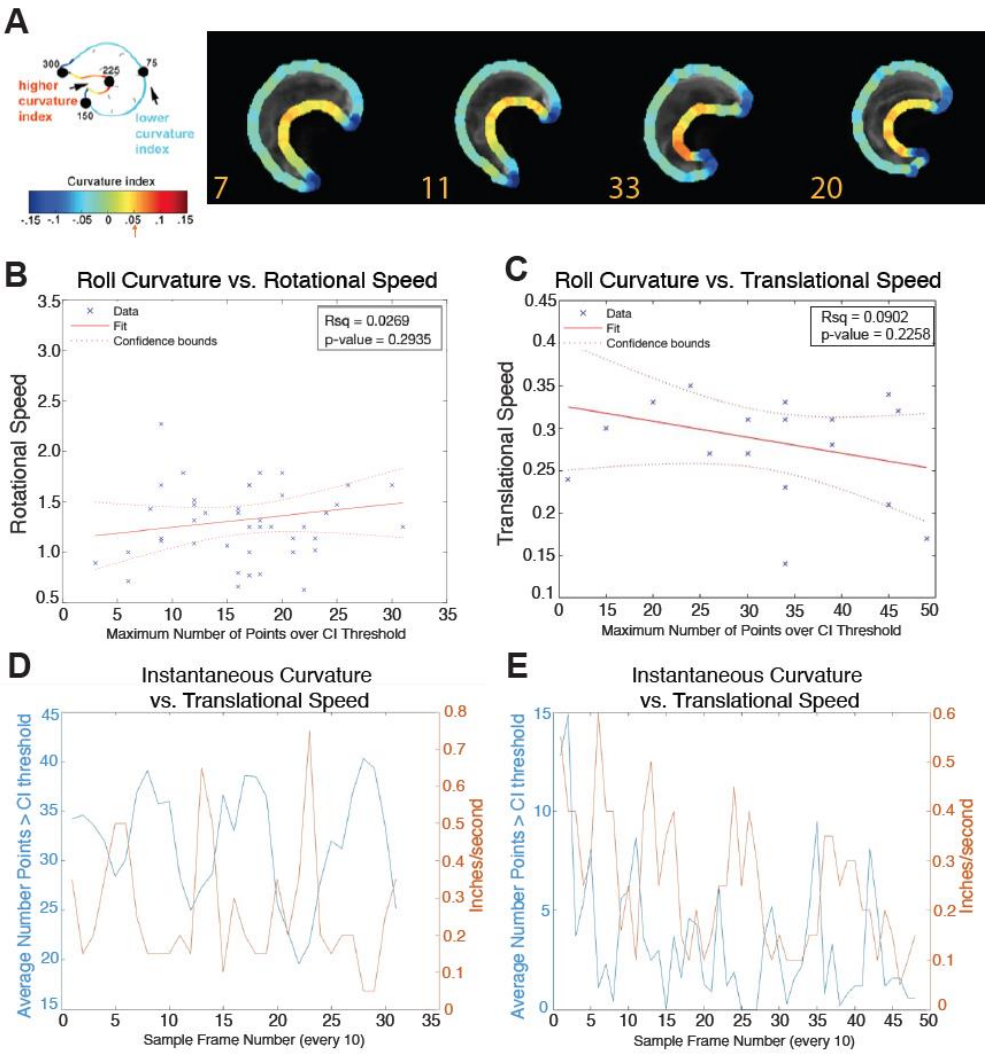


**Figure 2.10: Degree of bending does not impact net rotational or translation velocity during command neuron-evoked escape rolling.** (**A**) Schematic from Burgos *et al.*, 2018, and stills of curvature index (CI) measurements. The colored outline of

the larva demonstrates amount of curvature at each of 300 evenly spaced points on the larval outline. For subsequent measurements, number of points exceeding a CI threshold of 0.05 were automatically extracted frame-by-frame. Example counts in orange on the behavior frames. (**B**) For each roll, the max number of points over the CI threshold during any single frame were compared to the rotational speed (1/roll duration in seconds; n = 51 rolls, 100% optogenetic Goro activation). (**C**) For each roll, the max number of points over the CI threshold during any single frame were compared to the translational speed (inches/second; n = 17 rolls, 100% optogenetic Goro activation). (**D,E**) Example rolls showing average of the number of points above CI threshold and the distance travelled by the larva, sampled every 10 frames for 350 frames and 500 frames, respectively. Curvature and distance traveled are inversely related.

The above findings support that parallel circuits control escape locomotion in the larva. Larval bending can occur in the absence of larval rolling; however, sensory-evoked rolling appears to be less effective when bending is artificially decreased[56]. Because Goro is a command neuron downstream of DnBs, I hypothesized that degree of bending during rolling might be independent of degree of Goro activation. Surprisingly, different levels of Goro activation directly impacted amount of curvature during rolling (**Figure 2.11A**). Moderate Goro activation resulted in the greatest amount of body curvature during escape, while low and high levels of Goro activation resulted in less body curvature (**Figure 2.11A**). These results suggest that either Goro is indirectly upstream of DnB interneurons, allowing feedback excitation from roll motor programs to enhance bending, or Goro and DnB indirectly share downstream premotor circuits, allowing feedforward excitation of bending and rolling combined. Further, though amount of curvature during rolls varies at different levels of optogenetic Goro activation, rotational speed does not differ significantly (**Figure 2.11B)**, mimicking the population results from **Figure 2.10B**. This result further indicates that curvature might impact instantaneous translational or rotational velocity, but not overall escape velocities, possibly due to the nature of escape induction.

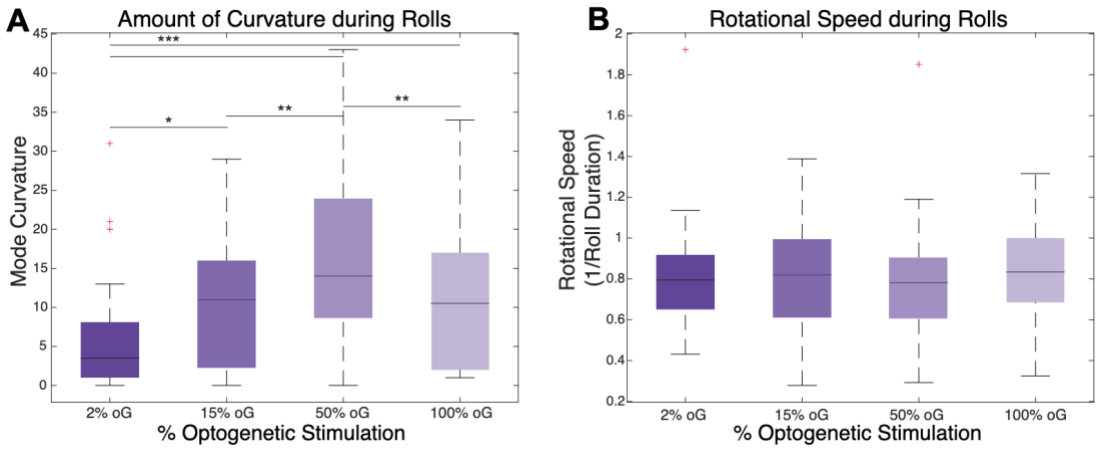


**Figure 2.11: Goro command neurons impact degree of bending during rolling.** (**A**) Mode curvature during rolling differs significantly based on intensity of optogenetic Goro activation (100%, n = 57; 50%, n = 48; 15%, n = 46; 2%, n = 19). (**B**) Rotational speed does not differ significantly based on intensity of optogenetic Goro activation. P values are indicated as *p<0.05, **p<0.01, ***p<0.001, as determined by Wilcoxon Rank Sum Test.

### Body-substrate interactions in escape rolling

The larva, though limbless, has small external features that contribute to its locomotion capabilities. Specifically, the larval body has mouth hooks in its head, posterior spiracles on its tail, and denticle belts—small triangular cuticle extensions with distinct orientations—at the posterior end of each segment. Biomechanical modeling and experiments combined have demonstrated that larvae use frictional forces between their body segments and the substrate to direct peristaltic crawling, and that their mouth hooks aide in forward crawling[126,127]. Larvae leave small indentations in agar substrates following crawling bouts. To test if larvae also utilize these body parts during escape behavior, I first observed behavioral videos for mouth hook or posterior spiracle engagement during rolling. I found that, on an agar substrate, larvae exhibiting "away from bend" escape appear to extend their posterior spiracles during rolling (**Figure 2.12A**). To verify whether spiracles or other body parts aided in rotational force generation during rolling, I observed impressions left in agar substrates during and after larval rolling events. Some larvae indeed left indentations with their posterior spiracles during "to bend" rolls (**Figure 2.12B**). Larvae also left indentations in the substrate with their mouth hooks during transitions to "to bend" rolls and transitions

from rolling to forward crawling (**Figure 2.12B,C**). Though these data are preliminary observations, this could suggest that larvae may use external features to aide in escape rolling, encouraging future study of this aspect of larval locomotion.

Though I observed mouth hook or posterior spiracle engagement in some larvae, I did not observe this across all trials. Further, I was unable to visualize denticle belt substrate indentations, if any were made, using my methods. Many of the genes that impact denticle belts also impact other larval features, like muscle morphology, making genetic manipulation and experimentation without denticle belts fraught with potential confounds. To test if body-substrate interactions are necessary for larvae to perform escape, I submerged larvae and induced escape. Larvae could perform escape bending and rolling while fully suspended in liquid and in soft molasses food (data not shown), demonstrating that body-substrate interactions are not essential for escape movements to occur, but highlighting that some level of friction is essential for larvae to translate in space while bending and rolling.

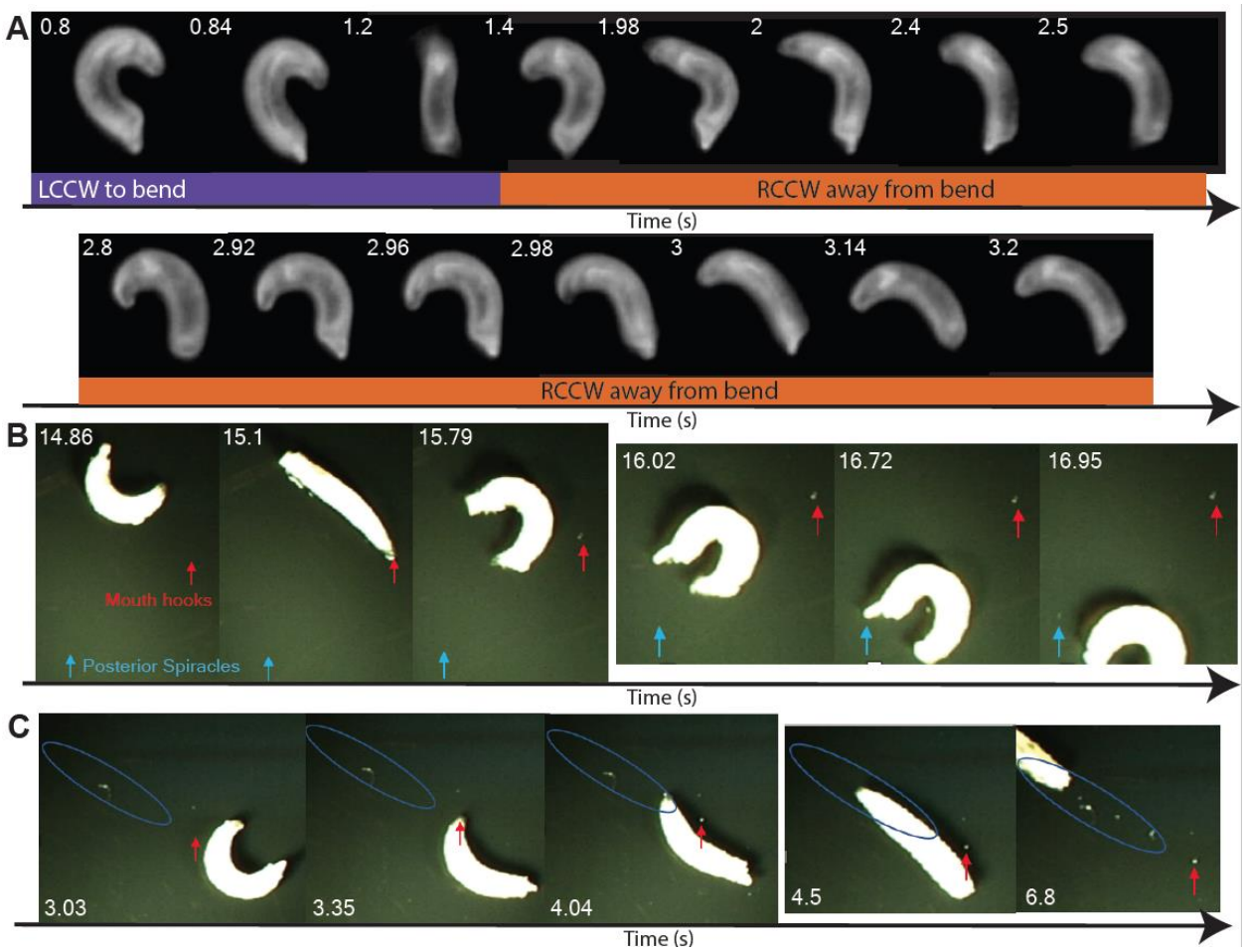


**Figure 2.12: Effect of body-substrate interactions in escape rolling.** (**A**) Stills from FIM video of larva transitioning from "to bend" to "away from bend", potentially by using its posterior spiracles to push off from the substrate. (**B**) Larva transitioning from "away from bend" to "to bend" roll plants its mouth hooks in the substrate during direction change (red arrow). Continued movement in "to bend" direction involves posterior spiracle substrate indentation (blue arrow). (**C**) Larva transitioning from bending and rolling into forward crawling plants mouth hooks to aide transition (red arrow), and leaves mouth hook tracks from forward crawling (blue oval).

## 2.4 Discussion

Escape behavior is a fundamental form of locomotion and critical for the survival of all animals. Here, I have characterized the kinematics and body-substrate interactions that comprise larval escape behavior using high-speed imaging. My behavioral data demonstrate that larval escape is comprised of four variant, flexibly interchangeable patterns. Further, I find that the body movement during escape differs

fundamentally from other forms of larval locomotion and from bending and rolling in other systems. Escape involves asymmetric recruitment of different parts of the larva's body, illustrating how distinct muscle groups could drive body propulsion during this behavior. Though body-substrate interactions permit high-speed lateral translation in escape, larvae can bend and roll in suspension, allowing the feature of potential predator avoidance to remain intact in any environment.

I found that larval escape behavior can take any of four variant combinations of bend and rotation directions. Larvae can alternate between these patterns even during a single roll bout. Such variability in escape behavior, and the ability of larvae to alternate between patterns, could increase the flexibility and efficacy of escape[16,18,29]. This idea is consistent with studies in the cockroach demonstrating that they flexibly select from several suboptimal trajectories when they perceive a threat, even though they could consistently utilize optimal escape trajectories[28]. Theoretical approaches have demonstrated that if prey were to consistently select the optimal escape trajectory, they would have decreasing escape success[29]. *Drosophila* larval escape circuitry may similarly permit variability in the escape pattern to increase success. Further, I observed that sensory-evoked escape preferentially resulted in "to-bend" escape, while command neuron-evoked escape resulted in roughly equal frequencies of escape patterns. In combination with our body-substrate findings, where some larvae use mouth hooks to pull their bodies as they transition into "to bend" rolls or fast forward crawling, this result could indicate that "to bend" rolls are more efficacious for the larva to escape global noxious stimuli. Sensory-evoked escape might also permit integration of body position information and noxious stimuli upstream of the command neuron and motor circuits prior to escape locomotion onset, whereas command neuron activation likely results in equivalently strong activation of the pair of bilateral Goro neurons. If the Goro neurons activate escape using a winner-takes-all circuit mechanism like that observed in fish escape[121], this could result in roughly equivalent frequency of activation of lateralized downstream motor circuits, and thus roughly equal frequency of emergent escape patterns.

High-speed widefield imaging of muscle positions in the body wall allowed greater characterization of kinematics during escape, demonstrating that larval rolling consists of segmentally synchronous

rotations. This stands in contrast to the peristaltically propelled snake robot and lamprey simulation bend and roll[124,125], as well as to peristaltic crawling behavior in the larva[100]. Segmental synchrony inspired the prediction that the muscle activity patterns that drive bending and rolling are likely circumferential waves around the larva. The kinematic result that bend direction changes occur more frequently than rotation direction changes during rolling supports this prediction. Namely, if the motor circuits driving a wave of circumferential muscle contractions must alter the larva's bend direction mid-roll, only the magnitude of activity in the opposite side's muscles must change while the sequence of muscle contraction itself remains the same; whereas altering the rotation direction mid-roll would require a switch in the sequence of muscle activation itself, essentially performing new action selection mid-escape—potentially a more complex and slower neural circuit computation. The hypothesis that a circumferential muscle activity pattern is occurring during rolling is tested in the next chapter.

I found that larval curvature is also variable during escape behavior, with highest curvature occurring when the ventral side is bent. I speculate that such curvature changes are due to muscle differences in the ventral side of the animal compared to the dorsal and lateral sides. In particular, the ventral oblique muscles span a greater body wall area than the other muscles. This could allow them to contract a greater proportion of each segment leading to stronger overall larval curvature. Such muscle structure and function differences are analogous to those seen in mammalian locomotion: leg muscles are greater in number and morphological complexity, and their sequential activities generate primary locomotor forces[128]; while trunk muscles are fewer in number and morphological complexity, and their sequential activities stabilize trunk position during locomotion[128,129]. One possibility could be that the ventral musculature is more active than other muscles as well, which will be tested in the next chapter, leading to a possibility that roll muscle patterns are primarily driven and synchronized by the ventral musculature. This idea is further supported by the preliminary data showing that alterations in curvature mid-roll correspond with concomitant decreases and increases in translational velocity. Namely, translational velocity decreases as larvae become maximally curved, then the body accelerates across the substrate after achieving max curvature. These results together suggest a spring-like mechanism for larval escape, where the ventral muscles serve as the

primary source of force generation. This is consistent with a recent finding of ventral muscle necessity in crawling and head-casting behaviors[103].

Different levels of optogenetic Goro activation result in different degrees of curvature during rolling, where moderate Goro activation results in maximal bending during escape. Future investigations should address whether this Goro-dependent curvature increase is due to increase in downstream premotor neuron activation, or if recurrence exists between Goro and the DnB interneurons that drive escape bending. Though DnBs do not receive direct input from Goro neurons[56], indirect recurrent connections could be at play, as is the case for Basins and their downstream nociceptive integrators TePn05 that are also indirectly upstream of Basins[87]. Goro neurons could indirectly disinhibit DnBs by exciting an intermediary inhibitory interneuron that inhibits the Handle-A interneurons that project onto DnBs, similar to what is seen in hunch vs. bend action selection circuits[15]. Such circuit mechanisms likely ensure the robustness and efficacy of larval escape when any components of escape circuitry are sufficiently triggered. Despite previous results demonstrating that decreased bending during sensory-evoked escape also decreases roll speed[56], amount of curvature did not correlate with overall escape speed metrics in my command neuron-evoked experiments. One possibility is that neuromodulatory circuits could contribute to bend-speed relationships in sensory-evoked escape. Supporting this idea, Goro activation elicits an escape sequence where larvae primarily transition out of rolling into forward crawling, but the speed of forward crawling is not as fast as sensory-evoked escape crawling[87]. This shows that the kinematics of behavior can be the same, but the speed of motor program execution is context- and circuit-dependent. Both dp-ilp7 and DnB nociceptive interneurons have been shown to express neuromodulators[56,89], providing two potential circuit mechanisms through which neuromodulators could impact amount of bending and locomotor speed, and explaining how escape activation that bypasses sensory circuits could also bypass activation of circuits that regulate speed.

Any animal's movements are directly impacted by how that animal's body interacts with the media it moves on or through. When walking, legged animals push off the ground to propel forward motion. When swimming, lateral sides of the fish undulate and push against surrounding water flow to propel forward motion. Here, I found that body-substrate interactions are essential for lateral translation during escape, and

that mouth hooks and posterior spiracles can aide in translation by pulling or pushing the larva relative to the substrate, respectively. The impact of body-substrate interactions on larval locomotion is not unprecedented. Neuromechanical modeling of larval crawling demonstrates that low-friction body-substrate interactions could cause larvae to slip in an unintentional direction during crawling[127]. The body slipping causes the larva to prolong muscle and neural activity duration during segmental peristalsis[127], making locomotor efforts more energetically costly and less efficient. Further investigation could manipulate these body parts to test the magnitude of contributions of these specific body parts or could model biomechanical contributions of friction and substrate interactions to escape rolling.

Altogether, the data presented in this chapter demonstrate the flexibility and robustness of escape and provide initial insight into the parallel circuit mechanisms that drive this behavior. Future experiments could further investigate how focal or naturalistic multisensory stimulation alters specific escape kinematic features. Additionally, utilizing semi-automated or automated pose tracking (as seen in Mathis *et al.*[120]) could increase the number and level of detail of kinematic findings, further contributing to our understanding of the circuits that generate escape.

## 2.5 Acknowledgments

I am grateful to Grace Shin, Rick Hormigo, Tanya Tabachnik, and Mark Sullivan for their contributions to modifying and optimizing the behavioral imaging setup. I thank Aref Zarin for genetic resources. I thank Aref Zarin and Wes Grueber for intellectual input and project conceptualization. This work was supported by a National Science Foundation Graduate Research Fellowship.

# Chapter 3: Motor Circuits & Muscle Activities that Drive Escape[ϕ]

## 3.1 Introduction

Escape behaviors across species often differ fundamentally from exploratory locomotion. For example, worms perform turns, insects jump, decapods execute tail-flip responses, and fish make C-shaped bends to avoid harm[16,19,20,130]. Even in mammals—for example, horses—high-speed gaits used for escape differ mechanically from lower-speed gaits[25,131]. This specificity suggests that dedicated neural circuits or unique activity patterns within shared locomotor circuits are employed during escape. While many studies have investigated how sensory input promotes escape[16,18] , few have characterized the neuromuscular activities that generate escape movements[22,132]. By characterizing escape motor circuits in a model with a well-studied sensory system and nearly complete connectome, we can understand how escape circuits differ from other locomotor circuits and how sensory input is transformed into motor output during escape.

*Drosophila* larval forward and backward crawling, driven by segmental peristalsis, are among the best studied locomotor patterns at the level of neural circuitry and muscle activity[98,100]. The *Drosophila* larval body consists of twelve segments, with abdominal segments containing up to 60 different muscles[98]. Forward crawling consists of consecutive segmental contraction that propagates from posterior to anterior segments, while sequential contraction of anterior to posterior segments results in backward locomotion[126]. In both behaviors, the left and right sides of a given segment contract at the same time with the same magnitude[51]. Crawling is supported by all thirty morphologically distinct muscles per hemisegment, each with a specific location and orientation[58,98,99]. The circuitry supporting larval crawling is well-studied[100]. Recently, a single-segment circuit diagram of premotor neurons (PMNs) to motor neurons (MNs) to muscles was generated using electron microscopy[52–54,58,114]. This detailed circuit reconstruction, alongside

[ϕ] I am thankful to my collaborators for their valuable contributions to this work. Wenze Li made modifications to the SCAPE microscope, helped troubleshoot protocol for imaging larvae during rolling, and performed SCAPE imaging experiments. Wenze Li and Elizabeth Hillman guided 3D data processing. Aref Zarin performed EM connectome analysis and guided muscle segmentation and data analysis. Wes Grueber and Aref Zarin guided project conceptualization. Wenze, Elizabeth, Aref, and Wes provided input on data analysis and the main text. This work is part of a submitted manuscript.

characterization of muscle activities during forward and backward crawling, have permitted the prediction of PMN activities[58], and testing of PMN function in particular aspects of motor coordination during forward and backward locomotion[52–54,57,113,133–135]. This work has revealed that distinct PMNs have specific roles in the promotion of forward or backward crawling[58], including intrasegmental coordination of MN firing[53,113,134], intersegmental coordination of peristaltic wave propagation[52,57,113], regulation of left-right symmetry[51], and regulation of speed[115] during crawling.

In addition to forward and backward locomotion, Drosophila larvae are capable of performing a nocifensive rolling escape behavior[77]. Upon experiencing harmful mechanical touch or heat, Drosophila larvae initiate C-shaped bending, rolling, and rapid forward crawling. Rolling causes fast lateral motion—faster than escape crawling alone[71,78] , and can dislodge attacking parasitoid wasps[78,85]. The sensory input and neural circuitry that promotes escape have been extensively characterized. The behavior is initiated by activity of class IV (cIV) dendritic arborization neurons, polymodal nociceptors that tile the body wall of the larva[69,77]. These neurons show differential activity patterns and use separate transduction receptors to detect different types of noxious stimuli[95]. When activated naturalistically or optogenetically, cIV neurons induce escape behavior[78]. Several downstream partners of cIV neurons have been identified and reconstructed using serial transmission electron microscopy[54,56,86,87,89]. Activation of any of a number of interneurons that are downstream of cIV neurons are sufficient to evoke escape behavior[54,56,86,87,89]. Despite much progress in understanding larval nociceptive circuitry, the motor program that generates bending and rolling remains unknown. This is primarily because of the difficulty in uncovering muscle activity patterns during rapid and complex three-dimensional movements, like larval escape.

In this chapter, we examine the muscle activities and motor circuits responsible for escape bending and rolling using a combination of high-speed 3D imaging of fluorescent calcium indicators expressed in larval muscles and connectomic approaches. We identify key features of neuromuscular function that support escape motor sequence progression. We compare these findings to the motor activity that drives crawling to identify shared and distinct features of these two modes of locomotion. Both behaviors occur via sequential motor activities, but our results suggest fundamentally different sequencing patterns, with

muscle contractions progressing along the anteroposterior axis of the larva during crawling, and muscle contractions progressing circumferentially around the larva during rolling. The neural circuit mechanisms for coordinating the rolling motor pattern could yield insights into escape motor pattern generation across species.

## 3.2 Methods

*Confocal Image Acquisition:*

Muscle activity during crawling was initially measured in Zarin et al., 2019[58]. Briefly, images were acquired using a 10x objective on an upright Zeiss LSM800 microscope. GCaMP6f and mCherry fluorescence values were extracted from a previously acquired forward crawling video and ratiometric values from muscle ROIs (see SCAPE analysis) were subsequently compared to ratiometric muscle ROI values from SCAPE escape images.

*SCAPE Image Acquisition:*

Many technical difficulties emerge when attempting to acquire quantifiable functional imaging data of neurons or muscles in freely moving transgenic animals. These issues include fluorescent tissues being out of focus due to changing tissue depth during behavior; low image acquisition speed relative to timing of neural or muscle activity; and variable brightness of tissues due to tissue compression or movement in the imaging plane rather than activity-dependent fluorescence changes. To overcome these issues, we used a custom-built Swept Confocally Aligned Planar Excitation (SCAPE) microscope, extended from that previously described[92,136], to acquire high-speed volumetric imaging of rolling larvae. Light sheet imaging approaches can acquire volumetric data at higher speed and with less photobleaching of living tissue than point-scanning microscopy approaches (*e.g.* conventional confocal and 2-photon approaches), overcoming the first two issues mentioned above[137]. However, conventional light sheet imaging relies on orthogonal objectives for planar excitation of fluorophores in the tissues of interest and signal detection[137]. Due to this configuration, the detection objective must be rapidly shifted in a precise manner relative to the light sheet's

position to acquire aligned, in-focus signal from the tissue, complicating and substantially slowing image acquisition[137]. SCAPE microscopy overcomes these issues by delivering an oblique light sheet for sample excitation and collecting emitted signal through the same, high numerical aperture objective[138]. SCAPE uses a scanning mirror that both allows the oblique light sheet to sweep through the tissue in the oblique x-direction for planar excitation, while also allowing the same optical path to collect emitted planar signal from that oblique x location, employing the scanning-descanning principles at play in a confocal microscope[138]. This imaging geometry makes it such that both the light sheet's sweeping position and the plane of emitted signal are consistently aligned in a manner that allows a constant, unmoving focal plane for the CMOS camera chip to collect functional imaging data from. This allows acquisition of whole volumes rapidly by simply altering the angle of the scanning mirror, rather than coordinating synchronous light sheet and detection objective positional changes[138]. These features of SCAPE provide an optimal solution for acquiring functional imaging data in freely moving, transgenic animals like the larva, as they allow rapid volume collection, accounting for unpredictable body motion and providing in-focus images of fluorescent tissues of interest across full time courses[138]. Later advances in SCAPE microscopy also permitted the collection of simultaneous volumetric dual-color images using an image splitter to separate different wavelengths of emitted light, permitting precise quantitative adjustment for movement-based fluorescence changes in tissues expressing activity indicators and non-activity dependent fluorophores[92,136].

Our specific SCAPE system utilizes a custom-made water chamber between the second and third objective lens to accommodate higher collection efficiency over a large field of view with 1.0 NA water immersion objectives throughout. 488nm and 561nm lasers were used to excite GCaMP and mCherry simultaneously, while also activating Chrimson for optogenetics. An image splitter with 561nm long pass dichroic mirror was used with 525/50 and 618/50 filters to split the image into two sCMOS cameras (Andor Zyla 4.2 plus) which enables acquisition of both green and red channels simultaneously with a field of view larger than 1.1mm in the lateral dimension. A 3D field of view with the size of the agar arena was acquired at 10 volumes per second to minimize the motion blur from the larva rolling behavior.

Larvae were raised and fed ATR for optogenetic activation as mentioned above. Larvae were imaged while in a thin 2% agarose chamber filled with distilled water. Each larva was assessed for brightness of muscle fluorophore expression and likelihood of rolling through epifluorescent screening, and the best overall larvae were placed into agar chambers using a fine paint brush. Each chamber was made using 3D-printed molds of different dimensions for late L1 and early L2 larvae of slightly different sizes.

*SCAPE Image Processing & Analysis:*

SCAPE volumetric data are inherently three-dimensional. To overcome 3D-segmentation difficulties but keep the richness of volumetric muscle data, we developed a custom MATLAB script to generate a 3D-averaged projection of all SCAPE data. Our 3D-averaging method generates separate GCaMP and mCherry 2D images. Each pixel in the 3D-averaged projection image is the mean of a z-depth window of 30 pixels that have fluorescence values greater than or equal to 50% of the difference between the voxel at that x,y coordinate that demonstrated maximum fluorescence and the voxel at that x,y coordinate that demonstrated minimum fluorescence in the mCherry channel. This allows inclusion of primarily voxels within the muscle plane into the 3D-averaged projection value for each pixel. The voxel with maximal fluorescence value was identified in the 3D-smoothed volume using a Gaussian kernel, eliminating noisy signal, but the 3D-averaged projection was generated using the raw fluorescence values for accurate ratiometric signal quantification. 3D-averaged projection images were then analyzed using modified versions of the custom MATLAB script from Zarin et al., 2019[58]. For rolling muscle activity analysis, ROIs were drawn manually on non-overlapping portions of each muscle for each segment from A2-A4 on a frame-by-frame basis. For behavioral transition analysis, ROIs were drawn manually outlining segments A1-A6 on left and right sides of the larva, and 0 pixel values were excluded in ratiometric quantitation. ROIs were drawn on the mCherry 3D-averaged projection. Because puncta were present throughout muscles in the mCherry images, pixels with a fluorescence value greater than 90% of the distribution of fluorescence values within the mCherry ROI were discarded in both the mCherry and GCaMP channels to prevent biased ratiometric signal. The ratio of fluorescence between the ROI pixels of

the mean depth-project GCaMP image and the mean depth projected mCherry image was calculated. The mean of this ratiometric value was extracted for each time point of the ROI.

Five roll bouts (one complete revolution based on muscle locations) from four larvae were selected for rolling muscle activity analysis, and three frames of "bend", "initiate", and "roll" moments were manually selected and averaged from dorsal and ventral views of four larvae for behavioral transition muscle activity analysis. Subsequent analyses were performed using custom MATLAB scripts.

For comparisons between ratiometric muscle activity values of crawling and rolling, normalized time at maximum ratiometric values were extracted. Statistical analyses were performed as described below.

For bend vs. stretch side comparisons of individual muscle activity during rolling, ROI centroids were tracked and, according to the bend and rotation directions of the larvae, divided into four quartiles based on spatial position within the larva's body at each time point. Ratiometric values from the most bent quartile and ratiometric values from the most stretched quartile were extracted and averaged for each muscle. These values were then compiled and averaged across segments and across all five roll videos, providing a single "bend" and single "stretch" ratiometric value for each muscle.

For bend vs. stretch side comparisons of broadscale muscle activity during bending, roll initiation, and rolling, large ROIs were drawn to encompass all dorsal or ventral muscles in left vs. right hemisegments A1-A6 for three consecutive frames during manually identified bend, initiate, and mid-roll moments. Only non-zero values were included in the ratiometric fluorescence calculation from GCaMP and mCherry channels to avoid effects of background pixels being included in the large, multi-segment ROIs. These values were averaged across larvae for subsequent statistical analysis.

*Statistical Analyses:*

Statistical analyses were performed using custom programs written in MATLAB. For the muscle activity unity plot and subsequent muscle activity categorizations, linear regression was performed and muscles were divided into relative levels of activity based on distance from the regression line. For bilateral muscle activity differences during bend, initiate roll, and mid-roll, paired t-tests were performed to compare

fluorescence values. Matlab codes for SCAPE image processing and subsequent analyses are available at the following Github repository: https://github.com/cooneypc4/larval_escape_manuscript .

*Electron microscopy and CATMAID reconstructions*

PMN-MN connectome previously reconstructed in Zarin et al., 2019[58] were used to generate **Figure 3.7-3.9.**

## 3.3 Results

**Volumetric SCAPE imaging captures muscle activity during escape behavior**

Analysis of escape kinematics suggests that a circumferential sequence of muscle contractions underlies rolling behavior (**Chapter 2, Figure 2.8**). To explicitly test this idea, we examined muscle activity patterns using Swept Confocally-Aligned Planar Excitation (SCAPE) microscopy, a volumetric imaging technique that permits high-speed, high-resolution dual-color 3D imaging[92,136–142]. We induced escape behavior optogenetically in larvae expressing mCherry and GCaMP6f in all body wall muscles through optogenetic Goro activation. Simultaneous dual-color volumetric imaging of GCaMP6f and mCherry enabled ratiometric imaging of muscle activity to correct for movement-dependent fluorescence changes. This approach resolved activity of individual muscles along the entire length of the larva and approximately half of the larval body thickness during freely moving behavior at 10 volumes per second (**Figure 3.1A-C**). We developed a 3D-averaging method to extract GCaMP and mCherry signals from individual muscles as the larva rotated (see **Methods**). We found that GCaMP and mCherry signals were highly correlated during behavior, while ratiometric signals revealed differences in muscle activity over time and across muscles during larval rolling (**Figure 3.1D,E**).

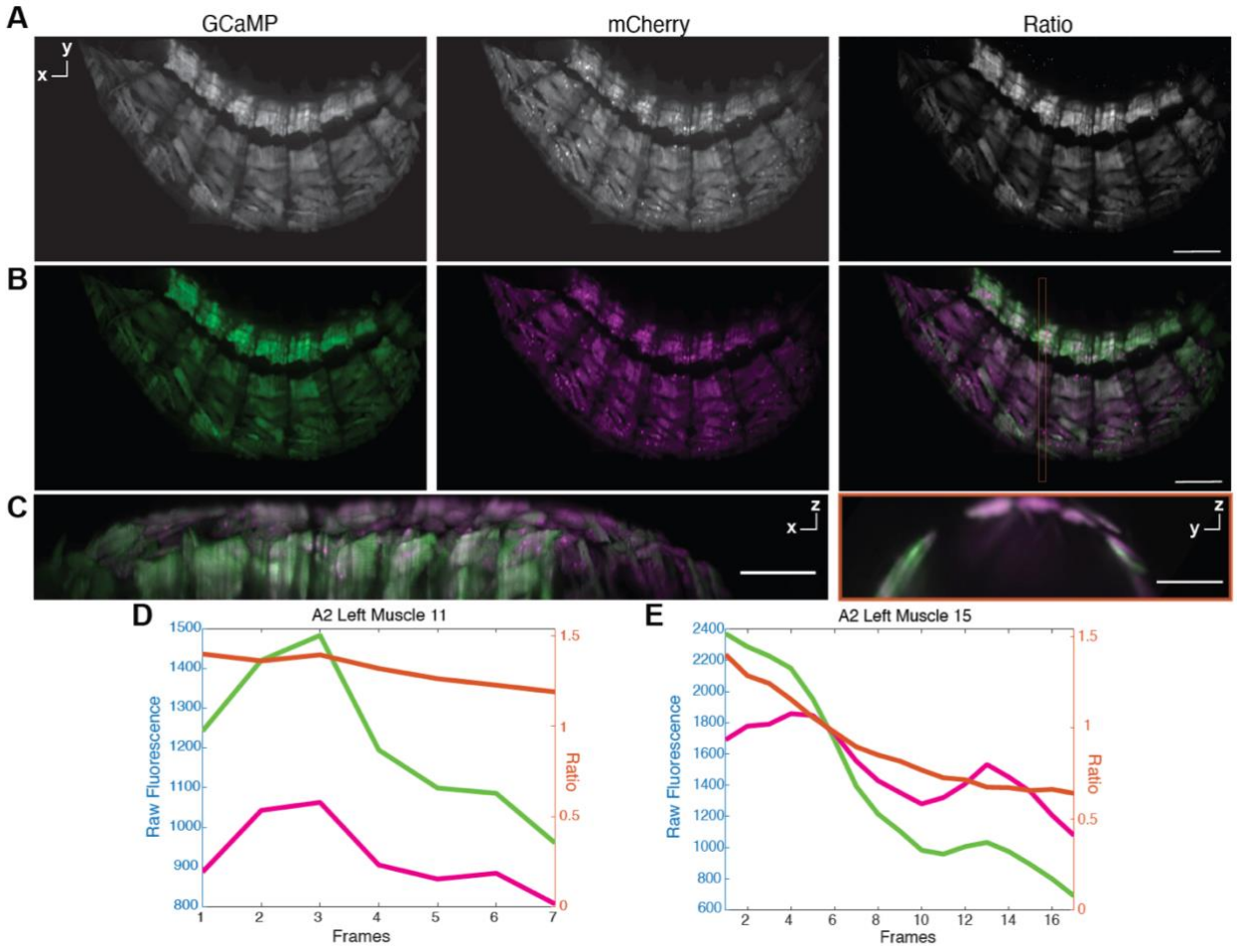


**Figure 3.1: Dual-color SCAPE captures individual muscle activities during escape behavior.** (**A,B**) Example stills from GCaMP, mCherry, and calculated ratiometric SCAPE images in grayscale (**A**) and in respective green and magenta and merged (**B**). (**C**) Side view of rolling larva showing prominent GCaMP signal in muscles within the bend (front) and prominent mcherry signal in muscles outside of the bend (back); Cross-section showing differing muscle depths along the circumference of the larva's body, with prominent GCaMP signal on bent side (left), and prominent mcherry signal in mid-section and on stretched side (right). Area used for cross-section is indicated by orange rectangle in final subpanel of **B**. (**D,E**) Fluorescence signals extracted from single example muscles during escape rolling demonstrate highly correlated GCaMP and mCherry signals. Example muscles show meaningful decreases in ratiometric signal during rolling, but demonstrate distinct dynamic ranges in activity during rolling: roughly 20% (**D**), and 60% (**E**), respectively.

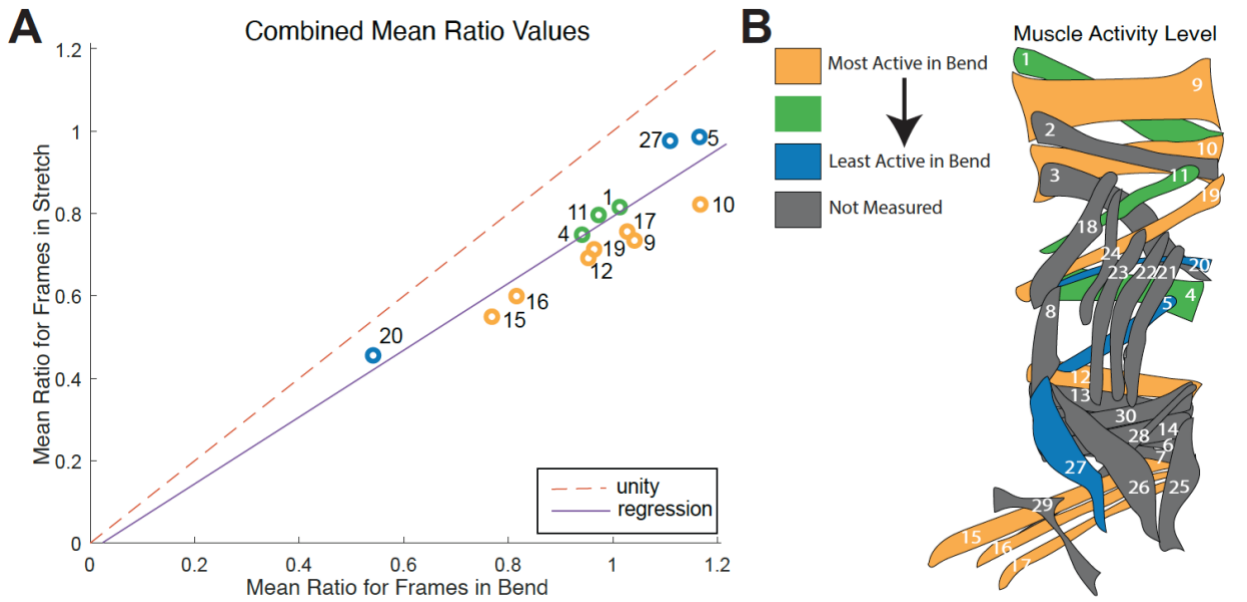


**Figure 3.2: Muscles are preferentially active in the bend during rolling.** (**A**) Within-muscle comparisons of mean ratiometric signal when muscles are in the bent side vs. when muscles are along the stretched side of the rolling larvae, averaged across all rolls (n = 5 rolls, n = 4 larvae). Unity line illustrates values at which muscles would have equivalent activity levels when in the bent sides or along the stretched side of the larva. All evaluated muscles fall below the unity line, indicating their bias towards being active in the bend. Regression line shows relationship between high activity levels (mean ratiometric values) and bias of being active in the bend ($R^2$= 0.97; p = 1.3631e-09). Points are color-coded based on activity preference for bend vs. stretched sides (distance from regression line), where muscles are grouped by strongest (mustard), moderate (green), and weakest (blue) bias towards being active in the bend. (**B**) Hemisegment schematic of most consistently measured muscles, color-coded according to preferential activity levels in A.

### Muscle activity travels in a circumferential wave during escape rolling

We analyzed SCAPE movies to determine whether a circumferential wave of muscle activity might occur during rolling, as schematized in **Figure 2.8B**. We find that muscles are most active along the bent side of the larva, consistent with asymmetric contractions maintaining the C-shaped bend (**Figure 3.2A**). Muscles at the dorsal and ventral midlines tended to be more active than lateral muscles while in the bend (**Figure 3.2A,B**), consistent with our kinematic observation that the ventral side of the larva is typically the most bent during rolling.

If a circumferential wave without a peristaltic component underlies rolling, we would expect that muscles in different segments would contract synchronously as they rotate. To test this, we visualized ratiometric signals from the same muscles in neighboring segments. While we were not able to measure the entire time course of each muscle during its rotation around the larva, we found that ratiometric signal tends to increase as muscles rotate into the bend (**Figure 3.3B,C**) and decrease as muscles move out of the bend (**Figure 3.3D-F**). Furthermore, muscle contractions during most escape rolling events occur via dorsoventral progression, and the sequence on the left side closely mirrors the sequence on the right side across segments.

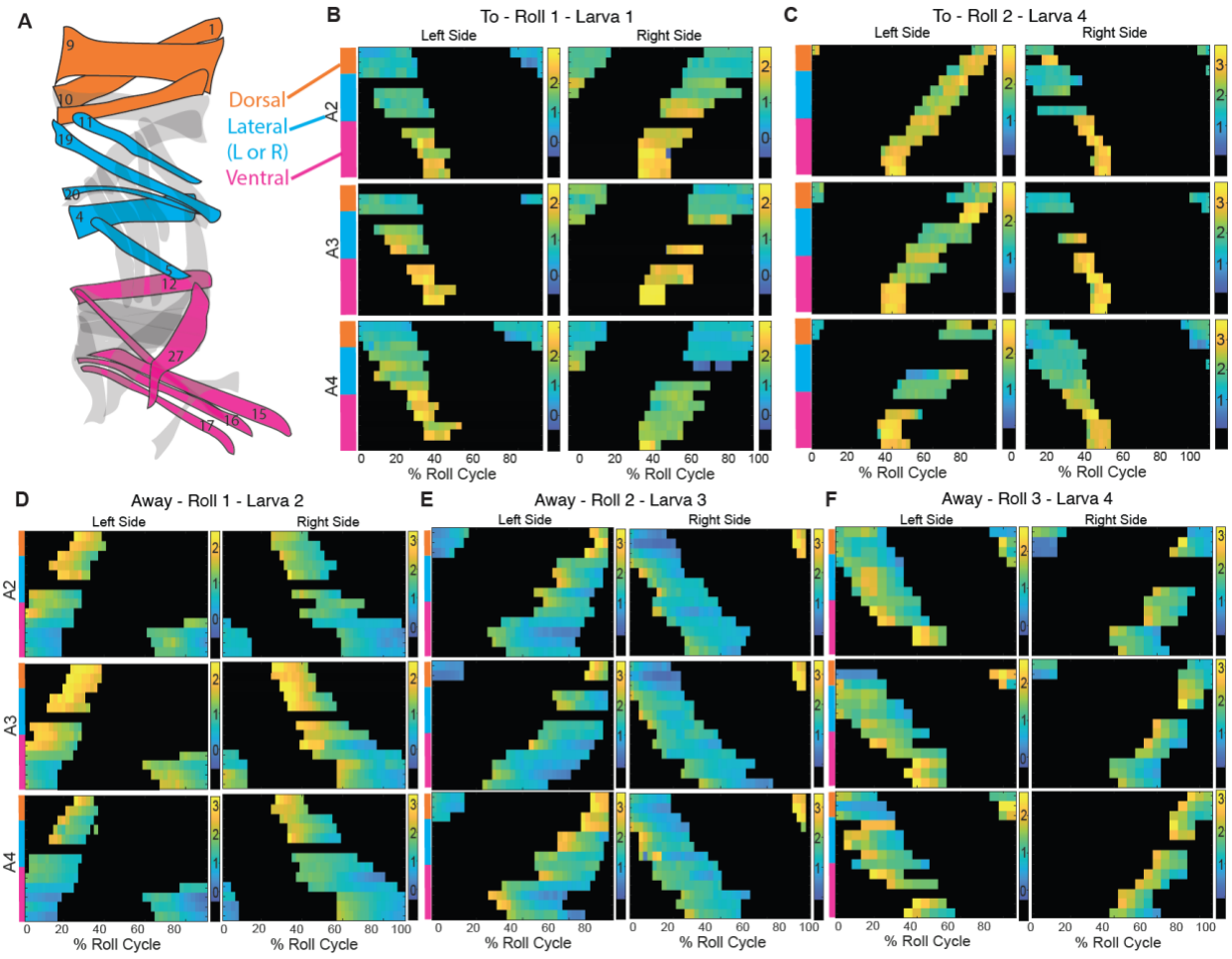


**Figure 3.3: Individual muscle activity patterns show symmetric dorsoventral propagation on left and right sides.** (**A**) Hemisegment color-coded by spatial muscle groups (dorsal, lateral, and ventral) that correspond with color-coded muscle labels to the left of the rows in heatmaps. (**B-F**) Heatmaps of z-scored ratiometric signal across most consistently measured muscles, divided by segment (A2-A4) and side (left and right). Each row for each heatmap panel is an individual muscle, organized from dorsal (top

row) to ventral (bottom row), and color-coded according to spatial muscle groupings in **A**. Colorbars to the right of the upper heatmaps show range of ratiometric values. (**B,C**) Traces from muscles moving into the bend during rolling show some mild increase in ratiometric signal. (**D-F**) Muscles moving out of the bend show moderate decrease in ratiometric signal. Notably, ratiometric signals in muscles moving into the bend from our imaging perspective have a less apparent activity pattern.

To contrast escape rolling and crawling at the level of individual muscles, we compared SCAPE imaging data collected during rolling to previously acquired dual-color 2D crawling muscle activity data from Zarin *et al.*[58] (**Figure 3.4A,B**). Peak activity measurements of segmentally homologous muscles during crawling revealed a time delay between successive segments, reflecting peristaltic wave progression (**Figure 3.4C,E**). By contrast, segmentally homologous muscles showed synchronous contractions and sequential muscle activity travelled around the circumference of the larva during rolling (**Figure 3.4D,F, Figure 3.5**), as observed in the full ratiometric trace data (**Figure 3.3**). This sequential wave of circumferential muscle activity during escape behavior maintains a constant bend direction as the larva rolls. Different rolling directions showed a different order of muscle activation (**Figure 3.5**). These data demonstrate fundamental distinctions between muscle activity during larval escape rolling and larval crawling: 1) rolling is segmentally synchronous while crawling is segmentally asynchronous; 2) rolling is left-right asymmetric while crawling is left-right symmetric; 3) rolling involves a progression of muscle contractions around the circumference of the larva while crawling involves progression along the anteroposterior axis.

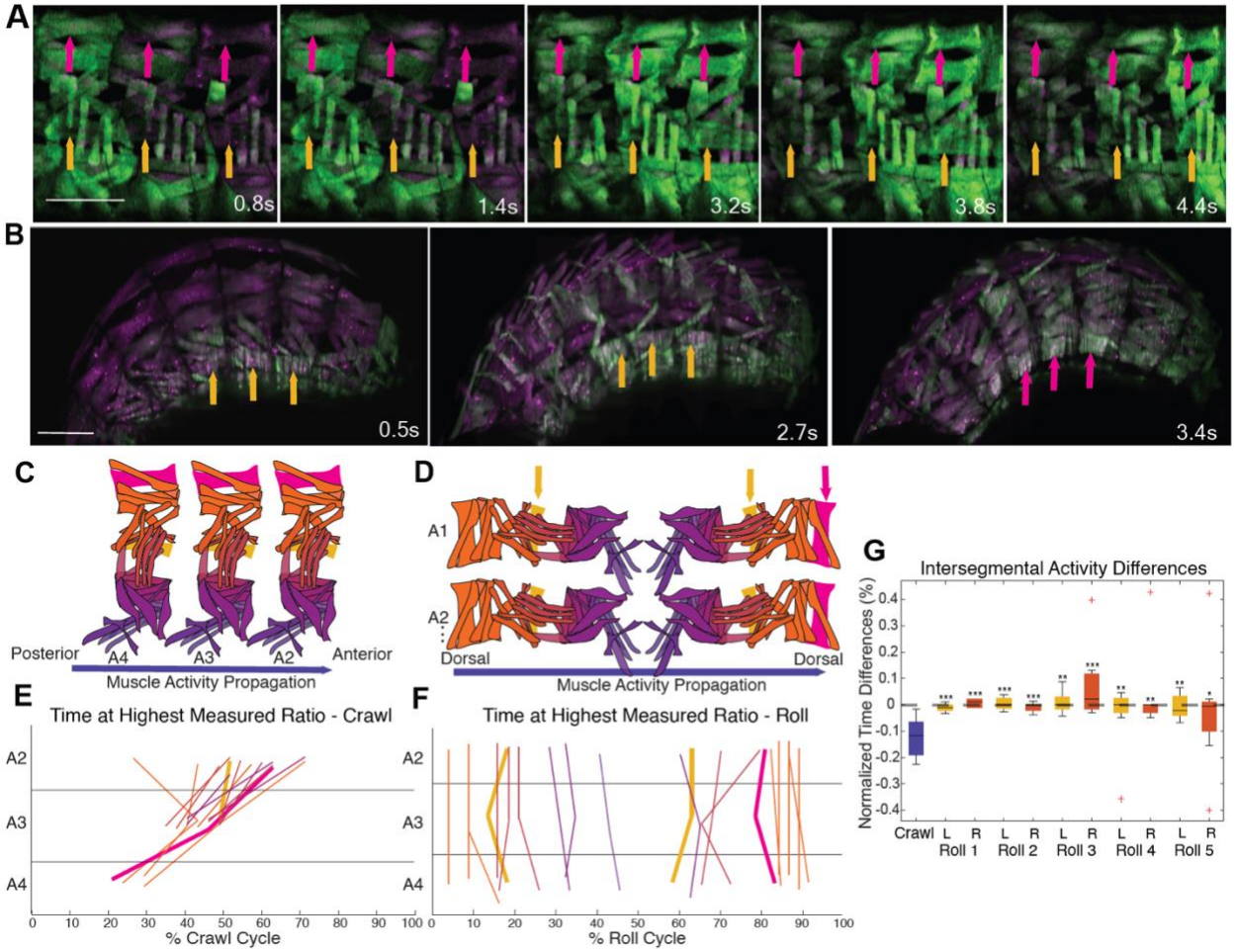


**Figure 3.4: Escape rolling is a segmentally synchronous behavior driven by a circumferential wave of muscle contractions**. (**A**) Confocal images from single crawl bout in larva expressing mCherry & GCaMP in the muscles. Arrows point to muscle 9 (magenta) and muscle 4 (mustard), showing the progression of increased GCaMP fluorescence in each of these muscles from posterior to anterior segments. Time indicated in bottom right (seconds). (**B**) SCAPE ratiometric stills from single roll bout, showing same muscle appearing in focal plane simultaneously across segments with increased brightness in when muscles are on the bent side of the animal. Arrows point to right muscle 4 (mustard), left muscle 4 (mustard), and right muscle 9 (magenta), showing the synchronous rotation and increase in GCaMP fluorescence in each of these muscles along three midsegments. Time indicated in bottom right (seconds). (**C**) Schematic of muscle arrangement in three neighboring hemisegments. Blue arrow indicates posterior-to-anterior propagation of muscle activity. Representative muscles and arrows highlighted in magenta and mustard. (**D**) Two-segment schematic of hemisegments, color-coded by activity order (dorsal to ventral to dorsal). Representative muscles and arrows highlighted in magenta and mustard. Blue arrow indicates circumferential propagation of muscle activity. (**E**) Peak ratiometric muscle fluorescence times during single crawl bout across three segments. During forward crawling, muscles of

segment A4 reach peak activity before A3, and muscles of segment A3 reach peak activity before A2 segment, demonstrating the propagation of peristaltic contraction from posterior to anterior segments. Representative lines of highlighted muscles from schematic are boldened in magenta and mustard. (**F**) Highest observed ratiometric muscle fluorescence times during single roll cycle with SCAPE across segments A2-A4. Same muscle types across segment a2 to a4 simultaneously reach their peak activity. Muscles are color-coded according to panel D, demonstrating dorsal to ventral to dorsal (circumferential) propagation of muscle contraction. Representative lines of highlighted muscles in schematic are boldened in magenta and mustard. (**G**) Comparison between time difference of muscles in segments A2-A4 for forward crawling versus rolling (crawl: n = 1; roll: n = 5 rolls, n = 4 larvae). Negative values indicate that muscles in A4 are active before muscles in A2 and "0" indicates synchronous contraction. Statistical tests were performed between roll side values from each roll bout and crawl values from a single crawl bout. P values are indicated as *p<0.05, **p<0.01, ***p<0.001. Scale bars = 100um.

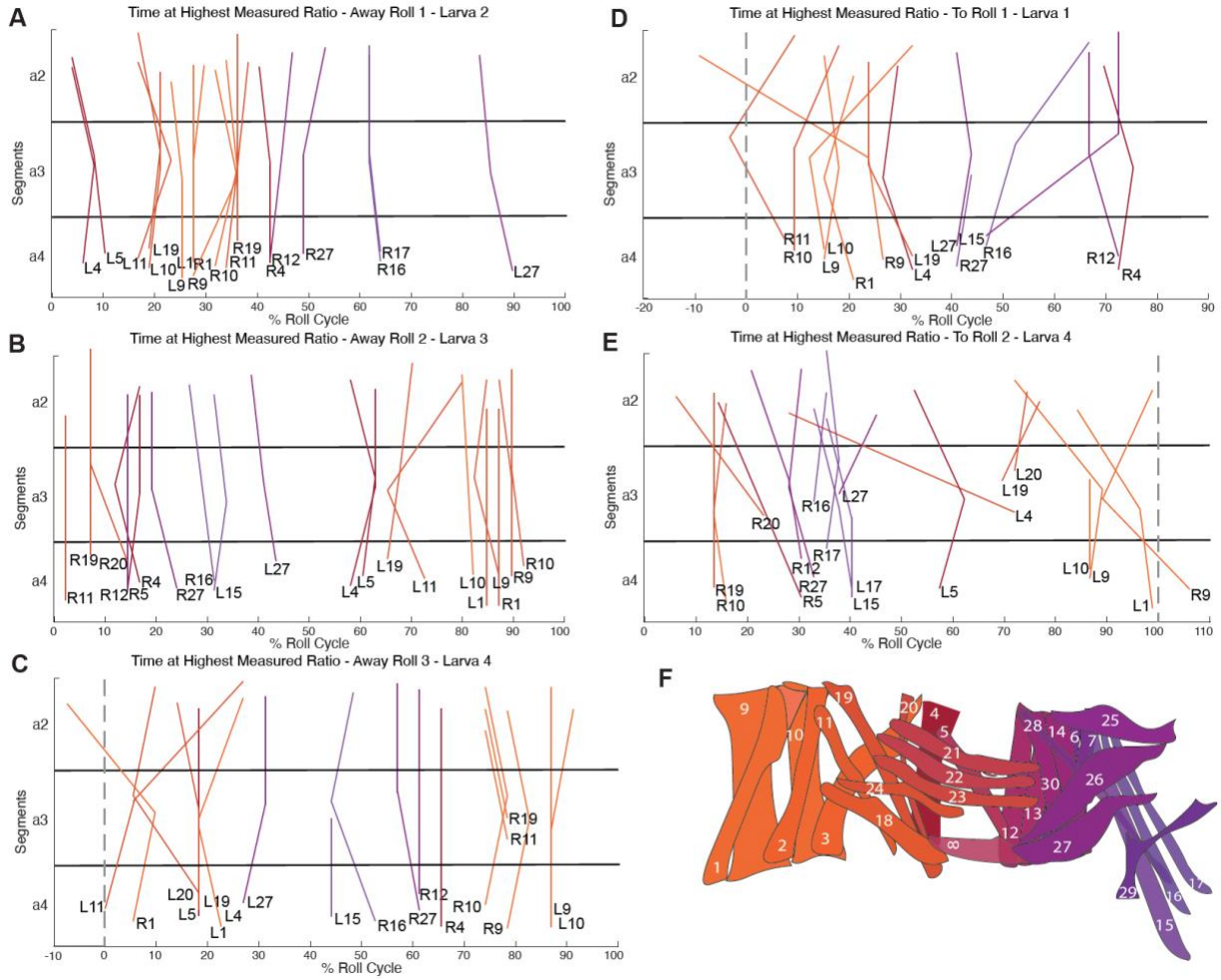


**Figure 3.5: Multiple roll bouts demonstrate segmentally synchronous circumferential wave of muscle contractions.** (**A-E**) Highest measured ratiometric muscle fluorescence times during single roll cycles where muscles rotate away/out of the bend (**A-**

**C**) or to/into the bend (**D**-**E**) (n = 5 rolls; n = 4 larvae). Note that, because rolling is a cyclical behavior, axes were adjusted in panels **C**-**E** to illustrate relative synchrony in segments where select muscles that appear twice during a single roll have offset peaks in linear time of a single roll (*e.g.* **D**, R11). (**F**) Single hemisegment muscle schematic, color-coded by spatial muscle groupings with muscle numbers (white).

### Changes in bilaterally asymmetric muscle activity drive bend to roll transition

SCAPE imaging revealed "hidden" muscle activity states in rolling that we had not identified by either kinematic or behavioral analysis. When larvae are in a bend-only (pre-roll) phase, bent and stretched sides of the larva showed the most pronounced activity differences (**Figure 3.6A,B,C-E**). As larvae begin to roll, muscles on the stretched side of the larva begin contracting, and muscles on the bent side decrease their activity, resulting in similar L-R activity levels (**Figure 3.6A',B',C-E**). During roll maintenance, muscles on the bent side of the larva show greater activity than stretched muscles; however, this asymmetry is less intense than the asymmetry that occurs during the pre-roll phase (**Figure 3.6A'',B'',C-E**). These results demonstrate that larval rolling behavior can be broken into three modules: bend (conversion from straight to C-shaped larvae), roll initiation, and roll maintenance. Muscles are active on the stretched side of the larva during roll initiation and maintenance, potentially contributing to the rotational force of the larva. Further, the partial coactivation of midline muscles during roll initiation and roll maintenance suggests a bilateral premotor drive generates rolling.

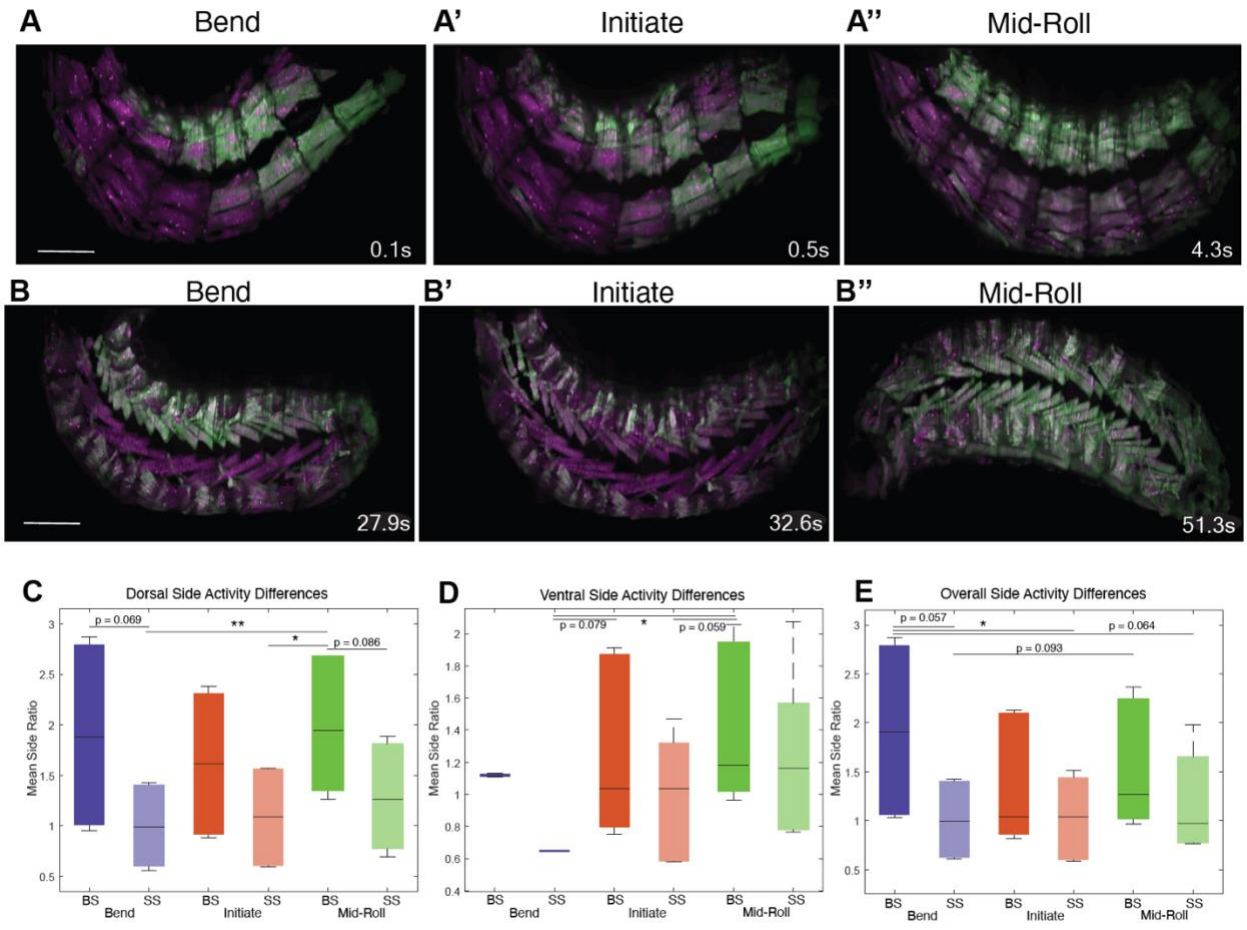


**Figure 3.6: Differences in bilaterally asymmetric activity in midline muscles drive the escape sequence.** (A-B'') Dual-color stills from SCAPE movies during example moments of larval bending (A,B), roll initiation (A',B'), and mid-roll (A'',B''). (A-A'') Dorsal musculature, (B-B'') ventral musculature. (C-E) Mean differences in total muscle ratiometric fluorescence on bent side (BS) vs. stretched side (SS) during bend, roll initiation, and mid-roll frames (C) Quantification of dorsal (C), ventral (D), and combined (E) asymmetric activity (n = 3 larvae each). P values are indicated as *p<0.05, or reported directly if p<0.1.

## A potential circuit basis for circumferential muscle contraction sequences

We next examined recently published electron microscopic (EM) connectome data[58] to determine whether PMN-MN circuit connectivity could provide insights into how circumferential contraction sequences are executed. We found that a majority of annotated PMN to MN synapses are located on ipsilateral MN dendrites (**Figure 3.7A**); however, some MNs receive inputs on ipsilateral and contralateral dendrites (**Figure 3.7A-D**). MNs with ipsilateral-only inputs primarily innervate muscles that are farther

from the body midline, including lateral transverse and dorsal oblique groups, while MNs with ipsilateral and contralateral synapses innervate muscles that are nearer to the dorsal or ventral midline (**Figure 3.7A,C,D**). This segregation of MN inputs could support midline muscle coactivity that progresses circumferentially to unilateral muscle activity and back to midline coactivity.

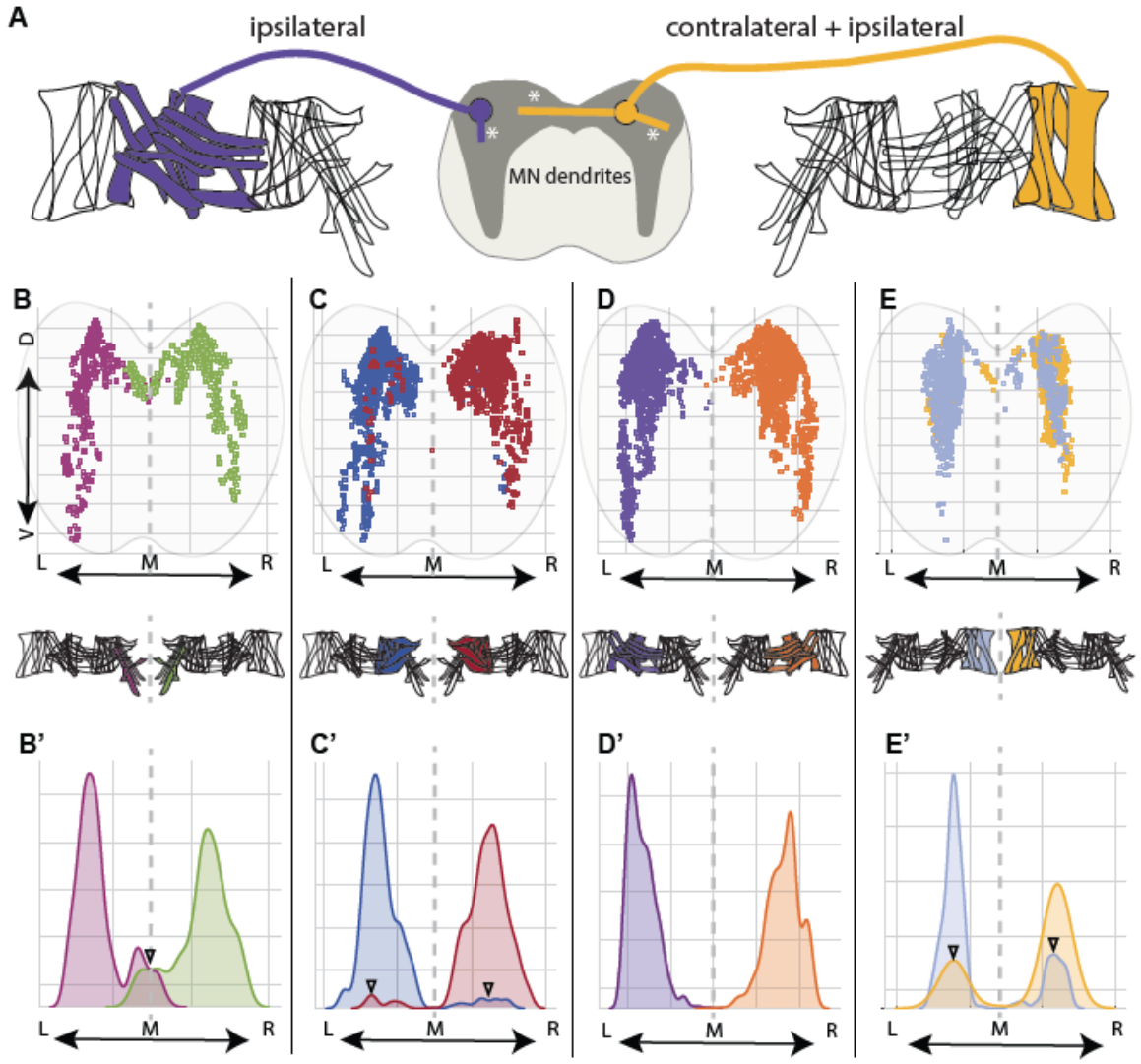


**Figure 3.7: Left and right midline muscles receive inputs from partially overlapping regions of neuropil**. (A) Schematic showing motor neurons whose dendrites receive postsynaptic input (indicated by white asterisks) either ipsilateral to their axon projections or both ipsilateral and contralateral to their axon projections. (B-E) Dorsoventral and mediolateral distributions of postsynaptic sites on MNs innervating the muscle groups indicated below each panel. Shaded gray area represents the cross-sectional view of the neuropil. Gray dashed lines define the midline (M) dividing the neuropil into left (L) and right (R) hemisegments, and the midline of dorsal and ventral body wall muscles, respectively. (B,C,E) Postsynaptic sites of MNs innervating

muscles near the dorsal or ventral midlines occupy partially overlapping regions of the neuropil. (D) Postsynaptic sites of MNs innervating lateral muscles are localized exclusively in either left or right hemisegment of the neuropil. (B'-E') 1D kernel density plot of MN postsynaptic sites on the mediolateral axis. Black arrowheads show overlapping localization of postsynaptic sites of left and right MNs.

Next, we examined the PMN-MN connectome relative to muscle activity of rolling behavior. In every larval VNC segment, there are two PMNs of the same type, one for each hemisegment. Any PMN in a given hemisegment could synapse onto MNs exiting either the left or right side (unilateral connectivity), or both the left and right sides (bilateral connectivity). The former would support left-right asymmetric coordination of muscles while the latter would support left-right symmetric coordination of muscles. Strikingly, muscles that demonstrate left-right asymmetry during rolling show a unilateral PMN-MN connectivity pattern (e.g. LT MNs innervating lateral muscles; **Figure 3.8A,B**). On the other hand, muscles that demonstrate moments of left-right symmetry during larval rolling show a bilateral PMN-MN connectivity pattern (e.g. MNs targeting dorsal longitudinal, ventral longitudinal and ventral oblique muscles; **Figure 3.8C-F**). Closer investigation of individual PMNs illustrate candidate microcircuits that could drive sequential bilateral coordination of midline muscles (**Figure 3.9B**), in juxtaposition with unilateral coordination of lateral muscles (**Figure 3.9A**). Thus, the unilateral or bilateral nature of PMN-MN connections, in conjunction with the MN synaptic input distributions observed in **Figure 3.7**, could provide a circuit mechanism for eliciting circumferential muscle activity progression during escape rolling.

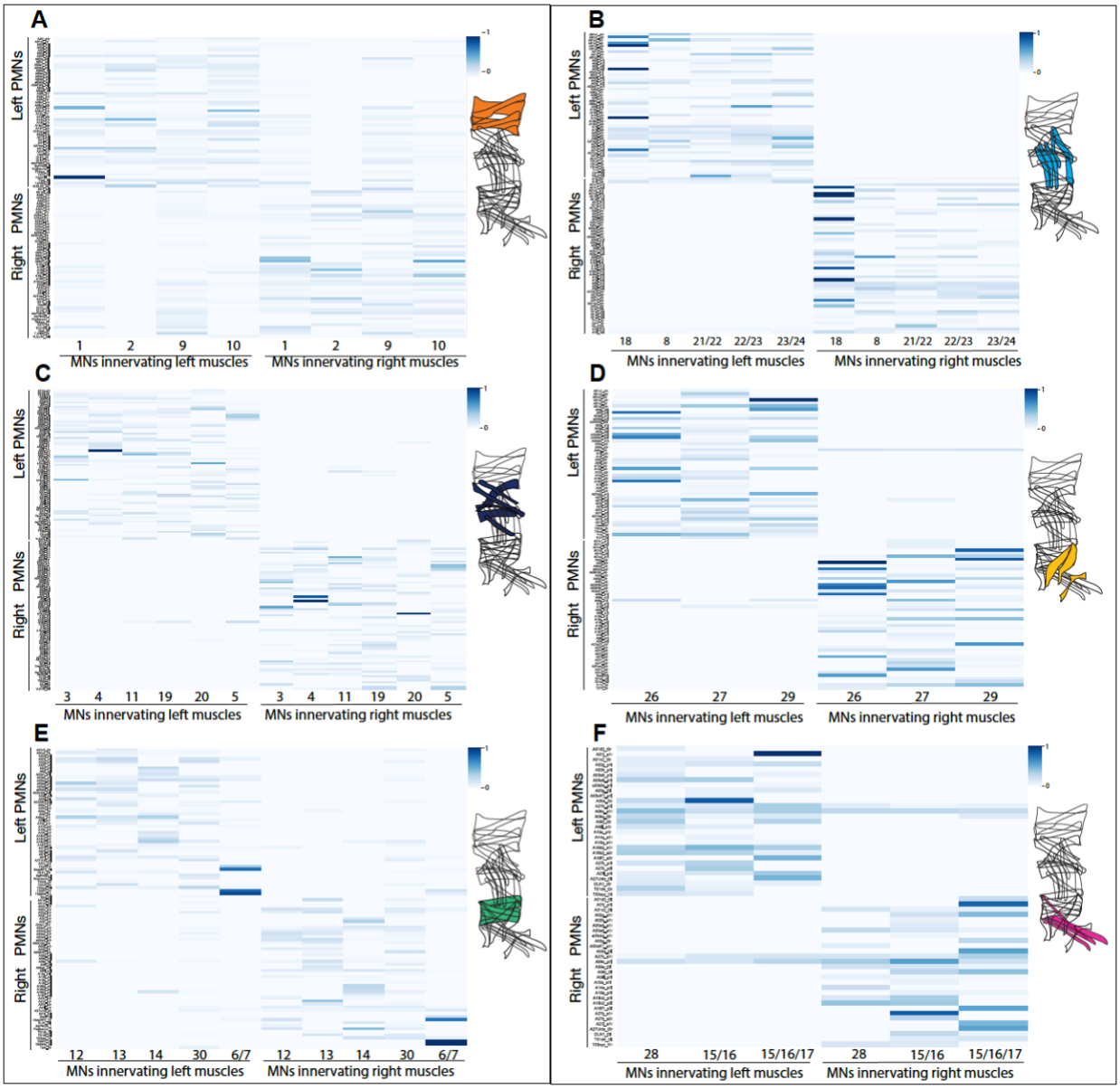


**Figure 3.8: MNs innervating midline muscles receive bilateral inputs from premotor neuron (PMN) left-right pairs.** (A-F) Heat maps representing the normalized weighted-synaptic output of a given left or right PMN (rows) onto a left or right MN (columns). Colored sketches next to heatmaps indicate the target muscles of MNs in heatmap. (A) Individual left or right MNs innervating dorsal longitudinal muscles 1, 9, and 10 receive synaptic inputs from both left and right counterparts of PMN pairs (bilateral PMN-MN connectivity pattern). While muscle 2 receives input only from left or right counterpart of any given PMN pair.

(B,C) MNs innervating lateral muscles show unilateral PMN-MN connectivity patterns. (D-F) MNs innervating ventral acute, longitudinal, and oblique muscles show some bilateral PMN-MN connectivity patterns.

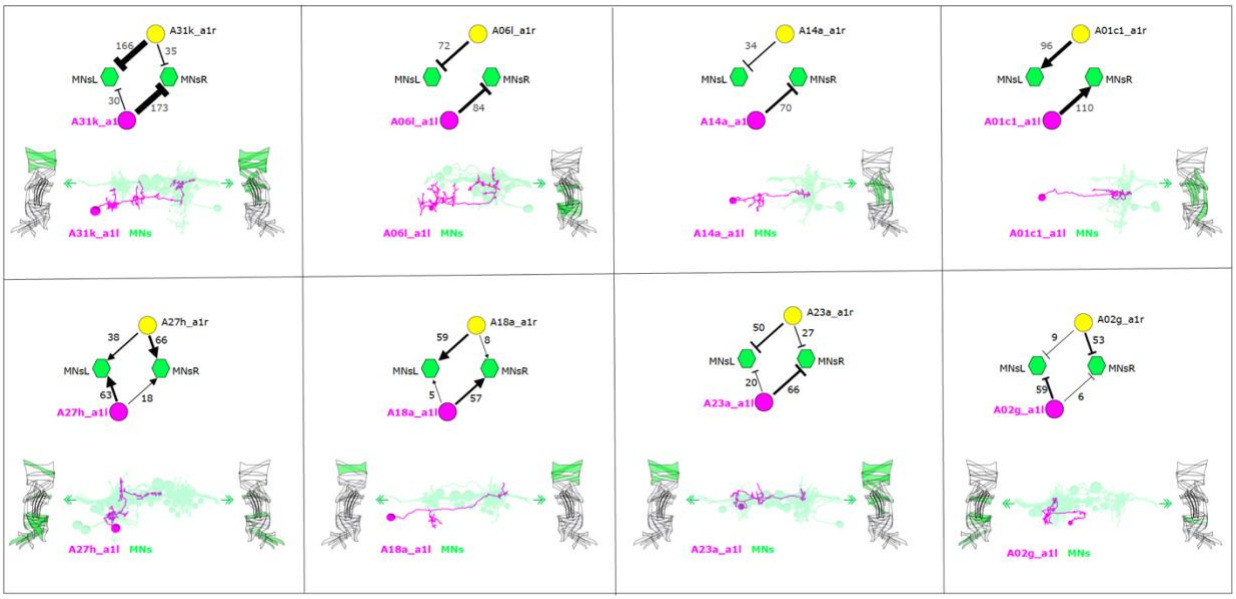


**Figure 3.9: Example PMNs demonstrate bilateral connectivity to midline muscles and unilateral connectivity to lateral muscles.** Microcircuit diagrams highlighting left (magenta) and right (yellow) PMNs' connections to left and right MNs (green) and the muscles they innervate (green). Excitatory PMNs connect to MNs with pointed arrowheads; inhibitory, flat arrowheads. Select PMNs demonstrate mostly unilateral connectivity to MNs that project to lateral muscles (first row), while others connect bilaterally to MNs that project midline muscles (second row).

## 3.4 Discussion

Escape behavior is a fundamental form of locomotion and critical for the survival of all animals. We have performed high-speed imaging of muscle activity and analyzed connectome data to identify potential motor circuitry underlying escape. Muscle activity data demonstrate that sequential muscle activity circumnavigates the larva's body during rolling, contrasting muscle activities that progress from tail to head that occur during crawling. Candidate motor circuit structures in the ventral nerve cord could support circumferential sequences of muscle contractions that drive rolling.

**Escape neuromuscular activities are distinct from other locomotor patterns**

During rolling, opposite sides of the larva contract asymmetrically. This contraction occurs synchronously along the length of the larva, leading to the characteristic C-bend of escape behavior. As the larva rolls the asymmetric contraction progresses either clockwise or counterclockwise around the larva. Therefore, we can think of escape muscle activity as a circumferential propagation of bend muscle activity. Interestingly, this circumferential sequence of muscle contractions must be generated by premotor circuits that fundamentally differ from the premotor circuits that control larval crawling. While crawling premotor circuits coordinate the timing of left-right symmetric, sequential muscle contractions along the length of the larva, the premotor circuits coordinating bending and rolling must perform left-right asymmetric, segmentally synchronous muscle contractions that occur sequentially around the girth of the larva. It remains to be seen if similar excitatory and inhibitory microcircuit motifs to the ones responsible for intrasegmental and intersegmental coordination of crawling are also responsible for rolling muscle contraction patterns. The fundamental differences in muscle contraction patterns suggest that, as with distinct locomotor patterns in leech[5] , larval crawling and rolling could be generated by partially overlapping premotor circuits that demonstrate unique activity patterns based on locomotion type. Population functional imaging and genetic circuit manipulations could reveal how the larval nervous system achieves distinct escape and exploratory motor sequences.

All patterns of escape bending and rolling appear to consist of this circumferential muscle activity, with the main distinction between patterns being the sequence of muscle activation. We posit that the directionality of escape bending and rolling is first decided by combined excitation of a population of interneurons, such as in cricket wind-evoked escape[28], or by a "winner-takes-all", competitive inhibition circuit mechanism, such as in larval zebrafish looming response[143]. Then, in order to prevent continual switching between escape patterns, the chosen escape pattern must be maintained by positive feedback loops or feedforward excitatory circuits[15,31]. As in the action selection and maintenance circuits for larval hunching and bending behaviors, competitive disinhibitory and feedback disinhibitory circuits could be employed to drive the bilaterally asymmetric muscle contractions that initiate and maintain escape patterns,

respectively[15]. Transitions between simple withdrawal-like bending and more elaborate escape rolling could also rely on feedforward excitatory circuits, as observed in *C. elegans* escape[31]. A combination of excitatory feedforward and competitive inhibitory circuits drives the flexible, context-dependent switching between freezing and flight behaviors in mice[33,38]. Together, these neural circuit templates across taxa provide multiple possibilities for what neural circuits could control: 1) bend selection, 2) roll initiation, 3) roll maintenance, and 4) flexible direction switches in Drosophila larval escape sequences. Future connectomic and behavioral screening data could identify these circuits.

Our imaging data demonstrate that muscles from different segments enter the bend synchronously and that contractions of segmentally homologous muscles are similarly synchronous. Our ability to identify patterns of muscle activity during rolling was greatly aided by the further development of dual-color SCAPE. SCAPE microscopy has previously captured high-speed, high-resolution, single-color data of muscles in the larva[144], and high-speed, high-resolution ratiometric data demonstrating proprioceptor activity during behavior[92]. Prior to expanding the SCAPE system to perform simultaneous dual-color imaging along the entire length of the larva, a concern was whether inactive muscles that happen to be in the bent side of the larva might falsely appear to be active due to passive compression and resultant increase in GCaMP density per area. This concern was verified when mCherry widefield images were observed. Our SCAPE setup enables simultaneous excitation and emitted signal collection from green and red channels, making ratiometric quantifications of muscle activity more accurate than imaging techniques that sequentially excite and collect from distinct fluorophores. This imaging method also allowed accurate measurement across muscles at different focal depths during freely moving behavior. Finally, because SCAPE captured muscle activity along the entire length of the larva, we were able to verify that muscle activity is synchronous across segments.

Our findings of segmental synchrony support the notion that rolling is similar to a circumferential propagation of “bend” muscle activity. This is surprising, in that previous work suggested segmental peristalsis as a mechanism for rolling: first, because larval crawling is segmentally peristaltic, we know that

neural circuits for segmental activity propagation exist in the larval neuromuscular system; second, the speed with which larvae transition from crawling into escape rolling and back into rapid forward crawling is suggestive of some priming for this mode of locomotion in circuit activity; third, there is a prevalence of segmental peristalsis in other instances of bend-and-roll behaviors, like in snake robots[124] in lamprey[125] and even in Drosophila embryos while they are developing[145]. Nevertheless, precedence for segmentally synchronous larval escape exists in the rapid escape gaits in quadrupeds, such as horses and mice [24,25]. In mice, for example, 'bounds', the most rapid gait used primarily to escape harm, involve synchronous activity of forelimbs and hindlimbs[24,39]. In both horses and mice, 'gallops' involve the near-synchronous activity of forelimbs and hindlimbs, and gradually slower gaits involve greater asynchrony across limbs[24,39]. Certain classes of commissural interneurons in the spinal cord regulate alternating patterns of limb movement, but the circuits that drive limb synchrony are yet to be uncovered[25]. However, the supraspinal nuclei that drive the choice between slower, exploratory gaits and escape gaits have been identified[39]. The premotor-motor connectivity patterns that we identified as potential drivers of larval escape could be mirrored in quadruped spinal circuits. Overlapping patterns of spinal interneuron outputs onto functionally similar motor neurons could yield near-synchronous activation, resulting in escape 'gallops' and 'bounds'. Identifying the specific premotor circuits that drive larval escape, other potential mechanisms for segmental synchrony, like gap junction-mediated coordination of motor neurons across segments[146], and the descending neurons that mediate decisions between crawling and rolling may generate deep insights into conserved principles of sensorimotor decision-making circuits.

**Motor circuit structure supports multiple functions**

During rolling we observed an alternation between moments of bilateral asymmetry and symmetry in rolling muscle activity. Specifically, moments of bilateral symmetry were observed in muscles flanking the dorsal and ventral midlines as the bending wave passes through these areas; while during bending alone, dorsal and ventral midlines show asymmetric activity. We find that the MN post-synapse distributions and the patterns of PMN-MN connectivity could support asymmetry in MNs innervating lateral muscles and

symmetry in MNs innervating muscles nearby the dorsal and ventral midlines. We propose that such circuit architecture supports bilaterally asymmetric behaviors, including the initiation and maintenance of body rotation during escape, turning, head-casting, or bending[15,54,74,147], but also bilaterally symmetric behaviors, like crawling and hunching[15]. Similar versatility of PMN-MN connections is present in the mammalian spinal cord[6,148]. For example, PMNs that are functionally upstream of trunk muscles show a bilaterally symmetric distribution, while PMNs functionally upstream of limb muscles are ipsilateral to their downstream MNs[148]. Thus, circuit structure-function relationships that must support both symmetric and asymmetric movements are conserved across species.

Connectivity-based computational modeling of neural circuits is feasible given the EM reconstructions made available for model systems[149], and recent efforts in Drosophila larvae that have revealed the connectivity and neurotransmitter expression patterns of PMNs and MNs[58]. This approach may be particularly insightful for rolling behavior because it could predict PMN activity patterns during escape. Subsequently, the necessity of those neurons for escape could be probed through genetic approaches. We predict based on vertebrate locomotion studies that inhibitory PMNs likely play a large role in mediating left-right asymmetry, while excitatory PMNs likely coordinate synchrony across segments[6]. Furthermore, biomechanical models of locomotion have demonstrated the necessity of sensory feedback and the importance of body-substrate interactions for motor control[127,150]. Combining connectome-based neural network predictions with a biomechanical model of rolling could yield insights into how sensory feedback and mechanical properties of the larva and its environment impact escape. These developments could be fruitful for soft-bodied robot design, potentially improving the set of locomotor programs these robots can generate in various environments[88]. Finally, future studies could also uncover how descending control and sensory feedback impact sequence transitions between escape bending and rolling, and forward crawling modules.

## 3.5 Acknowledgments

I am grateful to Wenze Li and Elizabeth Hillman for their technical expertise, imaging techniques, 3D-averaging code, and analysis guidance. I thank Aref Zarin for his motor expertise, genetic resources, EM connectome data, and analysis resources and training. I thank Wenze Li, Elizabeth Hillman, Aref Zarin, and Wes Grueber for intellectual input. This work was supported by a National Science Foundation Graduate Research Fellowship.

# Chapter 4: Premotor Circuits & Sensory Feedback in Escape[ϕ]

## 4.1 Introduction

Premotor and motor neurons comprise circuits in the spinal cord that can generate self-sustained, patterned movement. Ablation of distinct populations of PMNs can perturb rhythmic movement generation in ways that reveal their specific functions. For example, ablation of transcriptionally distinct subpopulations of excitatory ventral PMNs in mice prevents successful limb alternation for walking[25]. In fish, ablation of dorsal excitatory PMNs prevents high-frequency swimming while ablation of ventral excitatory PMNs prevents low-frequency swimming[41]. In larvae, silencing distinct segmentally repeated pairs of PMNs, or larger groups of segmentally repeated PMNs, has been shown to alter muscle contraction timing[53,114] and segmental coordination for peristaltic crawling[52,134]. Only one group of PMNs has been tested for necessity during escape rolling. Two pairs of PMSIs—a group of PMNs necessary for intrasegmental coordination of muscle contractions during crawling—are directly postsynaptic to DnB interneurons[56,114]. To test if any PMSIs are necessary for rolling, Burgos *et al*. constitutively silenced all twelve classes of segmentally repeated PMSI neurons and exposed larvae to global heat assay[56]. Larvae were more likely to only bend instead of bending and rolling and, upon rolling, performed fewer rolls when PMSIs were silenced[56]. This experiment revealed that silencing several PMNs did not abolish escape behavior but can impact its likelihood of occurrence. However, this work did not capture how escape kinematics were changed by this population of PMNs.

Computational models have served to make predictions about neural population activity that drives behavior for decades. More recently, neuroscientists have begun using connectome data to apply some components of the physical, biological connections between real neurons as constraints for the structure of

[ϕ] I am thankful to my collaborators for their valuable contributions to this work. Ashok Litwin-Kumar designed, provided template code and revisions, and guided conceptual development of preliminary modeling work. Amena Khair-Eldin performed neuronal silencing experiments and helped with behavioral analysis. Aref Zarin performed fictive preparation motor neuron imaging of escape. Wes Grueber, Aref Zarin, and Ashok Litwin-Kumar guided project conceptualization.

artificial neural networks[149]. Essentially, using the number of synapses—and when available, the neurotransmitter expression patterns—between individual neurons in a biological network as synaptic weights between the layers of artificial neurons in a network could provide more realistic predictions of how the brain performs specific computational tasks[149]. This has proven to be the case recently in a fly visual circuit, where predictions of neural activity are more accurate when connections between artificial neural network nodes are initially weighted to match connectome data[151,152]. Connectome reconstructions, alongside functional imaging, optogenetics, and electrophysiology in the larva, has permitted the prediction and greater interpretation of neural circuit activities in distinct contexts. For example, combining multiple microcircuit structures with a neural rate model based on connectome synaptic weights helped to predict circuit activity under distinct conditions and disambiguate how a complex, interconnected circuit mediates behavioral choice and transitions[15]. In the larval motor system, an anatomically constrained recurrent neural network model generated verifiable PMN activity predictions for driving forward and backward crawling in the first two abdominal segments of the larva, some of which have been verified as physiologically accurate[58]. This model demonstrated that pre-PMN, PMN, and MN connectivity patterns in segments A1 and A2 of the larva are sufficient to drive the rhythmic, segmentally peristaltic muscle activities that underlie forward and backward crawling. Because of the rich connectome data of *Drosophila* larval motor circuits, alongside the multitude of genetic tools available for manipulating specific neurons in larvae, determining the distinct roles of PMNs during escape behavior is an accessible goal for current research.

Sensory feedback is crucial for animals to execute and adapt movements, meeting the precise force, speed, and directional needs of movement goals under a given context. The premotor circuits that generate patterned movements are referred to as central pattern generators (CPGs). Though CPGs can generate repeated, rhythmic movement independent of descending control or sensory inputs, sensory feedback can alter both the timing of CPG activity and the magnitude of motor output across organisms, including legged insects and mammals, and limbless animals like lampreys[153]. In walking cats, for example, the CPG that controls alternation between flexor activity—the main driving component of the swing phase—and extensor activity—the main driving component of the stance phase—is modulated by sensory feedback[153].

Specifically, if artificially stimulated to mimic increased load (or amount of weight applied to the leg), proprioceptive inputs from the ankle extensor can increase the duration of the stance phase[153]. This sensory feedback-based response to increased load during locomotion is mirrored in legged insects. For example, if flies are weighted down during walking, their stance duration increases while their swing duration decreases in a sensory feedback-dependent manner[26]. If sensory feedback is removed and flies are challenged with increases in load, their stance phase increases, but their swing phase does not adjust appropriately, making it more challenging for flies to successfully walk in response to lower relative loads[26]. Soft-bodied animals also use sensory feedback to modulate CPG-based locomotion. Larval crawling is a CPG-based form of locomotion, proven by experiments showing that rhythmic motor output can be achieved in the larval ventral nerve cord without sensory input[116]. Sensory input modulates speed and magnitude of crawling motor output but does not alter the basic pattern of segmental peristalsis[91,116]. It remains to be determined if escape rolling is also a CPG-driven behavior, and whether sensory feedback mechanisms impact escape. Understanding whether and how sensory feedback impacts escape could permit a deeper understanding of the neural circuits that govern this form of locomotion.

Here, I modify a connectome-based feedforward neural network model to make predictions about PMN activities during escape. Despite caveats to this initial modeling approach, some of the model-based premotor activity predictions are congruent with behavioral and muscle activity results, specifically reinforcing the importance of bilateral, near-synchronous ventral muscle contraction in driving escape. Genetic silencing of a particular subset of PMNs does not impact exploratory or escape locomotor patterns at a global behavioral scale. Next, I refine approaches to effectively test PMN necessity during locomotor behavior. Applying these new approaches to proprioceptors during larval crawling yields novel behavioral insights into temporally restricted loss of proprioceptive feedback. Namely, larvae exhibit uncoordinated crawling and lateral instability with sustained low-intensity proprioceptor silencing. These findings provide an entry-point for further investigation into the sensorimotor circuits necessary for coordinated escape movements.

## 4.2 Methods

*Feedforward Neural Network Model:*

We built an anatomically constrained feedforward neural network based on connectome data between PMNs and MNs, and when available, neurotransmitter expression-based signs[58]. Based on the 1:1 connectivity between many type Ib MNs to individual body wall muscles, we inferred MN activity from preliminary muscle GCaMP data (data not shown in thesis), as in Zarin *et al.* We formulated our problem as a linear least-squares regression, wherein we minimized the difference between connectivity-weighted PMN activity and MN target activity (**Figure 4.1**). As in other anatomically constrained models[58,149], multiple PMN activity solutions might produce the MN-muscle activation patterns observed. However, the linearity of the model and convexity of the cost function limits the space of solutions to a single pattern. The formulation of our problem is as follows:

$$\text{minimize} \qquad L = (Cp - m)^T (Cp - m) + \lambda \mathbb{I} \text{ with respect to } p$$

$$\text{such that} \qquad Gp \leq h$$

where $L$ is the loss function, minimized to find $p$, the optimal predicted PMN activity from $C$, the connectivity matrix from PMNs to MNs, and $m$, the MN target activity. $G$ is a negative identity matrix while $h$ is a zero vector, constraining PMN activities, $p$, to be positive. To allow for MNs to be inhibited when inactive, rather than showing exactly zero output, we transferred the connectivity values between inactive MNs and PMNs from our matrix $C$ to our matrix $G$. To prevent PMN activity from exceeding biologically feasible firing rates, we introduce, a regularization term $\lambda$ to our loss function. Convex optimization was performed analytically using interior point methods (http://cvxopt.org/).

From this feedforward neural network, we predicted the PMN activities of two adjacent segments of the VNC with reconstructed PMN-MN connectivity patterns. Multiple hypothetical and GCaMP-only imaging-based muscle activity patterns were used to infer MN target, m. Validity of PMN predictions were then assessed by visually comparing Cp* to m. Python codes for this model are available at the following Github repository: https://github.com/cooneypc4/thesis_modelcodes_2022 .

*Fly Stocks:*

| **Reagent type (species) or resource** | **Designation** | **Source or reference** | **Identifiers** | **Additional information** |
|---|---|---|---|---|
| Genetic reagent (*Drosophila melanogaster*) | w1118 | | | Global heat + vibration assay line |
| Genetic reagent (*Drosophila melanogaster*) | OK6-Gal4 | BDSC | 64199 | Pan-motor neuron line |
| Genetic reagent (*Drosophila melanogaster*) | UAS-GtACR1-EYFP | Mohammed *et al.*, 2017 | 92983 | Optogenetic silencer, most sensitive to green light |
| Genetic reagent (*Drosophila melanogaster*) | UAS-Kir2.1-EGFP | BDSC | 6595 | Constitutive silencer, inward rectifying potassium channel |
| Genetic reagent (*Drosophila melanogaster*) | 36G02-Gal4 | BDSC | 49939 | A27h line |
| Genetic reagent (*Drosophila melanogaster*) | 221-Gal4 | Grueber *et al.*, 2003 | Flybase ID: FBti0187661 | Proprioceptor silencing; expressed in cI (ddaE, ddaD, vpda) and cII (vdaC) neurons; |

| Reagent type (species) or resource | Designation | Source or reference | Identifiers | Additional information |
|---|---|---|---|---|
| | | | | off-target brain and VNC expression present |
| Genetic reagent (*Drosophila melanogaster*) | 13xAop-Chrimson-mVenus | BDSC | 55137 | Optogenetic activator for Goro-LexA activations |
| Genetic reagent (*Drosophila melanogaster*) | 69E06-LexA | BDSC | 54925 | Goro-LexA line |
| Genetic reagent (*Drosophila melanogaster*) | 13xAop-Chrimson-mVenus; Goro-LexA/cyo; 20xUAS-GtACR.EYFP/T6 | Grueber lab | | Generated for future work stemming from this project |

*Behavior Experiments:*

For behavior experiments, flies were reared at 25 ˚C and tested as third instar larvae. Larvae were only tested once. Behavior experiments were conducted using the FIM, camera, heat, and LED setup as described in **Chapter 2**. Escape behavior and crawling behavior videos were acquired at 50 and 10 frames per second, respectively.

Global heat & vibration assays during constitutive PMN silencing were performed as described in chapter 2. For optogenetic experiments, two rings of green (525 nm) LED lights (WFLS-G30 × 3 WHT, SuperBright LEDs) of 5 inches and 8 inches diameter were placed approximately 5 inches underneath the FIM table. LED brightness was programmed for experiments using custom code in ARDUINO, as the

LEDs' pulse width modulation was controlled by an ARDUINO Mega 2560 board. For 100% proprioceptor or PMN silencing experiments, green LEDs were active at 1060 uW/mm$^2$. For 75%, 800 uW/mm$^2$; for 50%, 530 uW/mm$^2$; for 15%, 115 uW/mm$^2$; for 2%, 20 uW/mm$^2$. Power measurements were acquired with a ThorLabs PM100D with S120VC sensor for blue and UV (200nm - 1100nm range) (**Table 4.1**). An additional tracker IR LED (TSHA4401, Vishay Semiconductor Opto Division 875 nm) was mounted within the camera field of view to allow exact knowledge of when colored LEDs were on. Pulse-timing for motor neuron and proprioceptor silencing experiments occurred in 5 second bouts with 5 second gaps in between.

**Table 4.1: Optogenetic LED Pulse Width Modulation to Power Output**

| LEDs (nm) | 1% PWM, inner only (uW/mm^2) | 1% PWM | 2% PWM | 15% PWM | 25% PWM | 50% PWM | 75% PWM | 100% PWM |
|---|---|---|---|---|---|---|---|---|
| Red (650) | 10 | 30 | 40 | 290 | 470 | 960 | 1450 | 1920 |
| Green (525) | 4.5 | 10 | 20 | 115 | 270 | 530 | 800 | 1060 |
| Blue (470) | 10 | 20 | 40 | 160 | 540 | 1090 | 1660 | 2230 |
| UV (397) | 1.35 | 4 | 8 | 60 | 103 | 210 | 310 | 412 |

Larvae that failed to move at all during trials were excluded from any analysis. Bend and roll probabilities, number of rolls, roll latency, and bend and roll direction changes were quantified manually by evaluating TIFF stacks in FIJI (https://imagej.net/Fiji). Crawling behavior was quantified using FIMTrack[154]. The following parameters were quantified: velocity, spine length, right bend, perimeter, left bend, go phase, distance travelled, and coiling.

Curvature analysis was performed on PMN silencing data as in Burgos *et al.*[56] and as described in **Chapter 2**. Curvature index threshold-based analysis of overall body curvature and rotational speed were extracted as in **Chapter 2**. Statistical analyses of bend-roll quantifications and of crawling FIMTrack-based quantifications were performed using custom programs written in MATLAB. Wilcoxon Rank Sum tests were used to compare group metrics. Matlab codes for behavioral analysis are available at the following

Github repositories: https://github.com/cooneypc4/larval_escape_manuscript & https://github.com/cooneypc4/thesis_behavcodes_2022 .

## 4.3 Results

### Feedforward neural network for predicting premotor circuit activities during escape

Based off the connectome data and successful use of modeling for predicting premotor activities in Zarin *et al.*[58], we sought to combine the premotor-motor connectome data and escape muscle activity imaging data to make predictions about which PMNs would be active during and contribute most to larval escape. Though the recurrent neural network model of the larval motor system could be applied to escape rolling, we opted to simplify the complexity of our model for making PMN activity predictions by considering a backwards inference of premotor activity from muscle activity alone, rather than including inter-PMN connections (**Figure 4.1A**). Namely, we used a feedforward neural network structure constrained by connectome data to find optimal values of PMN activity. Optimal PMN activity patterns were selected by fitting a least-squares regression between MN target activity and the combined PMN predicted activity and connectivity weights (**Figure 4.1B**; see **Methods**). Additional constraints were added to the model to enforce the prediction of non-negative PMN activities, to prevent activity predictions with excessively high magnitudes, and to allow MNs to exhibit zero activity or be inhibited when not contributing to a MN target pulse (see **Methods**).

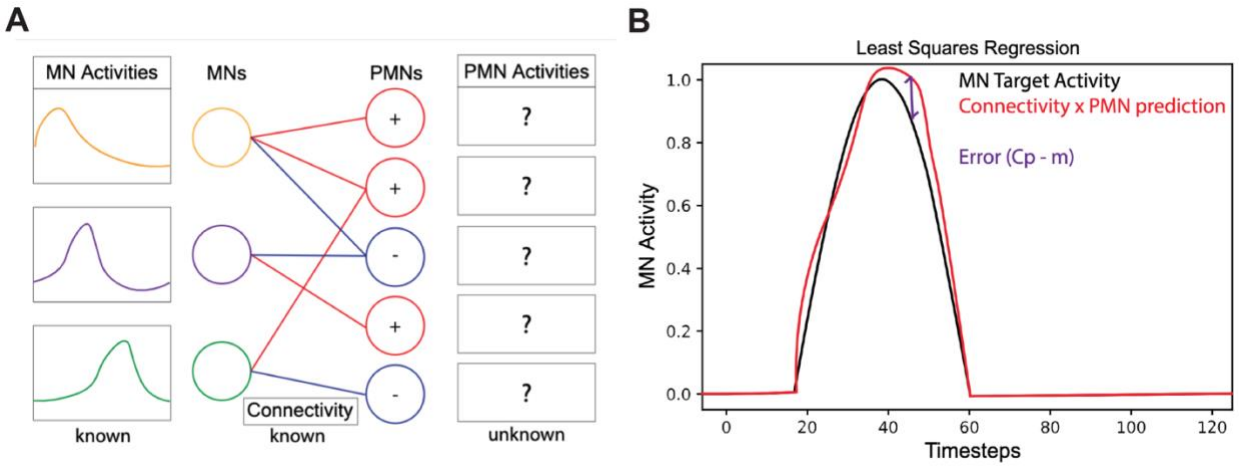

**Figure 4.1: Overview of feedforward neural network for predicting PMN activities during rolling.** (**A**) Schematic illustrating concept behind feedforward neural network, where MN activities are known (from observed or hypothetical muscle activity patterns that occur or could occur during escape), PMN-MN connectivity is known (EM reconstructed synaptic weights and neurotransmitter signs), and PMN activities driving escape are solved for. (**B**) Rather than fitting PMN activity to find a direct equality for MN target activity, the cost function of the feedforward neural network is a least-squares regression equation, where the difference between MN target activity activities and combined connectivity matrix and PMN activity predictions is minimized. This formulation was introduced because a direct equality (Cp = m) was not able to be computed by our model.

Multiple hypothetical and data-based MN target activities were used to generate PMN activity predictions. The data-based MN target activities for these initial modeling experiments were grounded in preliminary muscle activity imaging experiments, where larvae expressed only GCaMP6f in their muscles. Unlike subsequent dual-color SCAPE data where ratiometric calculations could represent activity more accurately, these data served as a coarse readout of the muscle activity pattern during rolling behavior. Many of these hypothetical motor patterns involved a circumferential progression of activity through the body wall muscles—and therefore, the type Ib MNs that innervate them. Sine wave pulses were used to model sequential MN onset and offset in most iterations (**Figure 4.2**), as in Zarin *et al.*, while a combination of sine wave pulses and tonic square waves were used to model potential tonic and phasic muscle activity during escape rolling (data not shown).

The neural network, though unable to predict probable PMN activities given too few constraints, allowed us to draw insightful conclusions about larval motor circuits and how they might drive this behavior. First, the model could not successfully recapitulate a MN target pattern in which every single muscle was activated with a simple sine wave on-off pulse in a circumferential sequence (**Figure 4.2A**). This was the case for circumferential waves comprised of individual onset times for every single muscle and its respective type Ib MN (data not shown), and for circumferential waves comprised of fewer muscle groups (**Figure 4.2A**). The hypothetical MN target patterns that the model could successfully recapitulate consistently involved fewer subgroups of coactive muscles. This suggests a relative difficulty of controlling individual muscles rather than coactivating groups based on how the larval motor system is structured.

Interestingly, when individual MNs that could not recapitulate the desired MN target output were eliminated one-by-one, the MNs that the model could drive pulse activity in individually were most of the muscles that are differentially recruited during forwards versus backwards crawling (*2, 11, 19, 15, 16,* & *17* **vs.** 1, *2, 11, 19, 15, 16, 17*, 26 & 27, respectively[58]), suggesting that the premotor-to-motor connectivity of these particular muscles allows greater flexibility in their recruitment order compared to other motor neuron-muscle pairs.

Second, the model also could not recapitulate MN target activities derived from preliminary GCaMP-only muscle imaging data. Based on individual muscle GCaMP levels across segments, some muscles were categorized as being tonic (modeled as constant square-wave pulse throughout the roll) or low phasic (modeled still as a sine wave pulse, but with lower magnitude than other muscles). Neither of these types of muscle group activations could be successfully recapitulated by the model (data not shown). Further, a GCaMP-based MN target pattern with as few as nine muscle groups that allowed other muscles to be passive (set to zero) also could not be recapitulated by the model (**Figure 4.2B**). These negative results could be in part due to brightness differences in GCaMP-only data being based on expression rather than based on activity level—a reason for utilizing dual-color muscle imaging data to set MN target patterns. Consistently, however, the model could recapitulate sparse MN activation patterns with coactivity of left and right ventral oblique muscles during rolling (**Figure 4.2C**). The muscle activity that could be recapitulated in this iteration of the model pointed to an interesting underlying pattern: the MNs that drive muscles 15, 16, 17, 21, 22, & 28 show relatively little shared excitatory PMN inputs with MNs outside of this grouping (**Figure 4.2D**). Therefore, these ventral midline- and lateral-projecting MNs could be easily co-driven with each other and driven independently of other MNs through excitatory input alone. Combined with the ventral side curvature results (**Chapter 2**), the ventral muscle symmetry in rolling and roll initiation, and the relatively high magnitude ventral muscle activity results (**Chapter 3**), these findings support a crucial role for ventral oblique muscles in performing escape. We predicted that if this iteration of the model is similar to ground truth rolling, then PMNs like A27h—that innervate primarily ventral

oblique muscles and are predicted to be active in this iteration of the MN target activity (**Figure 4.2E**)—should contribute to generating escape.

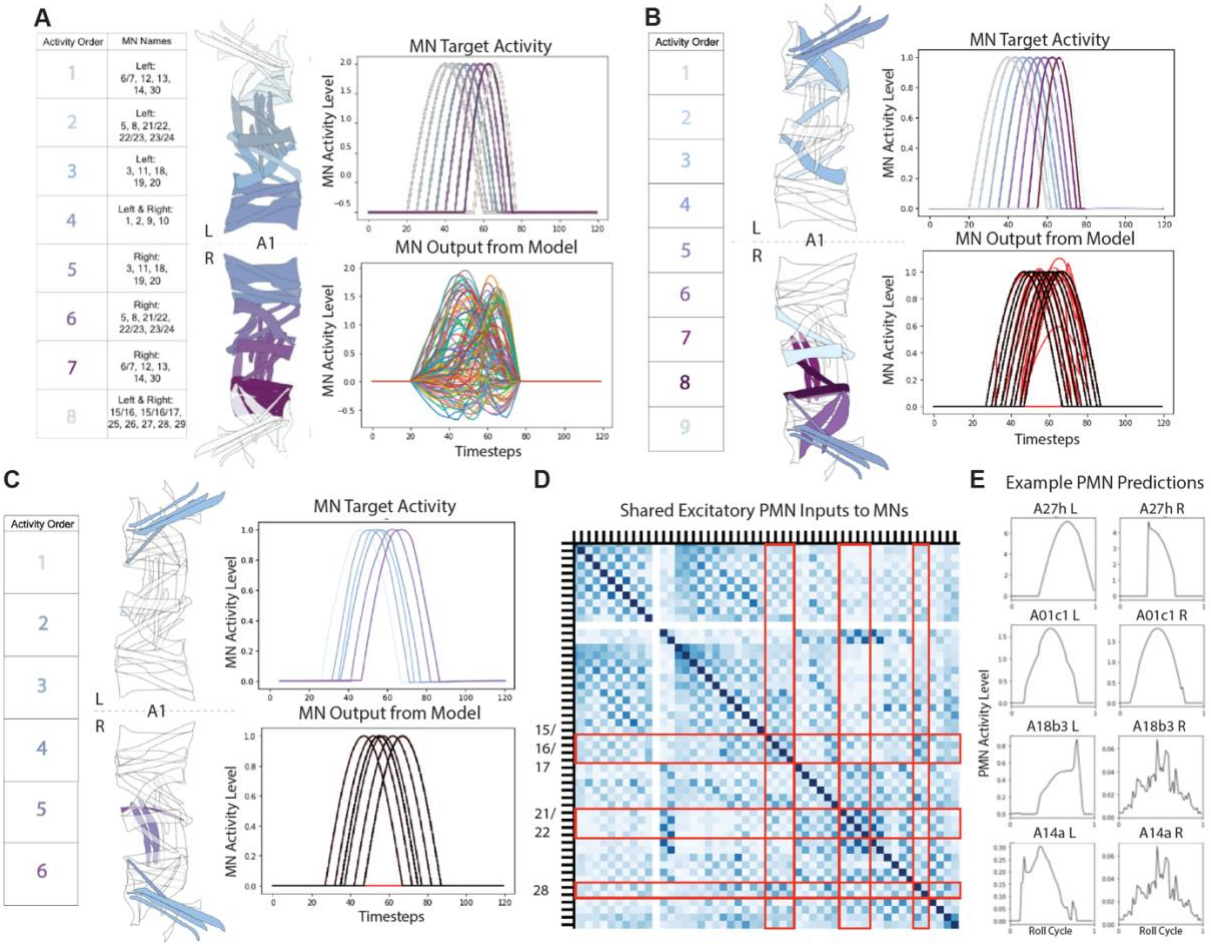


**Figure 4.2: Feedforward neural network emphasizes key motor recruitment features for larval locomotion.** (**A**) Hypothetical MN target activity pattern, consisting of 8 coactive muscle groups coordinated in a circumferential progression, cannot be recapitulated by the feedforward neural network model. (**B**) GCaMP-only muscle imaging data-based MN target pattern where some muscles are explicitly modeled as passively compressing could not be recapitulated by the feedforward neural network model. (**C**) Very sparse MN target pattern involving left-right ventral oblique symmetric contractions could be recapitulated by the model. (**D**) Correlation matrix showing how many excitatory PMN inputs each MN shares with other motor neurons in segment A1. Red boxes highlight the muscles deemed active by MN target pattern in 4.2C, and show lower shared excitatory PMN inputs with other non-target MNs. (**E**) PMN activity predictions from the model when fitted to the MN target pattern in 4.2C. These particular predictions are for PMNs previously identified as contributing to forward or backward crawling.

## Towards probing premotor neuron function in escape

Next, I sought to identify PMNs that actively drive escape rolling. Because of the recent EM reconstructions of each PMN in the first abdominal segment of the larva[58], we could identify candidates that either primarily demonstrate bilateral connectivity to motor neurons targeting midline muscles or unilateral connectivity to motor neurons targeting lateral muscles (**Figure 3.9**). Because near-synchronous activity of midline muscles occurs during escape rolling initiation and maintenance, I predicted that candidate bilaterally-projecting PMNs are most crucial to escape. Further, because the ventral side of the larva is the most bent during rolling, the ventral muscles show strong activity in the bend, and ablating ventral muscles abolishes other larval behaviors[103], I anticipated that excitatory PMN A27h would play a fundamental role in escape. Specifically, I hypothesized that silencing A27h PMNs would decrease roll probability, decrease amount of curvature during rolling, and potentially increase behavioral switches—whether through bend or rotation direction changes—because of difficulty maintaining roll motor activity.

To test these hypotheses initially, we constitutively silenced A27h PMNs and exposed larvae to the global heat and vibration assay to induce escape behavior. Surprisingly, we found that silencing A27h did not significantly impact roll probability, amount or latency of rolling, behavioral switches, or amount of curvature during rolling (**Figure 4.3A-H**). Previous work mapped A27h connectivity and demonstrated that it provides intersegmental excitatory input to an inhibitory PMN[52]. While the inhibitory PMN that A27h connects to is necessary for normal peristaltic wave propagation speed during crawling, the impact of A27h on crawling has not been measured[52]. To determine if global locomotor behavior is impacted by silencing A27h and to test whether temporally precise silencing is more impactful to ongoing motor behaviors, we optogenetically silenced A27h neurons during crawling. We found no impact on experimental group locomotion parameters, though we did observe some mild, statistically insignificant locomotor changes in control larvae in response to the optogenetic stimulus (**Figure 4.3I-K**). Overall, silencing one PMN pair per segment did not cause observable behavioral changes, though further testing with more precise measurements of movement, like muscle contractions, could better elucidate PMN roles in escape.

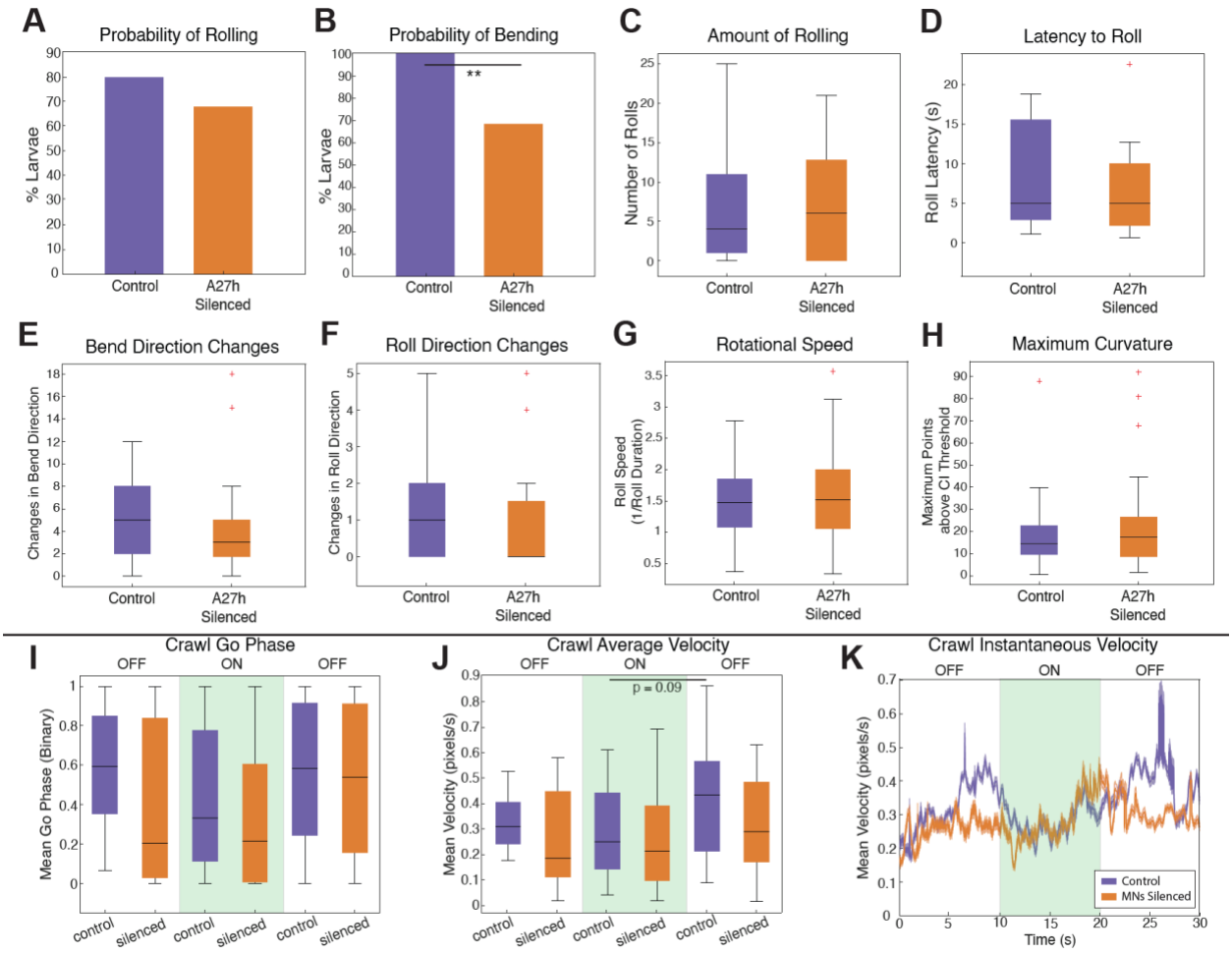


**Figure 4.3: Effect of silencing A27h on locomotion.** (**A-H**) Roll metrics did not differ significantly in larvae with constitutively silenced A27h PMNs, except for bend probability (control, 36G02-Gal4/+: n = 25 larvae; 119 rolls; experimental, 36G02-Gal4, UAS-Kir2.1: n = 9; 93 rolls). (**I-K**) Crawling metrics also did not differ significantly in larvae with constitutively silenced A27h PMNs (control, 36G02-Gal4, UAS-GtACR, ATR- : n = 15; experimental, 36G02-Gal4, UAS-GtACR, ATR+ : n = 15). P values are indicated as **p<0.01, or reported directly if p<0.1, as determined by Wilcoxon Rank Sum Test.

To establish a more precise protocol for neuron silencing during locomotion, we tested different light intensity levels for our optogenetic stimulations on larvae expressing an optogenetic silencer in a pan-MN pattern. As anticipated, when all MNs were silenced, the larvae froze and visibly elongated, demonstrating full-body muscle relaxation (data not shown). We compared MN-silenced locomotor behavior to control larvae to determine the light intensity level that would effectively silence neurons without otherwise impacting behavior. We found that, at 15% LED brightness, motor neuron-silenced

larvae decreased velocity (**Figure 4.4**). This effect appeared stronger at 50% and 75% LED brightness, but these higher brightness values also impacted control larvae (**Figure 4.4**). This experiment provided a more precise framework for effective, temporally precise optogenetic silencing of neurons during larval behavior.

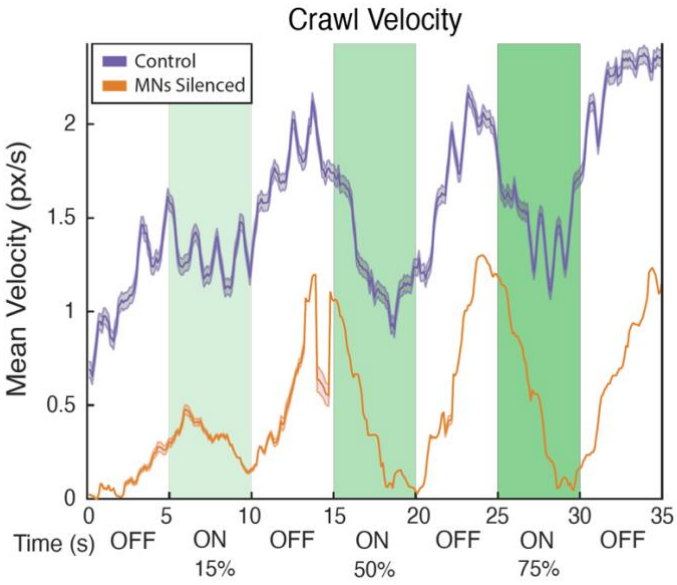


**Figure 4.4: Effect of motor neuron silencing on larval crawling.** Motor neuron silencing experiments performed at different light intensities demonstrate that optogenetic silencing of motor neurons at as little 15% LED brightness results in decreased crawling velocity. Both control larvae and motor neuron-silenced larvae show decreased velocity to 50% and 75% LED brightness values. Control, OK6-Gal4, UAS-GtACR, ATR+: n = 5; experimental, OK6-Gal4, UAS-GtACR, ATR-: n = 4.

### Towards probing the role of sensory feedback in escape

Our negative results from silencing A27h PMNs during exploratory and escape behaviors, alongside experimental results that raised the possibility that sensory feedback might be necessary for larvae to perform escape, encouraged us to silence proprioceptors during locomotion. Proprioceptors collectively tile the entire course of segmental contraction and stretching during crawling with activity [91,92]. Additionally, proprioceptors asymmetrically encode turning and bending movements in the freely moving larva[91,92]. While the MN and PMN activities that drive segmentally peristaltic larval crawling can be replicated in a fictive preparation, where the brain and nerve cord are isolated from the body, preliminary attempts to replicate escape rolling motor circuit patterns in a fictive preparation have proven unsuccessful

(data not shown). In response to optogenetic Goro activation, the isolated ventral nerve cord demonstrates asymmetric MN activity—where either the left or right motor neurons are activated, likely replicating "bend" behavior—but no further pattern of MN activity is observed (data not shown). Given proprioceptors' roles in encoding and promoting crawling coordination and speed[91,92,116], it is possible that the roll motor sequence is not fully recruited until proprioceptors send a "bend accomplished" signal to roll circuits, or that proprioceptors encode circumferential muscle contractions mid-roll, allowing larvae to select from other motor patterns in response to noxious stimuli if they do not successfully bend or roll.

We sought to test the role of sensory feedback in escape locomotion by silencing different populations of proprioceptors during larval escape. However, optogenetic proprioceptor silencing during larval locomotion has yet to be demonstrated. Temperature-dependent silencing of different populations of proprioceptors results in slower propagation of peristaltic segment contraction and intensified segment shortening[91]. To first establish the behavioral impacts of more temporally precise proprioceptor silencing on larval crawling, we performed optogenetic silencing of 221-Gal4, a genetic line with expression in class I proprioceptors that, when silenced using expression of a temperature-sensitive channel, results in mild decreases in segmental peristalsis speed[91]. We observed three main phenotypes during our proprioceptor silencing: head-casting (**Figure 4.5A**), uncoordinated S-shaped crawling and inability to remain upright (**Figure 4.5B**), and occasional escape rolling (**Figure 4.5C**). Interestingly, the S-shaped crawling and inability to remain upright are reminiscent of a phenotype observed when a pan-sensory neuron line is silenced with temperature-dependent methods[91]. This could suggest that sudden proprioceptor silencing has greater impacts on locomotion than more gradual temperature-dependent silencing techniques. Notably, 221-Gal4 is also expressed in unidentified neural populations in the larval brain and ventral nerve cord, a feature that could explain any of these behavioral phenotypes and that highlights a need for more precise neural manipulations of sensory feedback circuits during larval locomotion. When videos were tested for velocity differences and other general locomotor features using FIMTrack[154], no significant differences were observed between experimental and control groups. Future analysis could quantify curvature changes and number of sideways rotations during proprioceptor-silenced crawling.

Though genetic lines with more precise targeting of proprioceptors could be generated to improve experiments, this work has demonstrated initial optogenetic stimulus conditions that could effectively impact proprioceptor activity during escape. Further, I generated a new line permitting simultaneous optogenetic activation of Goro neurons to induce escape and optogenetic silencing of any Gal4- or split-Gal4 premotor or proprioceptor lines of interest (see **Methods**). Together, these developments make it possible to better test the sensorimotor circuit mechanisms that permit successful escape.

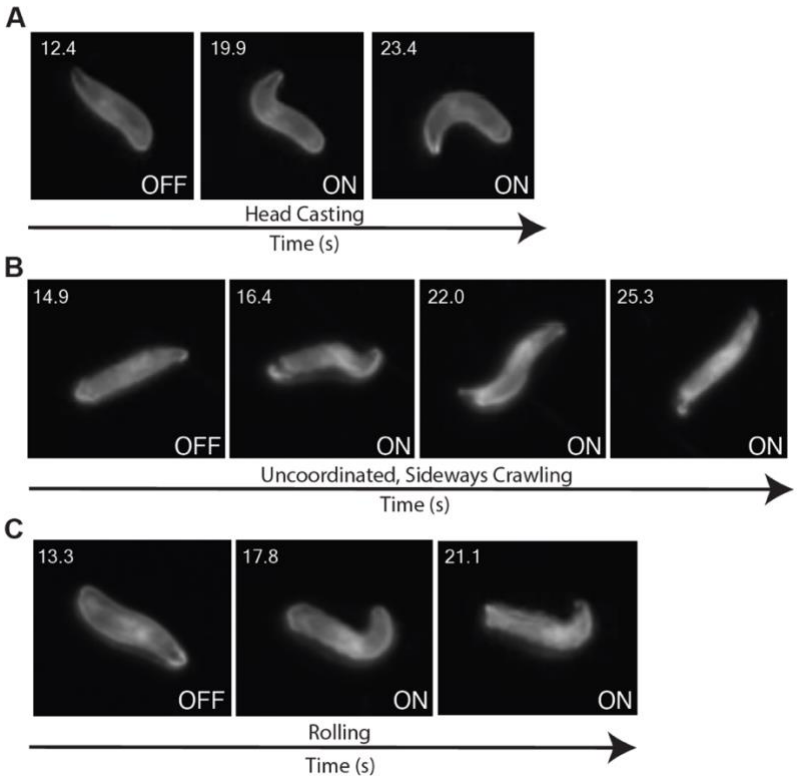


**Figure 4.5: Effect of proprioceptor silencing on locomotion.** (**A-C**) Optogenetic silencing of 221-Gal4 neurons results in (**A**) head-casting (n = 3/8), (**B**) uncoordinated sideways rotations and S-shaped crawling (n = 4/8), and (**C**) rolling (n = 3/8).

## 4.4 Discussion

Uncovering the specific components of motor and sensory feedback circuits that drive movement is essential for understanding the mechanistic basis of behavior. Here, I have applied initial approaches to move from understanding the kinematics, muscle activities, and motor circuit structures that comprise escape to identifying the specific sensorimotor circuit mechanisms that drive escape. My preliminary

modeling results confirm the connectivity-based individuation of specific muscles in larval behavior, and further highlight the likely importance of circuits that drive ventral oblique muscle coactivity in escape locomotion. Initial PMN silencing results imply that escape could be robust to perturbation of single classes of segmentally repeated pairs of PMNs. Proprioceptor silencing experiments demonstrate the potential of temporally precise stimulation tools to uncover more specific roles of sensory feedback circuits during larval behavior. The neural silencing experiments during behavior help to optimize stimulus parameters for future manipulations.

In this chapter, I demonstrate how a connectome-constrained feedforward neural network could predict PMN activities based on muscle activity patterns. The preliminary results from this model highlighted that some MNs share less excitatory PMN inputs than others, allowing them to be more easily independently controlled than other MNs. Of note, the ventral oblique muscles—muscles that are among the more strongly activated during rolling behavior, show distinct activity patterns during the transition between bending only to bending and rolling, and correspond with the region of the body that is most bent during larval rolling—show minimal shared excitatory PMN input with other muscles and are successfully recruited across multiple hypothetical muscle activity patterns with the feedforward neural network. This finding is congruent with the ventral obliques being recruited in distinct coactive muscles groups during forward versus backward crawling[58].

Notably, multiple additional constraints would help to optimize this model in the future. First, the results presented here were generated using GCaMP-only muscle imaging data, hypothetical muscle activity patterns, or some combination of the two. Though some of the tested patterns considered the possibility of sustained or low-level activity in subsets of muscles, none of the tested patterns reflected the muscle activity later measured via our dual-color imaging data. Specifically, from dual-color SCAPE data, we found that rolling involves high baseline activity in all muscles even on the stretched side of the larva, with higher magnitude activity when muscles rotate through the bent side of the larva. This MN output pattern has not yet been tested with the model. Further, because the rotational velocity of the larva's body varies during a single roll cycle, instead of using evenly spaced sine waves to craft MN target activity, MN

outputs should reflect the variable onset times and durations of muscle activity that occur during rolling. Using the specific dual-color findings from **Chapter 3** would allow us to make better predictions with our model.

Even with better constrained type Ib MN output, this model was generated agnostic to at least four other motor circuit features that could contribute to escape roll generation. First, type Is MNs that innervate large groups of muscles were not included in this model. One possibility is that type Is-based, large muscle group activation serves to drive the high continuous baseline activity observed in muscles during rolling. This would closely mirror observations for the roles of tonic vs. phasic motor neuron activation observed in mammalian motor unit drive, adult *Drosophila* flight and walking control[105,106], and crayfish escape behavior[102,107]. Such a division of function for type Is and type Ib MNs during behavior would be consistent with recent observations of how type Ib and type Is MNs differ physiologically[102], and would provide the first testable functional role of type Is MNs in larval behavior[102]. Second, because rolling behavior is segmentally synchronous along the entire larva, unlike crawling behavior, a two-segment EM reconstruction of the larva's premotor-motor synapses could provide insufficient constraints for inferring how intersegmentally connected premotor and motor circuits generate rolling. Long-range connections that currently remain unmapped and have unknown neurotransmitter identities could play a role in driving segmentally synchronous motor output. Third, type II octopaminergic and type III insulin-like peptide-releasing MNs could provide a modulatory signal that contributes to the high baseline of muscle activity observed during rolling. Interestingly, the type III MNs only innervate mid-segments of the larva—those which appear to have the highest magnitude muscle activity during rolling, and those that, when contacted by parasitic wasps, are most likely to induce escape rolling. Fourth, gap junctions between motor neurons could also contribute to the high baseline muscle activity throughout rolling, particularly in the midsegments where they have been shown to mediate motor signal propagation between segments A6 to A4 in fictive crawling[146], or could potentially contribute to the circumferential propagation of muscle activity. Some combination of these motor circuit components likely drives escape.

Another approach for uncovering the general circuit mechanisms that could drive the segmentally synchronous, bilaterally asymmetric circumferential wave of muscle activity in escape—without having to make and test assumptions about the above-mentioned unknowns—could be to model more general segmentally repeated excitatory and inhibitory subpopulations. Such a model would allow observation of how intersegmental and bilateral connections between such subpopulations could generate and shape escape-like motor output. This type of neural rate model successfully recapitulated left-right symmetric segmental propagation of crawling before sufficient connectome, muscle activity, and premotor circuit activity data was available for constraining and validating model-based predictions[155]. Essentially, by coupling outputs of neighboring excitatory and inhibitory equations in a segmentally repeated manner and providing an external input value to either of the end segments, Gjorgjieva *et al.* were able to build a model that successfully demonstrated self-sustained forward and backward segmental waves of activity that, when paired with a mechanism for sensory feedback in the model, closely resembled crawling kinematic output[155]. This model then could be used to elucidate the types of connections required to induce segmental peristalsis and left-right symmetry. Specifically, linking a bilateral pair of segmentally repeated E-I network nodes and altering connectivity between nodes demonstrated that left-right synchrony of wave propagation is most effectively maintained by E-E left-right connections[155], a feature that has since been validated by characterizing neural circuits that driving bilaterally symmetric crawl propagation[51]. Building a similarly simplistic model that abstracts away the specific neurons within the larva's motor circuits and permits more general understanding of motor control of escape could generate new hypotheses and predictions to be tested in this behavior.

My premotor neuron manipulations in this chapter failed to impact measured kinematics of escape and exploratory locomotion. This was particularly surprising because the manipulated A27h PMNs show strong bilateral innervation of ventral oblique muscles that are heavily recruited during rolling and are active during forward crawling[103]. One possibility is that the kinematic measurements performed are not fine enough to capture locomotor changes that could be occurring during escape. Using muscle imaging approaches similar to those in **Chapters 2 & 3**, either positional-only or positional and functional imaging,

could allow observation of how ventral oblique contraction timing might differ relative to other muscles during escape. A similar approach has recently demonstrated that A27h PMNs alter muscle contraction timing during crawling[156], suggesting that this level of resolution might be necessary to understand how specific PMNs impact behavior. It is also possible that escape locomotion is too robust for silencing of most specific segmentally repeated pairs of PMNs to impact coordinated movement. Reinforced by observing the high degree of excitatory PMN-MN overlapping input across MNs (**Figure 4.2D**), a substantial amount of redundant excitation to motor neurons could ensure behavioral robustness, and therefore silencing inhibitory PMNs could result in stronger behavioral phenotypes. This is corroborated by data demonstrating that the excitatory PMNs that drive antagonistic muscles during larval crawling have largely overlapping activity patterns and that the distinct timing of antagonistic muscle activation is driven by inhibitory PMNs[53]. These results, alongside evidence that silencing the inhibitory PMNs that delay A27h PMN firing during forward crawling decreases crawling speed and increases the duration of single peristaltic waves[52], suggest that inhibitory PMNs should be tested for their role in escape.

Optogenetic silencing of proprioceptors during crawling revealed that sudden loss of proprioceptive feedback has more profound behavioral effects than those previously reported[91]. Namely, previous silencing of proprioceptors using the same genetic line was performed with a temperature-sensitive silencing channel, requiring silencing to occur in a gradual onset manner before behavior was quantified[91]. The behavioral phenotypes I observed were more similar to those reported using gradual silencing of many more sensory neurons[91], and constitutive silencing of mechanosensory neurons during embryonic development has been shown to impact sensorimotor circuit formation and result in generally aberrant locomotor output[157]. Together, these data highlight the potential importance of testing sudden proprioceptor loss of function to reveal more about the precise role for real-time sensory feedback during behavior. One difficulty with testing sensory feedback necessity in behavior is that different proprioceptors encode distinct aspects of segmental contraction[92], and many of the genetic lines that drive expression in proprioceptors drive expression in multiple proprioceptors and also drive expression in off-target neurons in the brain lobes and ventral nerve cord (data not shown). One approach for bypassing these two experimental difficulties

could be to specifically silence any neurons expressing channels that are responsible for detecting different aspects of body movement[157].

Future studies should test whether and how proprioceptive feedback impacts escape kinematics. Doing so would help to clarify whether rolling is a CPG-based locomotor behavior and could provide insights into how premotor circuits drive the circumferential contraction wave that occurs during rolling. Ohyama *et al.* demonstrated that silencing a subset of proprioceptors reduces roll probability and decreases crabspeed—the speed that a larva moves perpendicularly to its anteroposterior axis—in larvae that do roll[71]. One possibility is that proprioceptor activity helps to expedite the circumferential handoff of muscle activities during rolling. This would imply a similar role for proprioceptors in rolling as their function in crawling, where their activity allows detection of segmental contraction and propagation of peristalsis to the neighboring segment[91,92]. Without proprioceptor input, this propagation is ten times slower and involves more intense segmental shortening[116,155]. Observing rotational velocity and amount of curvature during rolling could reveal if this is a function of proprioceptors in escape. Another possibility is that lack of sensory feedback during a noxious threat decreases roll probability by altering action selection circuit outputs. Specifically, proprioceptors could be responsible for detecting left-right asymmetric muscle activity during bending, as has been demonstrated via functional imaging of larval turning[92], and could be responsible for sending this asymmetric "bend accomplished" signal to downstream circuits that trigger the subsequent rolling motor pattern. Such a role for proprioception would be consistent with the negative results observed in preliminary fictive rolling experiments. Some combination of the proprioceptive input and nociceptive input could also be responsible for probabilistic switching between different behavioral responses to wasp attack[85]. This would be congruent with studies indicating that body position impacts withdrawal and escape behaviors in rats and flies[21,30]. Silencing proprioceptors and quantifying behavioral response types could inform whether such sensory feedback signals indeed impact escape locomotion.

## 4.5 Acknowledgments

I thank Ashok Litwin-Kumar for feedforward neural network coding framework and guidance through planning, implementing, troubleshooting, and interpreting model. I am grateful to Amena Khair-Eldin for performing behavioral experiments and analysis, as well as discussing experimental outcomes. I thank Aref Zarin and Wes Grueber for intellectual input and project conceptualization. This work was supported by a National Science Foundation Graduate Research Fellowship.

# Conclusions & Future Directions

How the brain converts perception and state into action remains one of the most fundamental and complex questions in neuroscience. Escape serves as an excellent model for understanding how neural circuits use sensory information to generate behavior across species. By elucidating the neuromuscular basis of escape in a model with comprehensive circuit mapping and a large toolbox of genetic resources, we can begin linking together how the nervous system processes pertinent sensory information rapidly to produce high-powered, life-saving movements. The *Drosophila* larva is an ideal model for studying sensorimotor circuit computations, given its genetic manipulability, established circuit reconstructions, robust behavioral responses, and well-studied sensory and motor systems. Altogether, the rich characterization of the *Drosophila* larva and many tools for investigating its nervous system and behaviors make it highly accessible for gaining traction on neural mechanisms underlying phenomena that are difficult to address, including action selection, behavioral sequences, and motor flexibility.

Larval escape behavior, comprised of a probabilistic sequence of C-shaped bending, lateral rolling, and fast forward crawling, stands at the nexus of detailed sensory and motor circuit investigations. Though the sensory transduction and circuit mechanisms responsible for promoting larval escape had already been well-characterized, until now, the neuromuscular basis of this behavior had not been investigated. In this thesis, I present the first detailed characterization of the kinematics, muscle activities, and motor circuit structures that comprise larval escape rolling. Through this work, I demonstrate that escape rolling is a flexible behavior, powered by sequential propagation of muscle activities around the girth and along the entire length of the larva's body. The neuromuscular coordination of this behavior stands in stark contrast to larval exploratory behavior (**Figure 5.1**); yet some features of these two forms of locomotion—like the importance of specific muscles for movement generation—are consistent. This work has combined behavioral analyses, high-speed volumetric functional imaging of muscles, and EM connectomics to uncover the principles of larval escape locomotion. Preliminary modeling and neural circuit manipulations began addressing circuit mechanisms for generating and coordinating this behavior. Further investigation

of the motor circuits, sensory feedback, and action selection mechanisms underlying escape could substantially expand our comprehension of how the brain generates behavior.

**Escape flexibility & locomotor pattern selection**

Tinbergen's conceptualization of behavior as a hierarchy of modules has proven a useful structure for identifying how finite motor circuits and muscles can yield infinite movements. With many examples of modular behaviors, muscle activities, and motor circuits identified in the literature, a new question about behavior emerges: how do neural circuits select specific motor modules in response to external and internal sensation, and how does the brain allow seamless switches between motor modules to permit flexible, adaptable behavioral outcomes? A role for descending control in action selection has been well established, yet descending control alone oversimplifies the multilevel computations that occur in the brain to yield behavior. For example, in flies and mice, context-dependent selection of freezing or flight behaviors, and even of specific gait selection, are mediated by descending control[32,33,39,40]. Hierarchical relationships, some mediated by lateral inhibitory interactions, can govern flexible switches between these behavioral modules[33]. While these examples of descending control act at the level of selecting specific behavioral modules, combinatorial descending control has been shown to mediate magnitude of motor output in flies as well[11]. However, these descending control mechanisms neglect how—particularly in behaviors like escape that may require rapid, lower-level computation for immediate withdrawal from danger—spinal circuits and descending control combine to impact behavioral output, and how smooth transitions through distinct motor patterns occur.

Larval nociceptive circuitry, successfully mapped via EM connectomics from cIV nociceptors through to Goro command neurons, consists of a multilevel circuit structure where distinct sensory modalities repeatedly converge and diverge in the ventral nerve cord and in the brain[56,87]. Though Goro command neurons reliably evoke escape, some second-order nociceptive interneurons exhibit direct connections to premotor and motor neurons[56], and others are capable of inducing escape in the absence of Goro activity[86]. Furthered by my kinematics results that demonstrate the remarkable flexibility of larval

escape behavior, especially in sensory-evoked assays, these findings encourage investigation of the balance between descending and local sensorimotor control of escape locomotion. In addition to promoting more flexibility in escape motor programs, sensory activation of escape impacts behavioral kinematics over a longer timescale. Namely, sensory-evoked escape involves a transition from bending and rolling into fast forward crawling, while Goro-evoked escape does not induce subsequent faster crawling[71]. Neuromodulators, like octopamine and serotonin, have been shown to alter locomotion in *Drosophila* larvae and adults. For example, serotonin and octopamine both modulate walking speed in adults, where serotonin is partially responsible for generating slower tetrapod gaits[158], while octopamine is partially responsible for generating faster tripod gaits[159]. Similarly, larvae demonstrate reduced locomotion speed in the absence of octopamine[160]. Given previously identified neuromodulatory nociceptive circuit components[56,89], alongside neuromodulator expression observed in type II and type III motor neurons[101], sensory-evoked escape could impact locomotor patterns, including subsequent fast forward crawling, via neuromodulatory mechanisms. Neuromodulatory impacts on the transition from rapid escape rolling into fast and then slower forward crawling would be congruent with identified neuromodulator roles in mediating walking speed and gait transitions in adult *Drosophila* locomotion[158,159]. Understanding how peripheral nociceptive circuits impact neuromodulatory control of escape remains an open question.

My kinematic analyses demonstrate that larval escape can occur as one of four patterns of combined bending and rolling. Larvae can alter either the direction of their body bend, or, less frequently, the direction of their body rotation mid-escape. The number of motor pattern switches was greatest in sensory-evoked assays, perhaps in part due to the nature of activation being global rather than localized to a single portion of the larva's body. Upon identifying the muscle activities that drive different patterns of escape and examining the premotor-motor circuit connections in the larva, a hypothesis for how the larva coordinates such behavioral flexibility emerges. If the larva is rotating in one direction but receives sensory input that it has not successfully evaded harm, it could forego transitioning to forward crawling by: 1) continuing the same, unsuccessful bending and rolling combination, 2) continuing the same bending direction, but changing which way it rotates, 3) continuing to rotate in the same direction, but changing which way it

bends. My muscle activity findings show that the larva transitions from bend-only to bend-and-roll movement by increasing bilateral muscle activity in dorsal or ventral midline muscles. PMN-MN connectivity patterns demonstrate frequent bilateral innervation of midline muscles, providing a mechanism for potential co-contraction of midline muscles but with different magnitudes (**Figure 5.2A**). Therefore, the larva's motor circuits could change the body bend direction mid-roll simply by altering which side of midline muscles receives the most input, without altering the direction of circumferential propagation (**Figure 5.2C**). Meanwhile, to change rotation direction mid-roll, motor circuits must undergo a more fundamental switch in the direction of the circumferential wave, potentially a more difficult circuit activity switch to achieve (**Figure 5.2C**), explaining the lower frequency of rotation switches observed across behavioral assays. Such switching mechanisms could stem from winner-takes-all Goro action selection interactions preferentially activating either the left or right PMN of a bilaterally-projecting PMN pair, similar to lateral inhibition circuit motifs in other action selection contexts[15,20,33]. Alternatively, because these behavioral switches occur more frequently in sensory-evoked escape, it is possible that they involve local interactions between sensory and motor circuits, or that continued sensory-weighting of one Goro neuron biases the circuit for specific directional switches. Uncovering the mechanisms for the behavioral switches observed in larval escape, alongside further circuit mapping, could lead to better understanding of how multilevel circuit computations decide motor outputs.

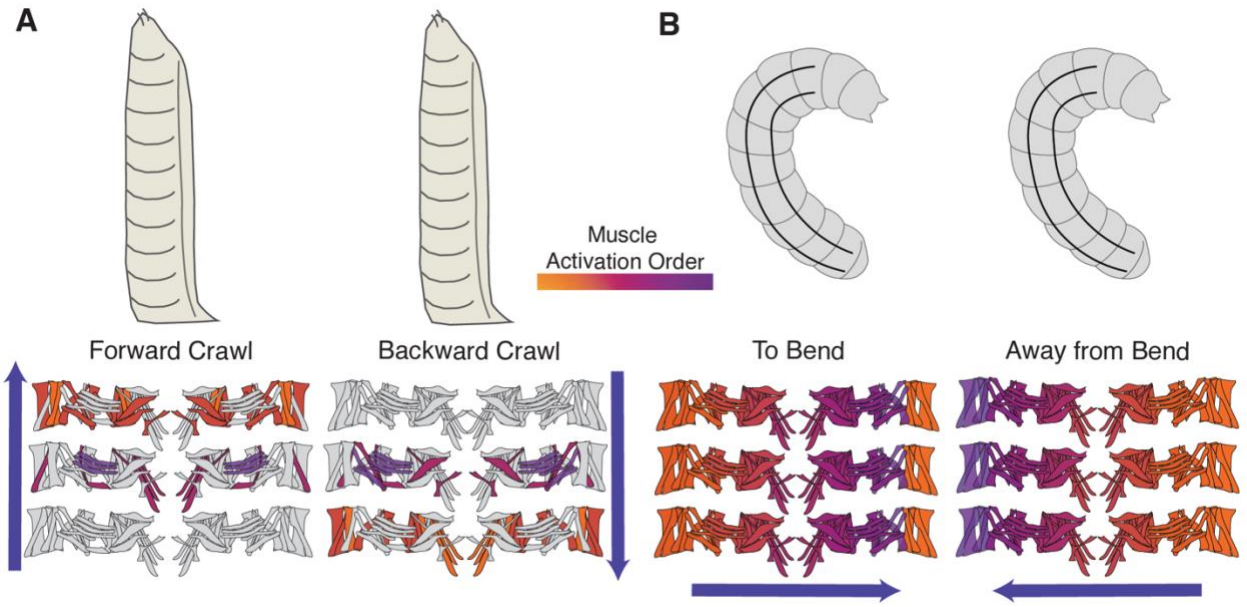


**Figure 5.1: Exploratory vs. escape locomotion muscle contraction patterns in *Drosophila* larvae.** (**A**) Schematics illustrating forward and backward crawling body movement and muscle activity sequences, adapted from Zarin *et al*[58]. (**B**) Schematics illustrating two patterns of escape bending and rolling body movement and muscle activity sequences—the "to bend" circumferential wave of muscle activity starts on bent right dorsal side, then propagates to the stretched left dorsal side and around the larva's girth; the "away from bend" circumferential wave of muscle activity starts on the bent right dorsal side, then propagates to the bent right lateral side and around the larva's girth. Orange to purple gradient indicates order of muscle activation.

### Circuit mechanisms for distinct patterns of motor coordination

The differences between larval crawling and rolling pose interesting possibilities about the circuit generation of these motor patterns. As summarized in **Figure 5.1**, crawling is a left-right symmetric, segmental sequence of muscle contractions[58], while rolling is a segmentally synchronous, circumferential sequence of muscle contractions, resulting in moments of left-right symmetry in midline muscles and asymmetry in lateral muscles. In the context of Tinbergen's modular breakdown of behavior, how the premotor circuits that coordinate specific muscle group activations during crawling would be recruited in the fundamentally different coordination of muscle activations in rolling is not immediately obvious. Previous PMN population activity imaging during swimming and crawling behaviors in the leech revealed that some PMNs are multifunctional, demonstrating the same or distinct activity patterns during two

different behaviors, while others demonstrated dedicated activity to a single locomotor pattern[5]. The observations from **Chapter 3,** that midline dorsal and ventral muscles are controlled in part by bilaterally-projecting PMNs, highlight the possibility that bilaterally-projecting PMNs could demonstrate similar functions and activity patterns during crawling and rolling. In the future, population imaging of PMNs during escape sequences could reveal fascinating insights into how PMNs with distinct activity patterns during locomotion types alter their activity patterns to transition between behaviors.

How the circumferential wave of muscle contractions that drives escape rolling is generated by premotor circuits requires further investigation. One possibility emerging from the circuit connectivity data presented in this thesis is that PMNs innervate groups of muscles in a directionally biased manner. Like the hypothesized mechanism for bend direction changes in the section above (**Figure 5.2C**), directionally preferential excitation or inhibition of neighboring muscles could generate the entire rolling muscle contraction pattern. Specifically, an excitatory PMN could innervate MNs that project to and drive contraction of multiple adjacent muscles, but with greater synaptic connectivity in one circumferential direction could mediate circumferential activity, as observed by example with A18j (**Figure 5.2B**). The opposite correlation between preferential synaptic weighting and resultant circumferential wave direction could be in effect for inhibitory PMNs, like A23a (**Figure 5.2C**). More candidate PMNs for propagating the wave around the entire circumference of the larva could be identified using connectome data. Alternatively, a different mechanism for generating a segmentally synchronous, circumferential wave could borrow from mechanisms identified in nervous system development. Across brain regions and taxa, synchronous waves of activity across neural populations impact circuit connectivity and development[161]. These waves, also observed in the developing spinal cords of fish, chicks, and mice, are frequently mediated by gap junctions between motor neurons[162]. Further, respiratory motor patterns in neonatal mice have been shown to synchronize rhythmically not only due to gap junctions between MNs, but also gap junctions between respiratory MNs and their input interneurons, allowing a more robust mechanism for synchronized activity wave generation[162]. Gap junctions in motor circuits could serve as a mechanistic basis for generating the segmentally synchronous circumferential wave of muscle activity observed in escape rolling,

as they have been identified as contributing to segmental peristalsis[146]. Observing escape kinematics in the presence of chemical gap junction blockers or in larvae with gap junction mutations could reveal if these structures contribute to segmental synchrony and circumferential wave generation[146].

In summary, the work presented in this thesis reveals the kinematic and neuromuscular basis of larval escape and sets the groundwork for uncovering circuit mechanisms of escape motor generation. In the future, expanding from these foundational data could allow a greater understanding of action selection, motor circuit multifunctionality, and behavioral flexibility.

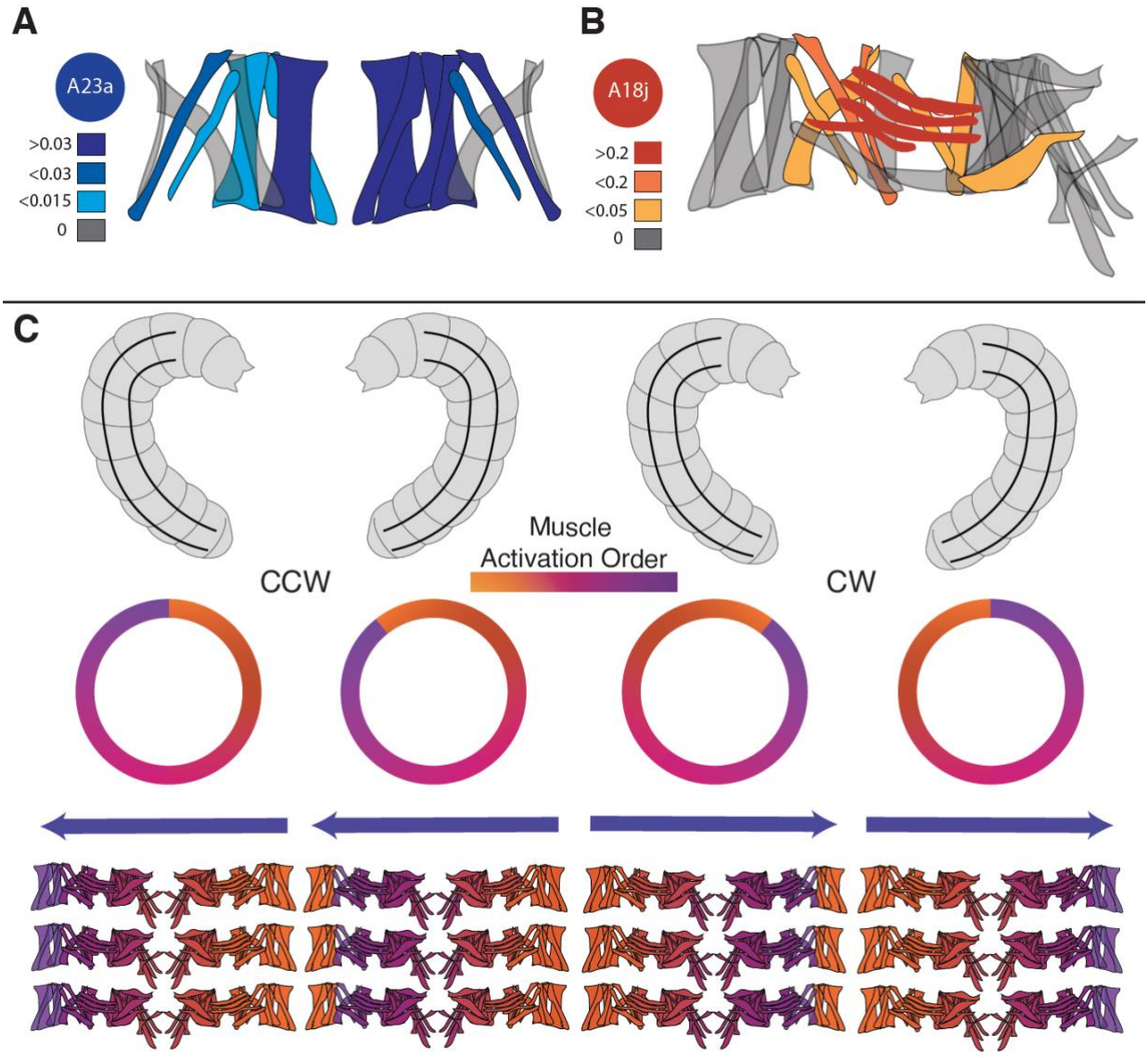

**Figure 5.2: Circuit mechanism predictions for generating escape.** (**A**) Connectome-based, hypothesized inhibitory PMN-based mechanism for promoting directional propagation of circumferential muscle activity in co-innervated dorsal longitudinal muscles, wherein preferential inhibition of right dorsal muscles by A23a-left promotes circumferential wave to propagate to left dorsal muscles. Synaptic weights are from left-only A23a PMNs. Roughly the opposite pattern of synaptic weights is observed in right-only A23a PMNs (data not shown). (**B**) Connectome-based, hypothesized excitatory PMN-based mechanism for promoting directional propagation of circumferential muscle activity in lateral muscles, wherein preferential excitation of neighboring dorsal oblique muscles (rather than ventral longitudinal muscles) relative to strongly activated lateral transverse muscles promotes ventral to dorsal contraction propagation. Synaptic weights are sum of left and right A18j PMNs. (**C**) Schematic illustrating all sequences of muscle contractions for the four patterns of escape rolling. Left two panels demonstrate cross-section and fillet prep visualizations of muscle activities that drive counterclockwise rotations (CCW). Right two panels, clockwise rotations (CW). Note that if a larva changes bend direction mid-roll, the sequence of muscle activity propagation does not change—only the magnitude of activity for the midline muscles switches before the same circumferential pattern of muscle activity resumes. Orange to purple gradient indicates order of muscle activation.

# References


1. Tinbergen, N. *The study of instinct.* (Clarendon Press, 1951).
2. Wiltschko, A. B. *et al.* Mapping Sub-Second Structure in Mouse Behavior. *Neuron* **88**, 1121–1135 (2015).
3. Riede, T. Rat Ultrasonic Vocalization Shows Features of a Modular Behavior. *Journal of Neuroscience* **34**, 6874–6878 (2014).
4. d'Avella, A. & Bizzi, E. Shared and specific muscle synergies in natural motor behaviors. *Proceedings of the National Academy of Sciences* **102**, 3076–3081 (2005).
5. Briggman, K. L. & Kristan, W. B. Imaging Dedicated and Multifunctional Neural Circuits Generating Distinct Behaviors. *Journal of Neuroscience* **26**, 10925–10933 (2006).
6. Arber, S. Organization and function of neuronal circuits controlling movement. *EMBO Mol Med* **9**, 281–284 (2017).
7. Grillner, S. Biological Pattern Generation: The Cellular and Computational Logic of Networks in Motion. *Neuron* vol. 52 751–766 Preprint at https://doi.org/10.1016/j.neuron.2006.11.008 (2006).
8. Guertin, P. A. The mammalian central pattern generator for locomotion. *Brain Research Reviews* vol. 62 45–56 Preprint at https://doi.org/10.1016/j.brainresrev.2009.08.002 (2009).
9. Purves, D. *et al. Neuroscience*. (2018).
10. Tresch, M. C., Saltiel, P., D'Avella, A. & Bizzi, E. Coordination and localization in spinal motor systems. *Brain Research Reviews* vol. 40 66–79 Preprint at https://doi.org/10.1016/S0165-0173(02)00189-3 (2002).

11. Namiki, S. *et al.* A population of descending neurons that regulates the flight motor of Drosophila. *Current Biology* **32**, 1189-1196.e6 (2022).

12. Briggman, K. L. & Kristan, W. B. Multifunctional Pattern-Generating Circuits. *Annu Rev Neurosci* **31**, 271–294 (2008).

13. Berkowitz, A. Physiology and morphology indicate that individual spinal interneurons contribute to diverse limb movements. *J Neurophysiol* **94**, 4455–4470 (2005).

14. O'Sullivan, A. *et al.* Multifunctional Wing Motor Control of Song and Flight. *Current Biology* **28**, 2705-2717.e4 (2018).

15. Jovanic, T. *et al.* Competitive Disinhibition Mediates Behavioral Choice and Sequences in Drosophila. *Cell* **167**, 858-870.e19 (2016).

16. Card, G. M. Escape behaviors in insects. *Current Opinion in Neurobiology* vol. 22 180–186 Preprint at https://doi.org/10.1016/j.conb.2011.12.009 (2012).

17. Hemmi, J. M. & Tomsic, D. The neuroethology of escape in crabs: From sensory ecology to neurons and back. *Current Opinion in Neurobiology* vol. 22 194–200 Preprint at https://doi.org/10.1016/j.conb.2011.11.012 (2012).

18. Branco, T. & Redgrave, P. The Neural Basis of Escape Behavior in Vertebrates. *Annu Rev Neurosci* **43**, 417–439 (2020).

19. Edwards et al. 1999-Fifty years of a command neuron- the neurobiology of escape behavior in the crayfish.

20. Eaton, R. C., Lee, R. K. K. & Foreman, M. B. The Mauthner cell and other identified neurons of the brainstem escape network of fish. *Prog Neurobiol* **63**, 467–485 (2001).

21. Blivis, D., Haspel, G., Mannes, P. Z., O'Donovan, M. J. & Iadarola, M. J. Identification of a novel spinal nociceptive-motor gate control for aδ pain stimuli in rats. *Elife* **6**, (2017).

22. Fotowat, H., Harrison, R. R. & Gabbiani, F. Multiplexing of Motor Information in the Discharge of a Collision Detecting Neuron during Escape Behaviors. *Neuron* **69**, 147–158 (2011).

23. Dunn, T. W. *et al.* Neural Circuits Underlying Visually Evoked Escapes in Larval Zebrafish. *Neuron* **89**, 613–628 (2016).

24. Bellardita, C. & Kiehn, O. Phenotypic characterization of speed-associated gait changes in mice reveals modular organization of locomotor networks. *Current Biology* **25**, 1426–1436 (2015).

25. Kiehn, O. Decoding the organization of spinal circuits that control locomotion. *Nat Rev Neurosci* **17**, 224–238 (2016).

26. Mendes, C. S., Bartos, I., Akay, T., Márka, S. & Mann, R. S. Quantification of gait parameters in freely walking wild type and sensory deprived Drosophila melanogaster. *Elife* **2013**, 1–24 (2013).

27. Cande, J. *et al.* Optogenetic dissection of descending behavioral control in Drosophila. *bioRxiv* (2017) doi:10.1101/230128.

28. Domenici, P., Blagburn, J. M. & Bacon, J. P. Animal escapology II: Escape trajectory case studies. *Journal of Experimental Biology* **214**, 2474–2494 (2011).

29. Domenici, P., Blagburn, J. M. & Bacon, J. P. Animal escapology I: Theoretical issues and emerging trends in escape trajectories. *Journal of Experimental Biology* **214**, 2463–2473 (2011).

30. Card, G. & Dickinson, M. H. Visually Mediated Motor Planning in the Escape Response of Drosophila. *Current Biology* **18**, 1300–1307 (2008).

31. Wang, Y. *et al.* Flexible motor sequence generation during stereotyped escape responses. *Elife* **9**, 1–27 (2020).

32. Zacarias, R., Namiki, S., Card, G. M., Vasconcelos, M. L. & Moita, M. A. Speed dependent descending control of freezing behavior in Drosophila melanogaster. *Nat Commun* **9**, (2018).

33. Fadok, J. P. *et al.* A competitive inhibitory circuit for selection of active and passive fear responses. *Nature* **542**, 96–99 (2017).

34. von Reyn, C. R. *et al.* Feature Integration Drives Probabilistic Behavior in the Drosophila Escape Response. *Neuron* **94**, 1190-1204.e6 (2017).

35. Ache, J. M. *et al.* Neural Basis for Looming Size and Velocity Encoding in the Drosophila Giant Fiber Escape Pathway. *Current Biology* **29**, 1073-1081.e4 (2019).

36. Tanouye, M. A. & King, D. G. *GIANT FIBRE ACTIVATION OF DIRECT FLIGHT MUSCLES IN DROSOPHILA. Jf. exp. Biol* vol. 105 (1983).

37. Oram, T. B. & Card, G. M. Context-dependent control of behavior in Drosophila. *Current Opinion in Neurobiology* vol. 73 Preprint at https://doi.org/10.1016/j.conb.2022.02.003 (2022).

38. Tovote, P. *et al.* Midbrain circuits for defensive behaviour. *Nature* **534**, 206–212 (2016).

39. Caggiano, V. *et al.* Midbrain circuits that set locomotor speed and gait selection. *Nature* **553**, 455–460 (2018).

40. Tovote, P. *et al.* Midbrain circuits for defensive behaviour. *Nature* **534**, 206–212 (2016).

41. McLean, D. L., Fan, J., Higashijima, S. I., Hale, M. E. & Fetcho, J. R. A topographic map of recruitment in spinal cord. *Nature* **446**, 71–75 (2007).

42. McLean, D. L., Fan, J., Higashijima, S. I., Hale, M. E. & Fetcho, J. R. A topographic map of recruitment in spinal cord. *Nature* **446**, 71–75 (2007).

43. Bolker, J. A. Model species in evo-devo: A philosophical perspective. *Evol Dev* **16**, 49–56 (2014).

44. Bolker, J. A. Exemplary and surrogate models: Two modes of representation in biology. *Perspectives in Biology and Medicine* vol. 52 485–499 Preprint at https://doi.org/10.1353/pbm.0.0125 (2009).

45. Kazama, H. Systems neuroscience in Drosophila: Conceptual and technical advantages. *Neuroscience* vol. 296 3–14 Preprint at https://doi.org/10.1016/j.neuroscience.2014.06.035 (2015).

46. Powsner, L. *THE EFFECTS OF TEMPERATURE ON THE DURA-TIONS OF THE DEVELOPMENTAL STAGES OF DROSOPHILA MELANOGASTER'*. http://www.journals.uchicago.edu/t-and-c (1935).

47. Gerhard, S., Andrade, I., Fetter, R. D., Cardona, A. & Schneider-Mizell, C. M. Conserved neural circuit structure across Drosophila larval development revealed by comparative connectomics. (2017) doi:10.7554/eLife.29089.001.

48. Almeida-Carvalho, M. J. *et al.* The Ol 1 mpiad: concordance of behavioural faculties of stage 1 and stage 3 Drosophila larvae . *J Exp Biol* **220**, 2452–2475 (2017).

49. Cardona, A., Larsen, C. & Hartenstein, V. Neuronal fiber tracts connecting the brain and ventral nerve cord of the early Drosophila larva. *Journal of Comparative Neurology* **515**, 427–440 (2009).

50. Schneider-Mizell, C. M. *et al.* Quantitative neuroanatomy for connectomics in Drosophila. *Elife* **5**, 1–36 (2016).

51. Heckscher, E. S. *et al.* Even-Skipped+ Interneurons Are Core Components of a Sensorimotor Circuit that Maintains Left-Right Symmetric Muscle Contraction Amplitude. *Neuron* **88**, 314–329 (2015).

52. Fushiki, A. *et al.* A circuit mechanism for the propagation of waves of muscle contraction in Drosophila. *Elife* **5**, (2016).

53. Zwart, M. F. *et al.* Selective Inhibition Mediates the Sequential Recruitment of Motor Pools. *Neuron* **91**, 615–628 (2016).

54. Takagi, S. *et al.* Divergent Connectivity of Homologous Command-like Neurons Mediates Segment-Specific Touch Responses in Drosophila. *Neuron* **96**, 1373-1387.e6 (2017).

55. Carreira-Rosario, A. *et al.* MDN brain descending neurons coordinately activate backward and inhibit forward locomotion. *Elife* **7**, (2018).

56. Burgos, A. *et al.* Nociceptive interneurons control modular motor pathways to promote escape behavior in Drosophila. *Elife* **7**, (2018).

57. Kohsaka, H. *et al.* Regulation of forward and backward locomotion through intersegmental feedback circuits in Drosophila larvae. *Nat Commun* **10**, 1–11 (2019).

58. Zarin, A. A., Mark, B., Cardona, A., Litwin-Kumar, A. & Doe, C. Q. A multilayer circuit architecture for the generation of distinct locomotor behaviors in Drosophila. *Elife* **8**, 1–34 (2019).

59. Morgan, T. H. *Sex Limited Inheritance in Drosophila*. *New Series* vol. 22 (1910).

60. Konopka, R. J. & Benzer, S. *Clock Mutants of Drosophila melanogaster (eclosion/circadian/rhythms/X chromosome)*. vol. 68 (1971).

61. Bellen, H. J., Tong, C. & Tsuda, H. 100 years of Drosophila research and its impact on vertebrate neuroscience: A history lesson for the future. *Nature Reviews Neuroscience* vol. 11 514–522 Preprint at https://doi.org/10.1038/nrn2839 (2010).

62. Simpson, J. H. & Looger, L. L. Functional imaging and optogenetics in drosophila. *Genetics* **208**, 1291–1309 (2018).

63. Brand, H. & Perrimon, N. *402 A.*

64. Gohl, D. M. *et al.* A versatile in vivo system for directed dissection of gene expression patterns. *Nat Methods* **8**, 231–237 (2011).

65. Pfeiffer, B. D. *et al.* Tools for neuroanatomy and neurogenetics in Drosophila. *Proceedings of the National Academy of Sciences* **105**, 9715–9720 (2008).

66. Nässel, D. R. *Neuropeptides in the nervous system of Drosophila and other insects: multiple roles as neuromodulators and neurohormones*. *Progress in Neurobiology* vol. 68 (2002).

67. Reiter, L. T., Potocki, L., Chien, S., Gribskov, M. & Bier, E. A systematic analysis of human disease-associated gene sequences in Drosophila melanogaster. *Genome Res* **11**, 1114–1125 (2001).

68. Kasture, A. S., Hummel, T., Sucic, S. & Freissmuth, M. Big lessons from tiny flies: Drosophila melanogaster as a model to explore dysfunction of dopaminergic and serotonergic neurotransmitter systems. *International Journal of Molecular Sciences* vol. 19 Preprint at https://doi.org/10.3390/ijms19061788 (2018).

69. Grueber, W. B., Jan, L. Y. & Jan, Y. N. Dendritic tiling in Drosophila. *Development* **129**, 2867–2878 (2002).

70. Singhania, A. & Grueber, W. B. Development of the embryonic and larval peripheral nervous system of Drosophila. *Wiley Interdiscip Rev Dev Biol* **3**, 193–210 (2014).

71. Ohyama, T. *et al.* High-Throughput Analysis of Stimulus-Evoked Behaviors in Drosophila Larva Reveals Multiple Modality-Specific Escape Strategies. *PLoS One* **8**, (2013).

72. Wreden, C. C. *et al.* Temporal Cohorts of Lineage-Related Neurons Perform Analogous Functions in Distinct Sensorimotor Circuits. *Current Biology* **27**, 1521-1528.e4 (2017).

73. Jovanic, T. *et al.* Neural Substrates of Drosophila Larval Anemotaxis. *Current Biology* **29**, 554-566.e4 (2019).

74. Tsubouchi, A., Caldwell, J. C. & Tracey, W. D. Dendritic filopodia, ripped pocket, NOMPC, and NMDARs contribute to the sense of touch in Drosophila larvae. *Current Biology* **22**, 2124–2134 (2012).

75. Yan, Z. *et al.* Drosophila NOMPC is a mechanotransduction channel subunit for gentle-touch sensation. *Nature* **493**, 221–225 (2013).

76. Turner, H. N., Patel, A. A., Cox, D. N. & Galko, M. J. Injury-induced cold sensitization in Drosophila larvae involves behavioral shifts that require the TRP channel Brv1. *PLoS One* **13**, (2018).

77. Tracey Jr., W. D., Benzer, S., Wilson, R. I. & Laurent, G. painless, a Drosophila gene essential for nociception. *Cell* **113**, 261–273 (2003).

78. Hwang, R. Y. *et al.* Nociceptive Neurons Protect Drosophila Larvae from Parasitoid Wasps. *Current Biology* **17**, 2105–2116 (2007).

79. Jang, W. *et al.* Impairment of proprioceptive movement and mechanical nociception in Drosophila melanogaster larvae lacking Ppk30, a Drosophila member of the Degenerin/Epithelial Sodium Channel family. *Genes Brain Behav* **18**, (2019).

80. Guo, Y., Wang, Y., Wang, Q. & Wang, Z. The Role of PPK26 in Drosophila Larval Mechanical Nociception. *Cell Rep* **9**, 1183–1190 (2014).

81. Luo, J., Shen, W. L. & Montell, C. TRPA1 mediates sensation of the rate of temperature change in Drosophila larvae. *Nat Neurosci* **20**, 34–41 (2017).

82. Terada, S. I. *et al.* Neuronal processing of noxious thermal stimuli mediated by dendritic ca2+ influx in Drosophila somatosensory neurons. *Elife* **5**, (2016).

83. Zhong, L., Hwang, R. Y. & Tracey, W. D. Pickpocket Is a DEG/ENaC Protein Required for Mechanical Nociception in Drosophila Larvae. *Current Biology* **20**, 429–434 (2010).

84. Walcott, K. C. E., Mauthner, S. E., Tsubouchi, A., Robertson, J. & Tracey, W. D. The Drosophila Small Conductance Calcium-Activated Potassium Channel Negatively Regulates Nociception. *Cell Rep* **24**, 3125-3132.e3 (2018).

85. Robertson, J. L., Tsubouchi, A. & Tracey, W. D. Larval Defense against Attack from Parasitoid Wasps Requires Nociceptive Neurons. *PLoS One* **8**, (2013).

86. Yoshino, J., Morikawa, R. K., Hasegawa, E. & Emoto, K. Neural Circuitry that Evokes Escape Behavior upon Activation of Nociceptive Sensory Neurons in Drosophila Larvae. *Current Biology* **27**, 2499-2504.e3 (2017).

87. Ohyama, T. *et al.* A multilevel multimodal circuit enhances action selection in Drosophila. *Nature* **520**, 633–639 (2015).

88. Kim, S. E., Coste, B., Chadha, A., Cook, B. & Patapoutian, A. The role of Drosophila Piezo in mechanical nociception. *Nature* **483**, 209–212 (2012).

89. Hu, C. *et al.* Sensory integration and neuromodulatory feedback facilitate Drosophila mechanonociceptive behavior. *Nat Neurosci* **20**, 1085–1095 (2017).

90. Mauthner, S. E. *et al.* Balboa binds to pickpocket in vivo and is required for mechanical nociception in drosophila larvae. *Current Biology* **24**, 2920–2925 (2014).

91. Hughes, C. L. & Thomas, J. B. A sensory feedback circuit coordinates muscle activity in Drosophila. *Molecular and Cellular Neuroscience* **35**, 383–396 (2007).

92. Vaadia, R. D. *et al.* Characterization of Proprioceptive System Dynamics in Behaving Drosophila Larvae Using High-Speed Volumetric Microscopy. *Current Biology* **29**, 935-944.e4 (2019).

93. Grueber, W. B. *et al.* Projections of Drosophila multidendritic neurons in the central nervous system: links with peripheral dendrite morphology. *Development* **134**, 55–64 (2006).

94. Zhong, L. *et al.* Thermosensory and Nonthermosensory Isoforms of Drosophila melanogaster TRPA1 Reveal Heat-Sensor Domains of a ThermoTRP Channel. *Cell Rep* **1**, 43–55 (2012).

95. Tracey, W. D. Nociception. *Current Biology* **27**, R129–R133 (2017).

96. Xiang, Y. *et al.* Light-avoidance-mediating photoreceptors tile the Drosophila larval body wall. *Nature* **468**, 921–926 (2010).

97. Im, S. H. *et al.* Tachykinin acts upstream of autocrine Hedgehog signaling during nociceptive sensitization in Drosophila. *Elife* **4**, (2015).

98. Bate, M. The embryonic development of larval muscles in Drosophila. *Development* **110**, 791–804 (1990).

99. Landgraf, M., Bossing, T., Technau, G. M. & Bate, M. The Origin, Location, and Projections of the Embryonic Abdominal Motorneurons of Drosophila . *The Journal of Neuroscience* **17**, 9642–9655 (1997).

100. Clark, M. Q., Zarin, A. A., Carreira-Rosario, A. & Doe, C. Q. Neural circuits driving larval locomotion in Drosophila. *Neural Development* vol. 13 Preprint at https://doi.org/10.1186/s13064-018-0103-z (2018).

101. Peron, S., Zordan, M. A., Magnabosco, A., Reggiani, C. & Megighian, A. From action potential to contraction: Neural control and excitation-contraction coupling in larval muscles of Drosophila. *Comparative Biochemistry and Physiology - A Molecular and Integrative Physiology* vol. 154 173–183 Preprint at https://doi.org/10.1016/j.cbpa.2009.04.626 (2009).

102. Newman, Z. L. *et al.* Input-Specific Plasticity and Homeostasis at the Drosophila Larval Neuromuscular Junction. *Neuron* **93**, 1388-1404.e10 (2017).

103. Zhou, Jinrun; Huang, Zenan; Li, Xinhang; Song, Zhiying; Sun, Yixuan; Ping, Junyu; Chen, Xiaopeng; Fei, Peng; Zheng, Nenggan; Gong, Z. Representation of Drosophila larval behaviors by muscle activity patterns. *bioRxiv* 1–62 (2021) doi:10.1101/2021.11.26.470133.

104. Schaefer, J. E., Worrell, J. W. & Levine, R. B. Role of intrinsic properties in Drosophila motoneuron recruitment during fictive crawling. *J Neurophysiol* **104**, 1257–1266 (2010).

105. Azevedo, A. W. *et al.* A size principle for recruitment of drosophila leg motor neurons. *Elife* **9**, 1–36 (2020).

106. Lindsay, T., Sustar, A. & Dickinson, M. The Function and Organization of the Motor System Controlling Flight Maneuvers in Flies. *Current Biology* **27**, 345–358 (2017).

107. Kennedy, D. & Takeda, K. Reflex control of abdominal flexor muscles in the crayfish. *J. Exp. Biol.* **43**, 221–227 (1965).

108. Arber, S. Motor Circuits in Action: Specification, Connectivity, and Function. *Neuron* **74**, 975–989 (2012).

109. Baek, M. & Mann, R. S. Lineage and birth date specify motor neuron targeting and dendritic architecture in adult Drosophila. *Journal of Neuroscience* **29**, 6904–6916 (2009).

110. Enriquez, J. *et al.* Specification of Individual Adult Motor Neuron Morphologies by Combinatorial Transcription Factor Codes. *Neuron* **86**, 955–970 (2015).

111. Landgraf, M., Jeffrey, V., Fujioka, M., Jaynes, J. B. & Bate, M. Embryonic origins of a motor system: Motor dendrites form a myotopic map in Drosophila. *PLoS Biol* **1**, (2003).

112. Mauss, A., Tripodi, M., Evers, J. F. & Landgraf, M. Midline signalling systems direct the formation of a neural map by dendritic targeting in the Drosophila motor system. *PLoS Biol* **7**, (2009).

113. Itakura, Y. *et al.* Identification of inhibitory premotor interneurons activated at a late phase in a motor cycle during drosophila larval locomotion. *PLoS One* **10**, 1–24 (2015).

114. Kohsaka, H., Takasu, E., Morimoto, T. & Nose, A. A group of segmental premotor interneurons regulates the speed of axial locomotion in drosophila larvae. *Current Biology* **24**, 2632–2642 (2014).

115. Babski, H. *et al.* A GABAergic Maf-expressing interneuron subset regulates the speed of locomotion in Drosophila. *Nat Commun* **10**, 1–17 (2019).

116. Pulver, S. R. *et al.* Imaging fictive locomotor patterns in larval Drosophila. *J Neurophysiol* **114**, 2564–2577 (2015).

117. Sato, Y. *et al.* Functional reorganization of locomotor kinematic synergies reflects the neuropathology in a mouse model of spinal cord injury. *Neurosci Res* **177**, 78–84 (2022).

118. Kawai, R. *et al.* Motor Cortex Is Required for Learning but Not for Executing a Motor Skill. *Neuron* **86**, 800–812 (2015).

119. Whitehead, S. C. *et al.* Neuromuscular embodiment of feedback control elements in Drosophila flight. doi:10.1101/2022.02.22.481344.

120. Mathis, A. *et al.* DeepLabCut: markerless pose estimation of user-defined body parts with deep learning. *Nat Neurosci* **21**, 1281–1289 (2018).

121. Domenici, P. & Hale, M. E. Escape responses of fish: A review of the diversity in motor control, kinematics and behaviour. *Journal of Experimental Biology* vol. 222 Preprint at https://doi.org/10.1242/jeb.166009 (2019).

122. Risse, B. *et al.* FIM, a Novel FTIR-Based Imaging Method for High Throughput Locomotion Analysis. *PLoS One* **8**, (2013).

123. Risse, B. *et al.* FIM 2c : Multicolor, Multipurpose Imaging System to Manipulate and Analyze Animal Behavior. *IEEE Trans Biomed Eng* **64**, 610–620 (2017).

124. Li Chen, Yuechao Wang, Shugen Ma & bin Li. Studies on lateral rolling locomotion of a snake robot. in 5070–5074 (Institute of Electrical and Electronics Engineers (IEEE), 2004). doi:10.1109/robot.2004.1302521.

125. Ekeberg, Ö. & Grillner, S. Simulations of neuromuscular control in lamprey swimming. *Philosophical Transactions of the Royal Society B: Biological Sciences* **354**, 895–902 (1999).

126. Heckscher, E. S., Lockery, S. R. & Doe, C. Q. Characterization of Drosophila Larval Crawling at the Level of Organism, Segment, and Somatic Body Wall Musculature. *Journal of Neuroscience* **32**, 12460–12471 (2012).

127. Pehlevan, C., Paoletti, P. & Mahadevan, L. Integrative neuromechanics of crawling in D. Melanogaster Larvae. *Elife* **5**, (2016).

128. Chvatal, S. A. & Ting, L. H. Common muscle synergies for balance and walking. *Front Comput Neurosci* **7**, 1–14 (2013).

129. Waters, R. L. & Morris, J. M. Electrical activity of muscles of the trunk during walking. *J Anat* **111**, 191–9 (1972).

130. Broekmans, O. D., Rodgers, J. B., Ryu, W. S. & Stephens, G. J. Resolving coiled shapes reveals new reorientation behaviors in C. elegans. *Elife* **5**, 1–17 (2016).

131. Huang, T.-C., Huang, Y.-J. & Lin, W.-C. Real-time horse gait synthesis. *Comput Animat Virtual Worlds* **24**, 87–95 (2013).

132. Donnelly, J. L. *et al.* Monoaminergic Orchestration of Motor Programs in a Complex C. elegans Behavior. *PLoS Biol* **11**, (2013).

133. Heckscher, E. S. *et al.* Even-Skipped+ Interneurons Are Core Components of a Sensorimotor Circuit that Maintains Left-Right Symmetric Muscle Contraction Amplitude. *Neuron* **88**, 314–329 (2015).

134. Hasegawa, E., Truman, J. W. & Nose, A. Identification of excitatory premotor interneurons which regulate local muscle contraction during Drosophila larval locomotion. *Sci Rep* **6**, (2016).

135. Yoshikawa, S., Long, H. & Thomas, J. B. A subset of interneurons required for Drosophila larval locomotion. *Molecular and Cellular Neuroscience* **70**, 22–29 (2016).

136. Voleti, V. *et al.* Real-time volumetric microscopy of in vivo dynamics and large-scale samples with SCAPE 2.0. *Nat Methods* **16**, 1054–1062 (2019).

137. Hillman, Elizabeth M.C.; Voleti, Venkatakaushik; Li, Wenze; Yu, H. Light-Sheet Microscopy in Neuroscience. *Annu Rev Neuroscie* **42**, 295–313 (2019).

138. Bouchard, M. B. *et al.* Swept confocally-aligned planar excitation (SCAPE) microscopy for high-speed volumetric imaging of behaving organisms. *Nat Photonics* **9**, 113–119 (2015).

139. Xu, L. *et al.* Widespread receptor-driven modulation in peripheral olfactory coding. *Science (1979)* **368**, (2020).

140. Benezra, Sam E.; Patel, Kripa; Campos, Citlali; Hillman, E.M.C.; Bruno, R. Learning enhances behaviorally relevant representations in apical dendrites. *bioRxiv* (2021) doi:10.1101/2021.11.10.468144;

141. Hillman, E. M. *et al.* High-speed 3D imaging of cellular activity in the brain using axially-extended beams and light sheets. *Curr Opin Neurobiol* **50**, 190–200 (2018).

142. Schaffer, E. S. *et al.* Flygenvectors: The spatial and temporal structure of neural activity across the fly brain. *bioRxiv* 2021.09.25.461804 (2021).

143. Koyama, M. *et al.* A circuit motif in the zebrafish hindbrain for a two alternative behavioral choice to turn left or right. *Elife* **5**, 1–23 (2016).

144. Bouchard, M. B. *et al.* Swept confocally-aligned planar excitation (SCAPE) microscopy for high-speed volumetric imaging of behaving organisms. *Nat Photonics* **9**, 113–119 (2015).

145. Baker, R. *et al.* Protein O-Mannosyltransferases Affect Sensory Axon Wiring and Dynamic Chirality of Body Posture in the Drosophila Embryo . *The Journal of Neuroscience* **38**, 1850–1865 (2018).

146. Matsunaga, T., Kohsaka, H. & Nose, A. Gap junction–mediated signaling from motor neurons regulates motor generation in the central circuits of larval Drosophila. *Journal of Neuroscience* **37**, 2045–2060 (2017).

147. Clark, M. Q., McCumsey, S. J., Lopez-Darwin, S., Heckscher, E. S. & Doe, C. Q. Functional genetic screen to identify interneurons governing behaviorally distinct aspects of Drosophila larval motor programs. *G3: Genes, Genomes, Genetics* **6**, 2023–2031 (2016).

148. Stepien, A. E., Tripodi, M. & Arber, S. Monosynaptic Rabies Virus Reveals Premotor Network Organization and Synaptic Specificity of Cholinergic Partition Cells. *Neuron* **68**, 456–472 (2010).

149. Litwin-Kumar, A. & Turaga, S. C. Constraining computational models using electron microscopy wiring diagrams. *Curr Opin Neurobiol* **58**, 94–100 (2019).

150. Wen, Q. *et al.* Proprioceptive Coupling within Motor Neurons Drives C. elegans Forward Locomotion. *Neuron* **76**, 750–761 (2012).

151. Ganguly, I. & Litwin-Kumar, A. Connectomics: Relating synaptic connectivity to physiology. *Curr Biol* **32**, R118–R120 (2022).

152. Kohn, J. R., Portes, J. P., Christenson, M. P., Abbott, L. F. & Behnia, R. Flexible filtering by neural inputs supports motion computation across states and stimuli. *Current Biology* **31**, 5249-5260.e5 (2021).

153. Büschges, A. Sensory Control and Organization of Neural Networks Mediating Coordination of Multisegmental Organs for Locomotion. *J Neurophysiol* **93**, 1127–1135 (2005).

154. Risse, B., Otto, N., Berh, D., Jiang, X. & Klämbt, C. FIM Imaging and FIMtrack: Two New Tools Allowing High-throughput and Cost Effective Locomotion Analysis. *Journal of Visualized Experiments* (2014) doi:10.3791/52207.

155. Gjorgjieva, J., Berni, J., Evers, J. F. & Eglen, S. J. Neural circuits for peristaltic wave propagation in crawling drosophila larvae: Analysis and modeling. *Front Comput Neurosci* **7**, 1–19 (2013).

156. Huang, Y. & Zarin, A. A. A premotor microcircuit to generate behavior-specific muscle activation patterns 1 in Drosophila larvae 2 3. doi:10.1101/2022.08.18.504452.

157. Agrawal, S. & Tuthill, J. C. The two-body problem: Proprioception and motor control across the metamorphic divide. *Current Opinion in Neurobiology* vol. 74 Preprint at https://doi.org/10.1016/j.conb.2022.102546 (2022).

158. Howard, C. E. *et al.* Serotonergic Modulation of Walking in Drosophila. *Current Biology* **29**, 4218-4230.e8 (2019).

159. Wosnitza, A., Bockemüh, T., Dübbert, M., Scholz, H. & Büschges, A. Inter-leg coordination in the control of walking speed in Drosophila. *Journal of Experimental Biology* **216**, 480–491 (2013).

160. Saraswati, S., Fox, L. E., Soll, D. R. & Wu, C. F. Tyramine and Octopamine Have Opposite Effects on the Locomotion of Drosophila Larvae. *J Neurobiol* **58**, 425–441 (2004).

161. Feller, M. Spontaneous Correlated Activity in Developing Neural Circuits. *Neuron Minireview* 653–656 (1999).

162. Kiehn, O. & Tresch, M. Gap junctions and motor behavior. *Trends Neurosci* **25**, 108–115 (2002).